Alma Mater Studiorum – Università di Bologna

DOTTORATO DI RICERCA IN

SCIENZE BIOMEDICHE E NEUROMOTORIE

Ciclo XXX

Settore Concorsuale di afferenza: 06/D6 – NEUROLOGIA

Settore Scientifico disciplinare: MED/26 – NEUROLOGIA

TITOLO TESI

THE ROLE OF MITOCHONDRIAL GENOME IN INHERITED OPTIC NEUROPATHIES

Presentata da: **DOTT. LEONARDO CAPORALI**

Coordinatore Dottorato	**Relatore**
PROF. LUCIO COCCO	**PROF. VALERIO CARELLI**

Esame finale anno 2018

ABSTRACT

Leber's hereditary optic neuropathy (LHON) is due in 90% of cases to three common point mutations affecting complex I subunit genes encoded by the mitochondrial genome (mtDNA). Besides these common mutations, there is a long and complex list of other mutations involved at various levels in the pathogenesis of LHON. On this scenario, we here report for the first time on the existence of LHON associated with peculiar combinations of individually non-pathogenic missense mtDNA variants, affecting the MT-ND4, MT-ND4L and MT-ND6 subunit genes of Complex I. The pathogenic potential of these mtDNA haplotypes is supported by multiple evidences: first, the LHON phenotype is strictly inherited along the maternal line in one very large family; second, the combinations of mtDNA variants are unique to the maternal lineages characterized by the recurrence of LHON; third, the Complex I-dependent respiratory and oxidative phosphorylation defect is co-transferred from the proband's fibroblasts into the cybrid cell model. Finally, all but one of these missense mtDNA variants clustered along the same predicted fourth E-channel deputed to proton translocation within the transmembrane domain of Complex I, involving the ND1, ND4L and ND6 subunits.

Hence, the definition of the pathogenic role of a specific mtDNA mutation becomes blurrier than ever and only an accurate evaluation of mitogenome sequence variation data from the general population, combined with functional analyses using the cybrid cell model, may lead to final validation. Our study conclusively shows that even in the absence of a clearly established LHON primary mutation, unprecedented combinations of missense mtDNA variants, individually known as polymorphisms, may lead to reduced OXPHOS efficiency sufficient to trigger LHON.

With this complexity in mind, mtDNA genetic variation itself may play a modifying role in LHON. Many studies reported the association of LHON and a specific mitochondrial haplogroup classified as J. Here we present the largest sequence survey of the entire mtDNA ever performed assessing 119 independent probands from all Europe carrying the m.14484T>C/MT-ND6 mutation. Besides the occasional finding of double mutants, we confirm the association with the haplogroup J root, but not with its more recent sub-clades. The phylogenetic analysis suggests a possible double role of this haplogroup: it may act as predisposing factor to mutagenesis at m.14484T position, or preserving the pathogenic

mutation during evolution. On the clinical ground, the penetrance of LHON due to m.14484T>C/MT-ND6 mutation increases on the haplogroup J background, especially in females, and multiple founder haplogroup J events can be recognized in our cohort.

Considering the strong association of mtDNA haplogroups with LHON, we also investigated if a similar association may act on Dominant Optic Atrophy (DOA). This is another inherited optic neuropathy similar to LHON, caused by mutations in the OPA1 gene, which encodes for a protein essential for mitochondrial fusion and mitochondrial homeostasis. Our results indicated that the relationship of DOA with mtDNA genetic variation is complex: no specific haplogroups resulted strongly associated with DOA, neither clearly modified its clinical outcome. We only documented a minor effect of the mitogenome variation in DOA, in particular when compared with what it seems a definitely stronger role as modifier played by nDNA.

INDEX

INTRODUCTION

Mitochondria: origin, structure and functions

Mitochondria are unusual organelles. They primarily act as the powerhouse of the cell, but they are also involved in programmed cell death, calcium homeostasis and several biosynthetic pathways. They are wrapped by two membranes, they have their own genome, an independent protein synthesis apparatus, and can change their shape to adapt to the different metabolic needs of the cell, from discrete isolated organelles to a large network.

Their origin, according to the endosymbiotic theory, was due to the increasingly oxygen-rich atmosphere and the primordial eukaryotic cell, unable to metabolize oxygen, acquired bacteria much better adapted to oxygen (Sagan, 1967; DiMauro et al., 2013).

The mitochondrial genome (mtDNA) is present in multiple copies and codes for a few fundamental protein components of the oxidative phosphorylation (OXPHOS) (Anderson et al., 1981).

The mitochondrial double-membrane is composed by the outer (OM) and inner (IM) membranes, this latter separating the inner membrane space (IMS) from the internal matrix. The OM has similar composition to the cell membrane; many transport channels (porin) are present and make the OM permeable to molecules of 5000 dalton or less (ions and small proteins). Differently, the IM contains high levels of cardiolipin, making it especially impermeable to ions, and selective transport proteins are needed to transport the molecules necessary to matrix enzymes or their metabolites. This membrane is fundamental for maintenance of an electrochemical gradient between the matrix and the IMS (Frey and Mannella, 2000). The IM is also organized in *cristae*, which can shift from tubular to lamellar structures, depending on the conformational state (Frey and Mannella, 2000). All *cristae* connect to the inner boundary membrane via a tubular structure, named *crista* junctions, that limits diffusion between the intracristal space and the intermembrane space (Frey and Mannella, 2000; Rampelt et al., 2017). *Cristae* are the specialized compartment for the respiratory chain complexes and the ATP synthase (Rampelt et al., 2017).

The fundamental mitochondrial function is energy conservation, in the form of ATP molecule, synthetized by the OXPHOS metabolism. Furthermore, other pathways take place in mitochondria: partial synthesis of steroids, heme-groups synthesis, Ca^{++} intracellular

homeostasis, reactive oxygen species (ROS) production and detoxification and apoptosis regulation.

Oxidative Phosphorylation

OXPHOS is the final step of cellular respiration and is a two-phases biochemical process: electron transport chain, with NADH and $FADH_2$ redox to generate a proton gradient, and ATP synthesis, exploiting the proton gradient. The OXPHOS uses the electrons flow that are transported through a series of protein complexes, which are embedded in the lipid bilayer of the mitochondrial IM, to provide most of cellular energy in the form of ATP (Balaban, 1990; Friedman and Nunnari, 2014).

The OXPHOS system is composed of five multimeric enzymatic complexes (CI-V) and consists of 87 subunits, 13 directly encoded by the mitochondrial DNA (mtDNA) (Figure 1).

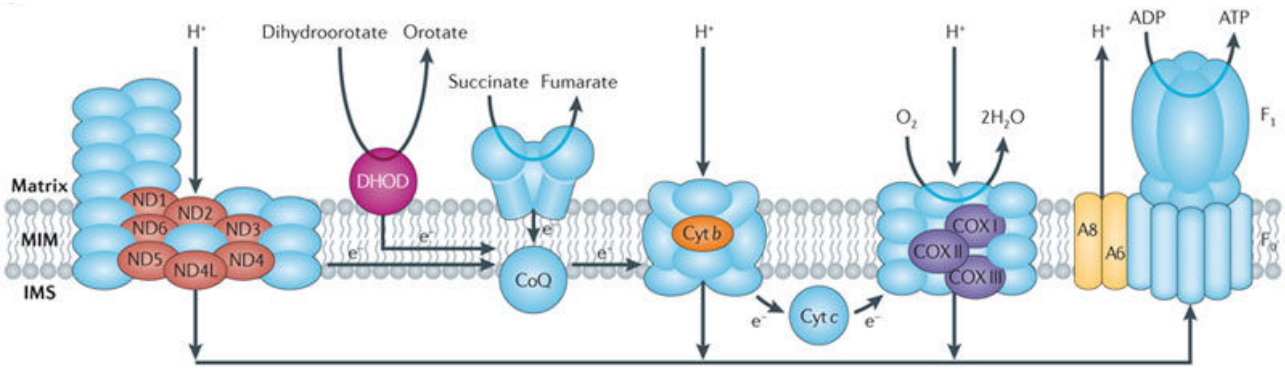

Figure 1. Mitochondrial respiratory chain (Schon et al., 2012)

All complexes are integrated in the lipid bilayer of the mitochondrial IM and together with two mobile electron carriers, ubiquinone (CoQ) and cytochrome c (cyt c), they make up the electron transport chain. The electron transport is coupled to the generation of a proton gradient across the IM and this is used by complex V to synthesize ATP from ADP (Mitchell, 1961). The electron carriers, nicotinamide adenine dinucleotide (NADH) and flavin adenine dinucleotide ($FADH_2$), are reduced during the Krebs cycle or the β-oxidation of fatty acids.

CI is the largest respiratory complexes, comprising 45 subunits, only seven mitochondrially encoded (Fiedorczuk et al., 2016). It's a L-shape structure protein, with two major domains: the hydrophilic matrix arm comprises flavin, involved in electron transfer, and the membrane arm, involved in proton translocation (Fiedorczuk et al., 2016). The electrons are transported

via iron/sulphur clusters to CoQ, reduced to $CoQH_2$ (Fiedorczuk et al., 2016), with the simultaneous translocation of four protons across the IM into the inner membrane space.

CII is formed by four subunits, completely encoded by the nucleus, and catalyzes the oxidation of succinate to fumarate. Reduced CoQ can move and transport the electrons to CIII (ubiquinone-cytochrome c oxidoreductase) (Lancaster and Kröger, 2000). CIII is a functional dimer and transfers electrons from $CoQH_2$ to cytochorme c, that donates electrons to complex IV through IMS (Darrouzet et al., 2001; Dibrova et al., 2013).

CIV is the terminal enzyme of the respiratory chain, composed of 13 subunits, of which three are encoded by the mtDNA. This complex reduces O_2 to H_2O, translocating protons from matrix to IMS. During the electron transfer, the energy released enables the proton pumping against gradient from the matrix to the IMS. The proton transfer occurs only in CI, III and IV. The electrochemical gradient, positive outside and negative inside the IM, is used by complex V (ATP synthase) to synthesize ATP.

CV consists of two major functional domains, a large extra-membranous portion (F_1) sector and a membrane-intrinsic portion (F_0) sector joined together by central and peripheral stalks (Walker, 2013). CV has two subunits encoded by mtDNA (MT-ATP6 and MT-ATP8), which take part to the membrane-bound portion (F_0) of the complex, and about 13 other subunits encoded by nDNA (Abrahams et al., 1994). Protons from the intermembrane space enter CV through the F_0 complex leading to the rotation of the catalytic complex. The rotational energy of the motor is transmitted to the catalytic domain by the central stalk, which is attached directly to the rotary motor, and then used for ATP synthesis (Walker, 2013). ATP formation requires a sufficient supply of ADP and phosphate, and specific carriers transport both substrates across the mitochondrial membranes: the adenine nucleotide translocator (ANT) and the phosphate carrier (Seelert and Dencher, 2011).

Morphology

Mitochondria appear as a dynamic network in balance between the processes of fusion and fission of both OM and IM (Chan, 2012; Liu et al., 2009). During fusion the membranes of two discrete mitochondria merge, uniting and mixing their content. Opposite, during fission a single mitochondrion splits into two organelles. Continuous rounds of fusion and fission are necessary to maintain mitochondrial homeostasis (Chan, 2012), in particular to meet the

energetic needs (Gomes et al., 2011; Mishra et al., 2014). A wide mitochondrial network is present in metabolically active cells and acts electrically as a unique system able to transmit mitochondrial membrane potential, allowing energy distribution and dissipation (Skulachev, 2001).

A "mitochondria-shaping" machinery, including both pro-fusion and pro-fission proteins, is involved in a dynamic control of the mitochondrial network, to efficiently maintain the mitochondrial population. During mitochondrial fission, the dynamin protein Drp1 is recruited from cytosol to the mitochondrial surface, self-assembles into ring-like oligomeric structures that encircle and pinch the outer mitochondrial membrane at sites of fission (Lee et al., 2017). Drp1 is essential for mitochondrial fission provoked by events like mitosis or stress, and for development of the nervous system (Ishihara et al., 2009; Wakabayashi et al., 2009). Drp1 is recruited at the mitochondrial surface by integral OM proteins (Fis1, Mff, MiD49 and MiD51). In mammals Fis1 can directly bind Drp1, although in yeast the recruitment requires Fis1 and the two WD40-containing adaptors (Griffin et al., 2005; Wells et al., 2007). Moreover, in mammals three other receptor proteins involved in fission events are reported: Mff, MiD49 and MiD51 (Losón et al., 2013; Otera et al., 2005). Mitochondrial fission plays a key role in both cell life and death. Fission occurs in the programmed cell death pathway (apoptosis), before the release of cytochrome c and caspase activation (Youle and Karbowski, 2005), and in cellular division, for correct distribution of mitochondria to daughter cells (Kashatus et al., 2011). Fission carries out a key role in mitophagy, because interruption of fission reduces the efficiency of mitophagy, suggesting that fission segregates mitochondria with loss of membrane potential (Frank et al., 2012; Stotland and Gottlieb, 2015).

Fusion is the reverse process of fission, when the inner and outer membranes of one mitochondrion melt with the respective membranes of another organelle. First, the OMs fuse, allowing the IMs to come into proximity for their fusion. In mammals, three proteins carry out this event: the mitofusins MFN1 and MFN2 for the OM fusion and OPA1 for the IM fusion (Chan, 2012). These proteins belong to the dynamin-like protein superfamily and contain GTPase activity essential for their functions (Praefcke and McMahon, 2004). MFN1 is essential to induce OM fusion, whereas the role of MFN2 is less defined. MFN2 can form hetero-oligomers with MFN1 and is suggested to participate in later steps of mitochondrial fusion (Ishihara et al., 2004; Koshiba et al., 2004). MFN2 has been shown to be involved also in

endoplasmic reticulum interactions, bridging the two organelles close at the level of mitochondrial associated membranes (MAMs), and the levels of MFN2 correlate with the oxidative metabolism of skeletal muscle (Bach et al., 2003; de Brito and Scorrano, 2008). OPA1 is essential for IM fusion, but it is also involved in shaping the cristae morphology, OXPHOS efficiency, and mtDNA maintenance (Belenguer and Pellegrini, 2013; Vidoni et al., 2013). OPA1 oligomerization, tightening cristae junctions, also controls the propensity to apoptosis by sequestering cytochrome c within the cristae and regulating its release in the IMS (Dotto et al., 2017; Frezza et al., 2006; Olichon et al., 2003). Fusion is important also for mitochondrial calcium homeostasis (Szabadkai et al., 2006), embryonic development (Chen et al., 2003), spermatogenesis and mtDNA maintenance (Chen et al., 2007).

The mitochondrial genome: mtDNA

The human mitochondrial genome (mtDNA) is a circular double-stranded molecule of about 16.6 kb, localized in the mitochondrial matrix, and represents 0,5-1% of the entire human genome. The mtDNA is present in multiple copies, ranging from tens to thousand per cell, according to the cell type. The two strands of mtDNA can be distinguished into 'heavy strand' (H-strand) and 'light strand' (L-strand), based on their nucleotide (GC) content (Fernández-Silva et al., 2003). The mtDNA is very compact, having none or only a few noncoding bases between genes and lacking in many cases the termination codons; termination is post-transcriptionally induced by polyadenylation of mRNAs (Anderson et al., 1981; Andrews et al., 1999).

The mtDNA encodes for 37 genes: 24 genes (22 tRNAs and 2 rRNAs, 12S and 16S) are necessary for transcription of 13 OXPHOS subunits, 7 for complex I (MT-ND1, MT-ND2, MT-ND3, MT-ND4, MT-ND4L, MT-ND5, MT-ND6), 1 for complex III (MT-CYB), 3 for complex IV (MT-CO1, MT-CO2, MT-CO3) and 2 for complex V (MT-ATP6, MT-ATP8) (Anderson et al., 1981) (Figure 2).

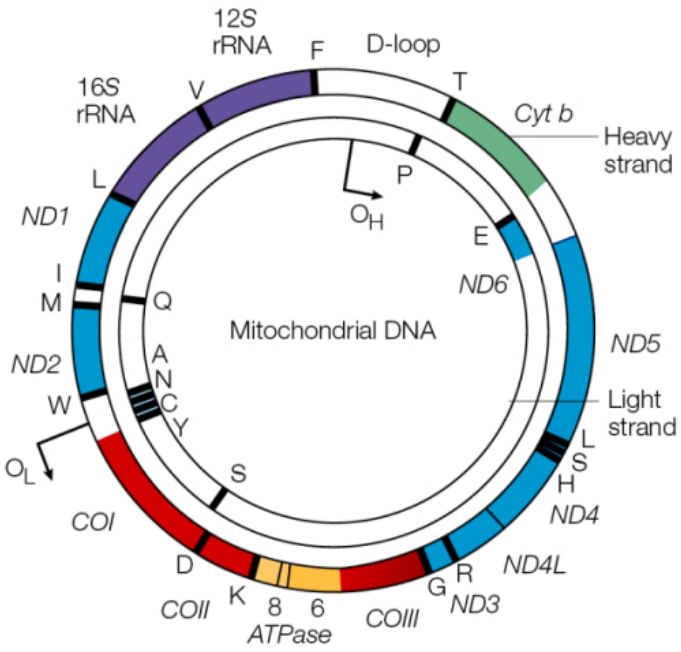

Figure 2. Map of mitochondrial DNA (Taylor and Turnbull, 2005)

Genes are distributed asymmetrically between the two strands: H-strand encodes for most genes, both rRNAs, 14 tRNAs and 12 mRNAs of 13 subunits, but ND6 and 8 tRNAs are in L-strand (Attardi and Schatz, 1988). Furthermore, two non-coding regions (NCR) are present in the mtDNA. D-loop (Displacement Loop) is a triple-stranded region found in the major NCR of many mitochondrial genomes, and is formed by stable incorporation of a third, short DNA strand known as 7S DNA (Nicholls and Minczuk, 2014). D-loop is involved in many function, especially in mtDNA replication and translation, but also in mtDNA topology, mtDNA recombination, membrane association and dNTPs metabolism (Nicholls and Minczuk, 2014). The second NCR contains the origin of L-strand replication (O_L) and is located in a cluster of five tRNA genes (MT-TA, MT-TN, MT-TC, MT-TY) on L-strand, between nucleotides 5512 and 5903, around two thirds of the mtDNA length from the O_H (Anderson et al., 1981; Fernandez-Silva et al., 2003).

Similar to bacterial chromosomes, mitochondrial DNA is organized into tightly-packed nucleoprotein complexes called nucleoids. Nucleoids are found associated with the inner mitochondrial membrane, but can also freely diffuse through the mitochondrial network (Albring et al., 1977; Brown et al., 2011; Nicholls and Minczuk, 2014). The most thoroughly characterized nucleoid protein is the high-mobility group box protein TFAM (Parisi and Clayton, 1991).

The mtDNA replicates according to the strand-displacement model, with an asynchronous and asymmetric modality. DNA synthesis occurs continuously on both strands without Okazaki fragments (Clayton, 1991). There are two specific origins of DNA replication, one for each strand, the H-strand origin (O_H) and the L-strand origin (O_L). This is necessary to ensure correct DNA synthesis for both strands. Replication starts at O_H, and DNA synthesis proceeds in 5'-3' direction to produce a new H-strand. During the synthesis of the new H-strand, mtSSB covers the displaced, parental H-strand and blocks POLRMT transcription (Miralles Fusté et al., 2014). When the replication machinery exceeds O_L, it becomes single-stranded and folds into a stem-loop structure. The stem inhibits mtSSB binding and leaves the single-stranded loop region accessible for POLRMT, which initiates primer synthesis from a poly-T stretch (Fusté et al., 2010; Miralles Fusté et al., 2014). After about 25 nucleotides of primer synthesis, POLRMT is replaced by POLγ, and L-strand DNA synthesis begins. The replication of the two strands is interconnected because H-strand synthesis is required for the initiation of L-strand synthesis. Once initiated, H- and L-strand synthesis proceed continuously in opposite directions until the two events reach a full circle (Gustafsson et al., 2016).

Besides the replication origin of H-strand, D-loop contains a dedicated promoter for the transcription of each strand of mtDNA, the L-strand promoter (LSP) and the H-strand promoter (HSP). Transcription initiation at LSP or HSP produces near-genome-length polycistronic transcripts that encompass all of the coding information on each strand. The primary transcripts are processed to release the individual RNA molecules. The steady-state levels of the longer unprocessed transcripts are low and, therefore, processing is likely to occur co-transcriptionally. According to the "tRNA punctuation model" model, tRNAs are specifically recognized and cleaved in the polycistronic transcripts, thus leading to the release of tRNAs, mRNAs, and rRNAs (Anderson et al., 1981; Ojala et al., 1981), which subsequently undergo further maturation by, for example, base modifications, CCA addition, and polyadenylation (Hällberg and Larsson, 2014). In mammalian mitochondria, the 5' ends of tRNAs are cleaved in the polycistronic transcript by an all-protein version of ribonuclease (RNase) P, consisting of three subunits (MRPP1–3), whereas the 3' ends of tRNAs are processed by RNase Z (ELAC2) (Hällberg and Larsson, 2014).

Mitochondrial genetics

The mitochondrial genome differs from the nuclear one (nDNA) in many respects. First, the mtDNA genetic code uses only two stop codons: AGA and AGG (Temperley et al., 2010) (compared with UAA, UGA and UAG in nDNA), conversely UGA encodes tryptophan. To compensate for this UAA codons have to be introduced at the post-transcriptional level. In addition, AUA, isoleucine in nDNA, encodes for methionine in mtDNA (Chinnery and Hudson, 2013).

Second, mtDNA is maternally inherited. The prevailing theory of an "active elimination model" for paternal mtDNA suggests that sperm mitochondria are ubiquitinated and removed through different routes, such as proteosomal, lysosomal pathways or mitophagy (Carelli, 2015; Rojansky et al., 2016; Sato and Sato, 2013; Sutovsky et al., 1999). Moreover, autophagy has been recently highlighted as the mechanism for paternal mtDNA elimination in *Caenorhabditis elegans* (Al Rawi et al., 2011; Sato and Sato, 2011). Finally, a passive "dilution model" due to disproportionate amount of paternal *versus* maternal mtDNAs in mammals has been proposed. This was observed in mice (Luo et al., 2013), but not confirmed in humans (Pyle et al., 2015). Occurrence of paternal mtDNA transmission has also been documented in human (Schwartz and Vissing, 2002), and more often in animals (Dokianakis and Ladoukakis, 2014; Gyllensten et al., 1991; Zhao et al., 2004).

Finally, mtDNA variants may be present in homoplasmy or heteroplasmy, not in homozygosity or heterozygosity. Homoplasmy occurs when the sequence of multiple mtDNA copies are identical. However, heteroplasmy arises when a variant co-exists with its wild-type counterpart in various proportions, due to the polyploid nature of mtDNA (Chinnery and Hudson, 2013; Payne et al., 2013). A heteroplasmic variant can be inherit from mother to child and segregate in different tissue with varying loads, according to the 'mitochondrial bottleneck theory'. During oogenesis and meiosis, cells incur to mtDNA reduction and amplification, leading to a purportedly random shift in mtDNA mutational load between cells (Chinnery and Hudson, 2013; Schon et al., 2012).

Mitochondrial haplogroups

The rate of evolution of the mitochondrial genome appears 10-fold higher than nuclear genome, mostly due to an elevated mutation rate of mtDNA (Brown et al., 1979). Due to the

high rate of evolution, mtDNA is an extremely useful molecule to exploit for high-resolution analysis in a wide range of fields, including evolutionary anthropology and population history, medical genetics, as well as forensic science (van Oven and Kayser, 2009). Thus, the mtDNA sequence evolved as a result of the sequential accumulation of mutations along maternally inherited lineages. All mtDNA types in the human gene pool can ultimately be traced back to a common matrilineal ancestor that lived approximately 200,000 years ago in Africa (Behar et al., 2008; Macaulay et al., 2005; Mishmar et al., 2003; van Oven and Kayser, 2009) and by migration colonized the world (Kivisild, 2015). Haplogroups are used to represent the major branch points on the mitochondrial phylogenetic tree and the migrations (Figure 3).

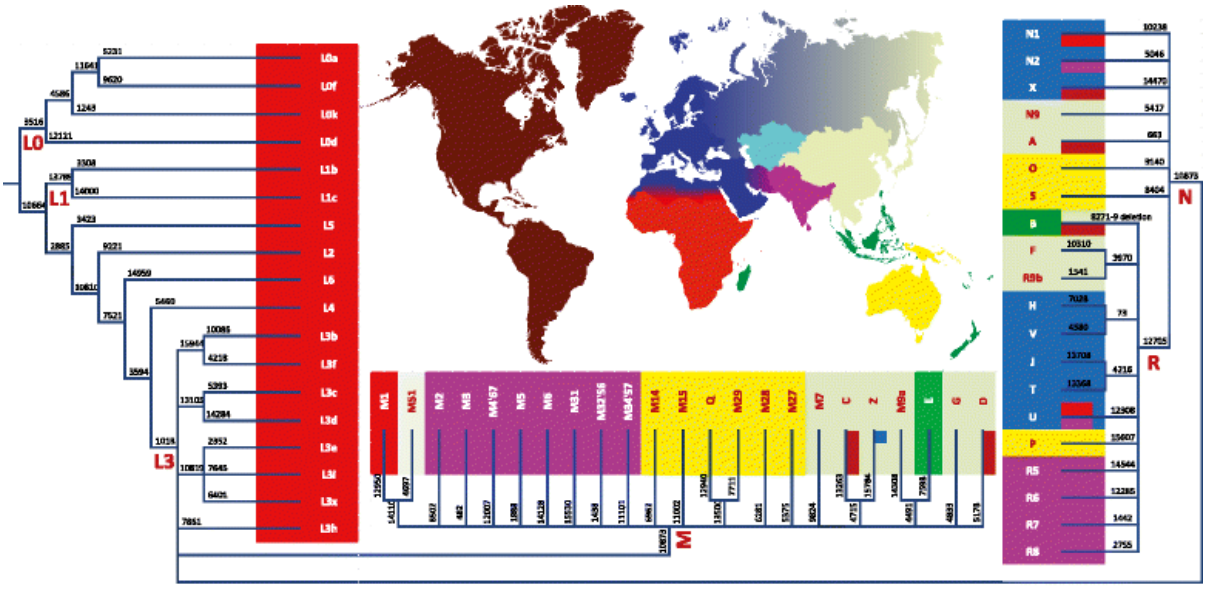

Figure 3 mtDNA haplogroup tree and distribution map (Kivisild, 2015).

The European population origins from the African haplogroup L3, followed by emergence of the major out-of-Africa haplogroups M and N (and N's descendants, R) in the vicinity of a putative "Gulf oasis" (Richards et al., 2016), subsequently followed by haplogroup R divergence (Pinhasi et al., 2012).

In the last decades, the possible role of mtDNA haplogroups in modulating mitochondrial function and pathology has been massively investigated. Interestingly, many studies have shown the associations of haplogroups with IQ (Skuder et al., 1995), sperm motility (Ruiz-Pesini et al., 2000), ability to adapt to climatic conditions (Ruiz-Pesini et al., 2004), body fat mass (Yang et al., 2011) and longevity (Cai et al., 2009; Santoro et al., 2006). Furthermore, this

association of mitochondrial haplogroups has been noticed in some pathologies, such as psychosis in bipolar disorder (Frye et al., 2017), motor function in long-term HIV-1 infected individuals (Azar et al., 2017), autism spectrum disorders (Chalkia et al., 2017), cardiomyopathy (Shin et al., 2000), multiple sclerosis (Kalman et al., 1999), Parkinson's disease (Ghezzi et al., 2005), Alzheimer's disease (Krüger et al., 2010; van der Walt et al., 2004), Friedreich's disease (Giacchetti et al., 2004), Amyotrophic Lateral Sclerosis (Mancuso et al., 2004) and Leber's Hereditary Optic Neuropathy (LHON) (Carelli et al., 2006; Hudson et al., 2007).

Leber's hereditary optic neuropathy (LHON)

LHON (OMIM #535000) is a blinding disorder, maternally inherited, characterized by acute or subacute loss of central vision, which affects predominantly young males, and is now recognized as the most frequent mitochondrial disease (Carelli et al., 2004, 2016; Yu-Wai-Man et al., 2011). The prevalence of LHON mutations in the population may vary from 1:10,000 in North East of England to 1:50,000 in Finland (Man et al., 2003; Puomila et al., 2007).

Clinically, LHON is characterized by painless, rapid loss of central vision in one eye, followed by a similar involvement of the other eye, usually in a short time laps, associated with dyschromatopsia (Carelli et al., 2004). In the acute phase, axonal loss in the papillo-macular bundle leads to temporal atrophy of the optic nerve, and the endpoint of the disease is generally a full optic atrophy with permanent severe loss of central vision, but with relative preservation of the peripheral visual field and pupillary light responses (Carelli et al., 2004). However, patients show occasionally a spontaneous recovery of visual acuity (Carelli et al., 2004; Mackey and Howell, 1992; Pezzi et al., 1998; Stone et al., 1992).

The peculiar feature of LHON is the selective degeneration of a single cell type, the retinal ganglion cells (RGCs). Thus, RGCs display somehow a unique sensibility to the mitochondrial energy defect generated by LHON pathogenic mutations. The 1.2 million axons that form the optic nerve originate from the RGCs in the inner retina (Carelli et al., 2004). These axons do not present a saltatory conduction of action potential until past the *lamina cribrosa*, due to absence of the myelin sheet, in order to maintain the optical transparency and consequently a good visual resolution (Howell et al., 2002). Thus, the high energy dependence of these cells

on mitochondrial OXPHOS may explain the particular sensitivity of RGCs and the related visual loss due to mitochondrial dysfunction (Carelli et al., 2004).

LHON is maternally inherited, due to the presence of point mutations on mtDNA. The most common pathogenic mutations are m.11778G>A/MT-ND4, m.3460G>A/MT-ND1, and m.14484T>C/MT-ND6, characterizing about 90% of LHON cases (Howell et al., 1991; Mackey and Howell, 1992; Wallace et al., 1988; Yu-Wai-Man et al., 2011). These "primary" pathogenic mutations are usually established as homoplasmic over multiple generations in LHON maternal lineages. However, two further features remain peculiar in LHON, i.e. the incomplete penetrance and the male prevalence (Caporali et al., 2017). Mitochondrial biogenesis, which is boosted in females by estrogens (Giordano et al., 2011), seems a major compensatory mechanism that determines incomplete penetrance (Giordano et al., 2014). On this, environmental factors, such as tobacco smoke (Sadun et al., 2004), and genetic modifiers, both in nDNA and mtDNA, are assumed to play a further role (Caporali et al., 2017).

Besides the 3 common "primary" LHON mutations, several other rarer pathogenic mutations have also been reported in single cases or families (Achilli et al., 2012). Moreover, additional recurrent polymorphic mtDNA variants were also associated with LHON and called "secondary" mutations (Brown et al., 1992; Johns and Berman, 1991; Johns and Neufeld, 1991). The role of these "secondary mutations", widely debated (Mackey et al., 1996), was elucidated by firmly establishing these variants as mtDNA haplogroup-related polymorphic markers (Torroni et al., 1996). Thus, multiple research groups confirmed the association of some LHON "primary" mutations with a specific mtDNA haplogroup, haplogroup J, as penetrance enhancer: in particular, this association is observed with the LHON m.11778G>A/MT-ND4 and m.14484T>C/MT-ND6 mutations (Brown et al., 1997; Lamminen et al., 1997; Torroni et al., 1997). Over the years, this association was refined to specific clades of haplogroup J, the J1c and J2b clades characterized by accumulation of missense variants affecting both complex I and III (Carelli et al., 2006; Hudson et al., 2007). This association were validated in large cohorts of LHON patients of European descent, but a similar scenario seems to be confirmed also in LHON cohorts of Asian ancestry (Ji et al., 2008; Kaewsutthi et al., 2011). Furthermore, the complete sequence analysis of mtDNA carrying rare LHON mutation allowed to identifying private variants that may also act as genetic modifiers (Achilli et al., 2012). Multiple reports on Chinese LHON families indicated the occurrence of mtDNA backgrounds

characterized by an unusually high or even complete penetrance, frequently due to coexisting pathogenic mutations (Yang et al., 2009; Zhang et al., 2012). Opposite, in other maternal lineages it was observed an extremely reduced penetrance (Qu et al., 2009). Thus, different combinations including mtDNA haplotypes as defined by specific arrays of polymorphisms, private variants and co-existing mutations may all impinge on the pathogenic potential and, ultimately, on penetrance of LHON primary mutations. Remarkably, the role of the same mtDNA variant may vary drastically, for example, from adaptation at high altitudes, due to an environmental positive selection on the mtDNA sequence, to a pathogenic potential predisposing to LHON in different interacting environments (Caporali et al., 2017; Ji et al., 2008).

Interestingly, the pathogenic role of the m.14484T>C/*MT-ND6* mutation was initially not recognized because of the low phylogenetic conservation of the affected amino acid (Howell et al., 1991; Mackey and Howell, 1992). Remarkably, the m.14484T>C/*MT-ND6* change found on non-J mtDNA backgrounds displays a very low penetrance and has been occasionally reported in genetic surveys of control populations, thus behaving borderline and similarly to a polymorphic variant (A. Torroni, unpublished data) (Howell et al., 2003a; Palanichamy et al., 2004). Furthermore, different sets of two or more mtDNA variants have been postulated as modulators of penetrance, such as combinations of multiple private "weak" pathogenic mutations or combination of established LHON pathogenic mutations with variants, already known as markers of specific haplogroups, but detected outside the usual haplogroup background (La Morgia et al., 2008, 2014a).

A few studies tackled the issue of providing a functional evidence for the modifying role of the mtDNA haplotype and/or the private variants or co-existing mtDNA mutations. Initial studies based on MR-spectroscopy were unable to detect differences between LHON patients carrying the m.11778G>A/MT-ND4 mutation associated or not with the mtDNA haplogroup J (Lodi et al., 2000). Exploiting the cell model of transmitochondrial cytoplasmic hybrids, "cybrids", it has been shown *in vitro* that different mtDNA haplogroups may have slight, but significant differences in bioenergetic efficiency, production of ROS and stability of respiratory complexes assembly (Carelli et al., 2002; Gómez-Durán et al., 2010, 2012; Pello et al., 2008), thus substantiating their possible role as modifiers for LHON penetrance. Controversial results

were instead provided by the few studies on cases of LHON carrying double primary mutations (Brown et al., 2001; Caporali et al., 2017; Cruz-Bermúdez et al., 2016; Jiang et al., 2016).

Dominant optic atrophy (DOA)

Dominant optic atrophy (DOA, OMIM#165500), also known as Kjer's optic atrophy, is the most common amongst hereditary optic neuropathies, with an estimated disease prevalence varying from 1:10,000 to 1:30,000 (Lenaers et al., 2012). In year 2000, two independent groups identified pathogenic mutations in the OPA1 gene as causative for DOA (Alexander et al., 2000; Delettre et al., 2000). Nowadays, about 70% of DOA families have been linked to OPA1 mutations and more than 350 pathogenic mutations have been submitted to OPA1 databases, spread throughout the protein (Ferré et al., 2015; La Morgia et al., 2014b). The 50% of DOA patients carry stop-codon, frame-shift and deletion-insertion, leading to incomplete transcription and decreased protein content, with haploinsufficiency as the genetic mechanism. The remaining patients present missense mutations, which are thought to act through a dominant negative mechanism. In 2008, a particular group of missense mutations, affecting the GTPase domain, have been related to a syndromic form of DOA, associated with sensorineural deafness, ataxia, late-onset chronic progressive external ophthalmoplegia (CPEO) and mitochondrial myopathy with cytochrome c oxidase negative. This new phenotype was defined as DOA "plus" syndrome (Amati-Bonneau et al., 2008; Hudson et al., 2008; Yu-Wai-Man et al., 2010). Importantly, these patients harbored multiple deletions of mtDNA in their skeletal muscles, confirming the OPA1 function in mtDNA stability, as previously reported for its orthologue in Saccharomyces cerevisiae (Jones and Fangman, 1992; Guan et al., 1993). Thus, OPA1 has been added to the list of genes (ANT1, Twinkle, POLG, MFN2) associated with human disorders characterized by mtDNA deletions (CPEO syndromes) (DiMauro and Schon, 2008; Rouzier et al., 2012). Recently, other phenotypes have been reported within the frame of the DOA "plus" syndrome, including MS-like features (Yu-Wai-Man et al., 2016), Behr-like spastic paraparesis (Marelli et al., 2011), Parkinsonism and dementia (Carelli et al., 2015) and cases with absent or very mild ocular phenotype (Milone et al., 2009), thus expanding the spectrum of OPA1 spectrum.

As LHON, DOA is a hereditary neurodegenerative disorder, characterized by a tissue specificity, which is limited to RGCs and their axons forming the optic nerve, with a

preferential involvement of the small fibers belonging to the papillomacular bundle, which serve central vision. The main difference with LHON is slowly progressive course of bilateral visual loss, and as in LHON, DOA is usually symmetrical, associated with centrocaecal scotomas, impairment of color vision, temporal pallor of the optic disks and relative preservation of the pupillary reflex (Delettre et al., 2002; Lenaers et al., 2012; Yu-Wai-Man et al., 2010). The onset of DOA is usually during childhood, although the defect most frequently is diagnosed early in adult life. However, this optic atrophy shows wide variability in clinical expression between and within families, and visual impairment ranges from subclinical vision impairment to legal blindness (Barboni et al., 2014; Carelli et al., 2009; Yu-Wai-Man et al., 2010).

Postmortem histologic studies showed diffuse atrophy of the ganglion cell layer in the retina, with loss of myelin and axons within the optic nerves (Johnston et al., 1979), similar to the histopathology of LHON (Kjer et al., 1983). Analysis of the retinal nerve fiber layer (RNFL) thickness in DOA patients with optical coherence tomography (OCT), a non-invasive technique used to obtain high-resolution images, revealed generalized loss of fibers, typically prevalent on the temporal sector, with a smaller average optic disk size compared to a control population (Barboni et al., 2011, 2014; Milea et al., 2010).

Due to the variable clinical severity and incomplete penetrance observed in DOA, similar to LHON, the possible role of mtDNA haplogroups was investigated in DOA patients carrying OPA1 mutations. The two studies currently published reached contrasting conclusions on the possibility that the mtDNA background may act as modifying factor for DOA penetrance (Han et al., 2006; Pierron et al., 2009). Both studies examined a limited series of patients (29 and 41 respectively) and the study design did not take into consideration that DOA is a dominant disorder where the mtDNA haplogroup may be co-inherited with the OPA1 mutation from the mother or, alternatively, may change when the OPA1 mutation is inherited from the father. As a consequence, a study design just considering the simple association of the mtDNA haplogroup with OPA1 mutations does not take into account for these intricacies. Thus, only further studies of large cohorts of patients, with multiple segregations, may lead to a properly supported conclusion on the possible role played by mtDNA haplogroups in OPA1-related DOA (Caporali et al., 2017).

AIMS

The two most common inherited optic neuropathies due to mitochondrial dysfunction, Leber's Hereditary Optic Neuropathy (LHON) and Dominant Optic Atrophy (DOA), are both characterized by an incomplete penetrance and variable clinical severity, and in LHON there is also a clear-cut prevalence in males. These features remain poorly understood. LHON is genetically determined by missense point mutation in Complex I subunits genes encoded by the mitochondrial genome, whereas DOA is mostly due to heterozygous mutation in the OPA1 gene, encoding a mitochondrial fusion protein. In LHON, 90 % of patients carry one of three common primary mutations (m.11778G>A/MT-ND4, m.3460G>A/MT-ND1, and m.14484T>C/MT-ND6), the remaining 10% harbor a rarer mutation (Achilli et al., 2012). Since the identification of the first pathogenic mutation in mtDNA (Wallace et al., 1988), the role of the entire mitogenome has been investigated in many aspect of medicine, and particularly in LHON, suggesting a complex interaction between the pathogenic mutations, and the adaptive and private variants.

The first aim of this study is to determine the molecular basis of optic neuropathy in four families, negative for the common LHON pathogenic mutations, but still characterized by a clinical phenotype undistinguishable from LHON, which is maternally inherited at low penetrance. We will carry out the sequence of the entire mitochondrial genome in each of the four probands and perform confirmatory functional studies by assessing mitochondrial bioenergetics, taking advantage of the cybrids cell model to isolate the mitogenome contribution to the pathogenesis.

The second aim of this study is a large-scale analysis of the entire mitogenome in a large European cohort of LHON patients previously diagnosed as carrying the m.14484T>C/MT-ND6 mutation, the less frequent of the primary mutations. This analysis is specifically carried out to dissect the modifier role of the mitogenome genetic variation. The association of the three primary LHON mutation with specific mitochondrial backgrounds is largely known (Carelli et al., 2006; Hudson et al., 2007), and this is particularly stringent for the m.14484T>C/MT-ND6 mutation, but only a few families have been analyzed to date, and never at the resolution level of the entire sequence of the mitogenome.

Finally, the last aim is the analysis of the mitochondrial genome variability in DOA patients carrying OPA1 mutations. It is well established that DOA patients present a wide clinical variability between and within families, without a clear genotype-phenotype correlation with the OPA1 mutations. In previous studies, the association with the mitogenome genetic variation was tested, but the results of these study were unclear due to a faulty design (Han et al., 2006; Pierron et al., 2009). Thus, we re-consider the mitogenome genetic variation as possible modifier of patients' clinical outcome, measured as retinal nerve fibers layer (RNFL) thickness by OCT (optic coherence tomography). We will also investigate the possible relevance of coadaptation between the nuclear and mitochondrial genomes, by considering the mother-children segregations, where the mtDNA segregates with the OPA1 mutation, and father-children segregations, where the mtDNA does not segregate with the OPA1 mutation. For each mitogenome, we will define the mtDNA haplogroup, highlighting the private mutations, not belonging to the evolutionarily fixed changes, and predicting the effect by integration of conservation analysis and on-line prediction tools.

RESULTS

PART 1 - *Peculiar combinations of individually non-pathogenic missense mitochondrial DNA variants cause low penetrance Leber's hereditary optic neuropathy*

Pedigrees investigated

We observed three multigenerational pedigrees (Families 1a, b, and c in Figure 4) with multiple affected individuals fitting the clinical diagnosis of LHON and with a clear maternal transmission of the phenotype. Noticeably, all three pedigrees were from the same geographical area of southern Italy (Campania region).

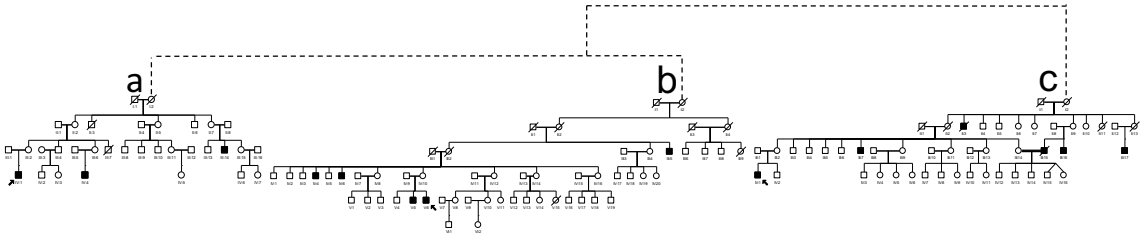

Figure 4. Pedigree of Family 1 with the reconstructed genealogy (indicated by dashed lines) of its three branches (a, b, c). Affected individuals are indicated in black; probands are indicated by arrows.

A fourth smaller pedigree (Family 2; Figure 5) from northern Italy (Emilia-Romagna region) was observed with a single affected individual obeying the LHON clinical diagnosis. All four families tested negative for the three common LHON mutations at positions m.11778G>A/MT-ND4, m.3460G>A/MT-ND1 and m.14484T>C/MT-ND6.

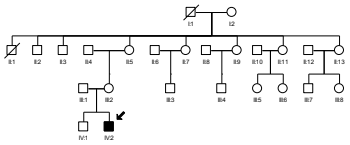

Figure 5. Pedigree of Family 2. Affected individuals are indicated in black; proband is indicated by arrow.

Skeletal muscle investigations reveal normal activity of respiratory chain complexes but increased mitochondrial biogenesis

Histological analysis of skeletal muscle biopsies from the probands of Families 1a, 1b and 2 (Figures 4, 5) showed no overt signs of myopathy with minimal variability in fibers size, and histoenzymatic stain showed normal COX activity, but some increase of subsarcolemmal SDH reactivity (Figure 6A). Ultrastructure (TEM) analysis confirmed the presence of proliferated mitochondria under the sarcolemma and, occasionally, between fibers (Figure 6B). Mitochondrial DNA copy number and CS activity were both increased in skeletal muscles of patients as compared to controls (Figure 6C-D). Similarly, the specific oxidoreductase activities of Complex I, Complex II+III, Complex III and Complex IV were increased (Figure 6E), whereas when normalized on citrate synthase (CS) activity they were comparable to controls (Table 1). Taken together these data indicate the occurrence of an activated compensatory mitochondrial biogenesis, most likely due to a compensatory response caused by a mild mitochondrial defect, as previously reported (Giordano et al., 2014; Iommarini et al., 2012).

	CI	**CII+III**	**CIII**	**CIV**
Controls (mean ± SD)	31.7±20.0	20.3±18.5	197.94±119.8	54.6±23.6
Family 1a IV:1	48.10	29.32	202.63	85.23
Family 2 IV:2	31.93	35.83	281.37	68.25

Table 1. Respiratory chain enzyme activity on skeletal muscle normalized for CS activity

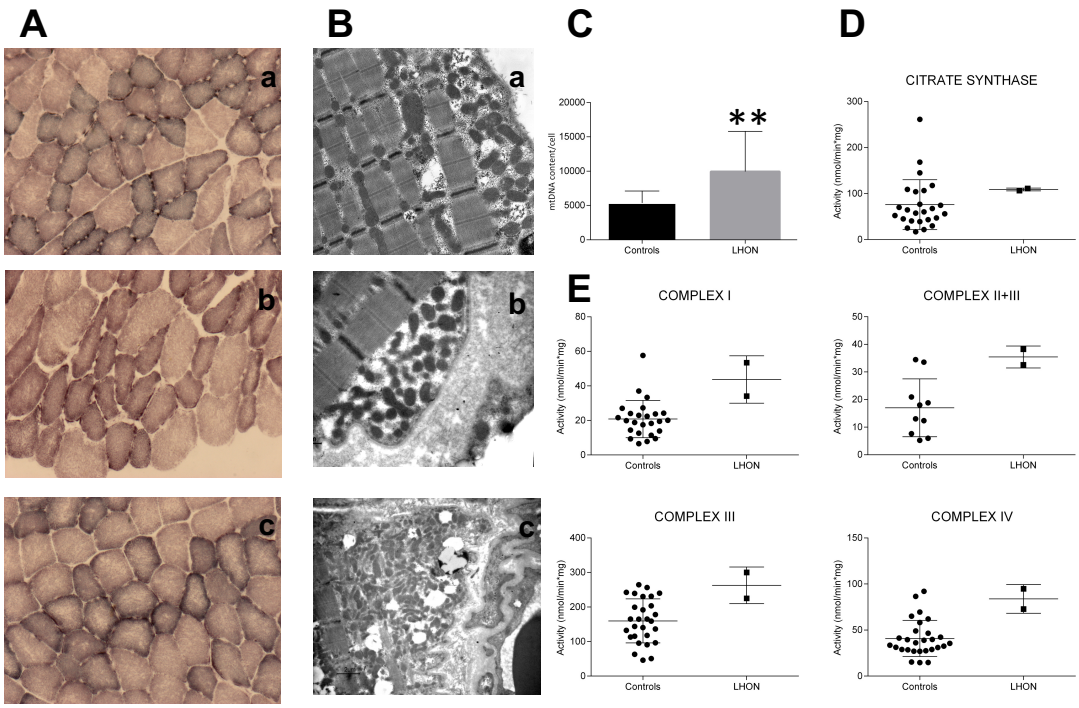

Figure 6. Morphological, molecular and biochemical analysis on skeletal muscle biopsies. A. SDH staining of skeletal muscle biopsies from individuals IV:1 from Family 1a (a), V:6 from Family 1b (b) and IV:2 from Family 2 (c). **B**. Transmission electron microscopy of the same muscle specimens as in A. Both SDH histoenzymatic staining (A) and ultrastructural evaluation (B) demonstrate mitochondrial proliferation as highlighted respectively by subsarcolemmal increase of SDH reaction and corresponding accumulation of mitochondria. **C.** Assessment of mtDNA content per cell, presented as column with mean ± SD (*n*=3; **p<0.001), confirms the activation of mitochondrial biogenesis as shown by the significant increase in LHON samples. **D.** The evaluation of citrate synthase activity, presented as scatter plot with mean ± SD, parallels again the results observed in C, with an increased mean value in the LHON samples. **E.** Evaluations of Complex I, Complex II+III, Complex III, Complex IV activities, presented as scatter plot with mean ± SD, reveal an increase of all activities in LHON samples.

Molecular investigations, protein conservation, frequency, and phylogenetic analyses of the identified variants

Sequencing of the entire mitochondrial genome (mtDNA) from each of the probands independently ascertained for Families 1a, 1b and 1c revealed the same identical sequence, indicating that they descend from the same maternal ancestor, as also suggested by their geographical proximity. They all shared the diagnostic variants for haplogroup K1a and the following private mutations: non-coding m.2281A>G/MT-RNR2 and m.16129G>A/MT-HV1; synonymous m.6137T>C/MT-CO1, m.6329C>T/MT-CO1, m.8994G>A/MT-ATP6, m.11038A>G/MT-ND4 and m.15253A>G/MT-CYB; and missense m.14258G>A/MT-ND6 and m.14582A>G/MT-ND6. The m.14258G>A/MT-ND6 mutation causes the amino acid

substitution p.P139L, and the m.14582A>G/MT-ND6 the amino acid substitution p.V31A. Both missense mutations affect poorly conserved positions of the ND6 subunit of Complex I and are not predicted to be damaging (Figure 7, Table 2). However, the P139 position showed a higher conservation degree in mammals (37%) compared to eukaryotes (22%), being highest in primates (66%). Furthermore, the P139 position in mammals sits two amino acidic residues away from an invariant position (G141) and, in primates is contiguous to another invariant position (D138) within a moderately conserved domain (6 invariant positions out of 21) (Figure 7). The V31 position shows similar features. In eukaryotes and mammals, glycine is prevalent at position 31 with a low conservation (49% and 46%, respectively). In primates, at this position valine becomes prevalent with a higher conservation (77%). Most relevantly, V31 is within a highly conserved domain (10 invariant positions out of 21) in mammals, and is even more conserved in primates (16 invariant positions out of 21) (Figure 7).

Complete mtDNA sequence analysis of the proband from Family 2 showed all the variants diagnostic for haplogroup H5b and the following private mutations: synonymous m.10248T>C/MT-ND3; missense m.9966G>A/MT-CO3, m.10680G>A/MT-ND4L, m.12033A>G/MT-ND4 and m.14258G>A/MT-ND6. Besides the m.14258G>A/MT-ND6 nucleotide change, Family 2 also harbored the m.10680G>A/MT-ND4L and the m.12033A>G/MT-ND4 mutations that induce the amino acid changes p.A71T in ND4L and the p.N425S in ND4 subunits of Complex I, respectively. The p.A71T change affects a highly conserved ND4L position (86% in eukaryotes, 97% in mammals, invariant in primates), within an invariant stretch of 16 amino acids in primates (Figure 7, Table 2). Conversely, the p.N425S affects a highly conserved ND4 position only in primates (41% in eukaryotes, 70% in mammals, 87% in primates), in a moderately conserved domain (9 invariant positions out of 21) (Figure 7, Table 2). Both variants were considered neutral for the protein function by most of the prediction tools employed.

The m.14258G>A/MT-ND6 change, found in both Families 1 and 2, has been previously reported according to Mitomap and HmtDB in 10 different haplogroups, being diagnostic for haplogroups U3a1a1 and H1q3. Conversely, the m.14582A>G/MT-ND6 (Family 1) variant has been previously reported in seven different haplogroups, being diagnostic for haplogroup H4a. In these databases, the sample classified as GenBank: KC878720 is from our Family 1 and it was previously published (Costa et al., 2013) without considering the recurrence of a clinical

phenotype (A. Torroni, personal communication). The coexistence of m.14258G>A/MT-ND6 with the m.14582A>G/MT-ND6 variants is, however, unique to Family 1, when compared to all the other reported cases (Table 3).

Concerning the m.10680G>A/MT-ND4L variant, this has been found in 14 haplogroups and it has been previously reported as the only pathogenic change in three LHON families, arising as independent mutational events in haplogroups B4a1e, M13a1b and D6a1 (Zhang et al., 2012; Zou et al., 2010). In addition, this mutation has also been found in association with the m.14484T>C/MT-ND6 mutation in a further LHON family with a haplogroup B4d1 background (Yang et al., 2009). However, the m.10680G>A/MT-ND4L change has also been recognized in ten different maternal lineages with no pathology reported (Table 4).

Finally, the m.12033A>G/MT-ND4 variant has been reported in five different haplogroups in the general population, without being associated with any pathologic phenotype. Overall, the combination of the three coexisting missense changes m.10680G>A/MT-ND4L, m.12033A>G/MT-ND4 and m.14258G>A/MT-ND6 is a unique feature of Family 2.

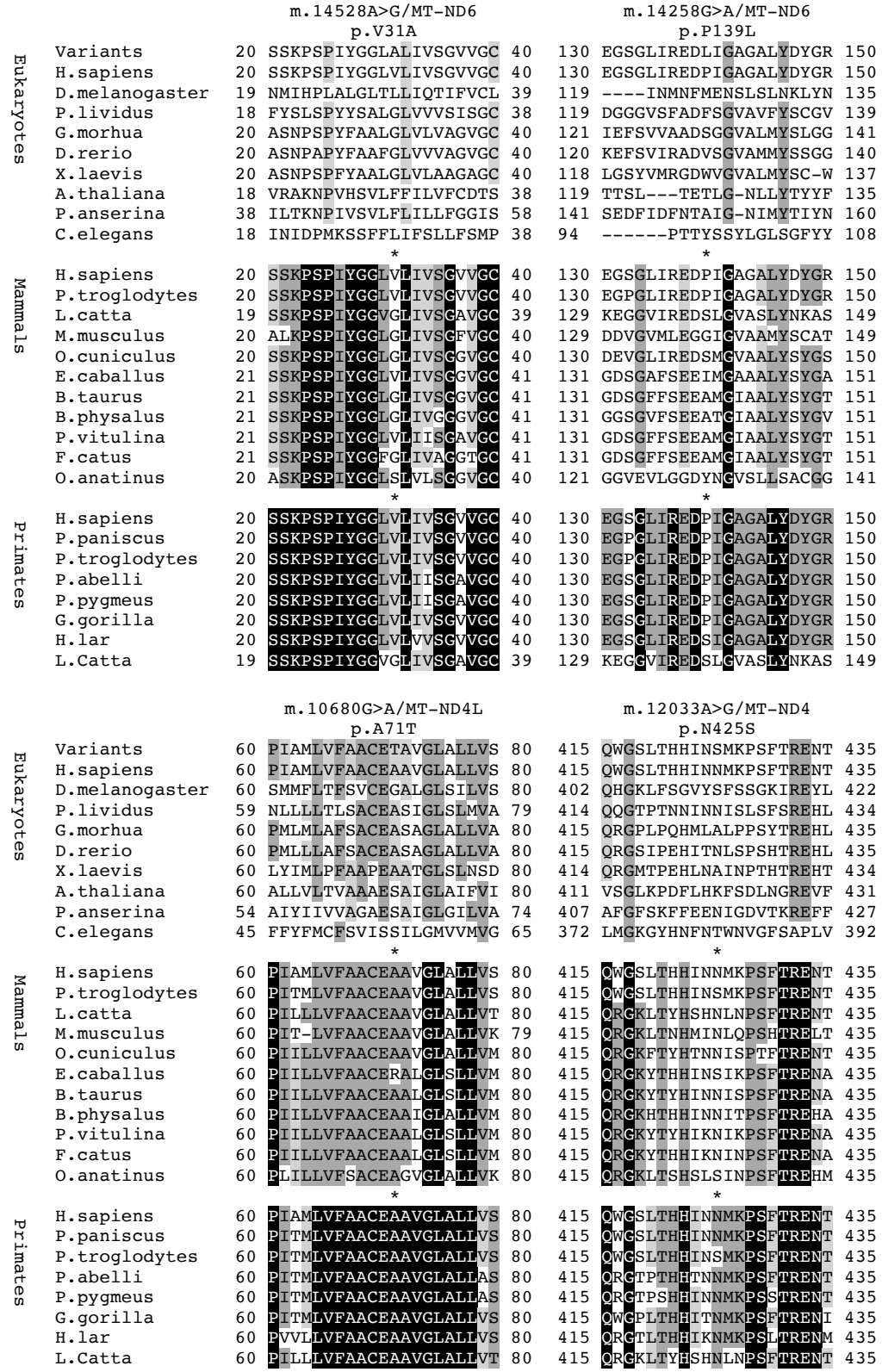

Figure 7. Amino acid conservation analysis. Global alignment of ND1, ND4L and ND6 protein sequences from a wide range of eukaryotes, mammals and primates. The neighborhoods (20 amino acids) of m.14582A>G/MT-ND6, m.14258G>A/MT-ND6, m.10680G>A/MT-ND4L and m.12033A>G/MT-ND4 are shown. Rectangles frame these specific variants. Amino acid residues with a percentage of conservation ranging between 70.0% and 79.9% are highlighted

in light grey, those between 80.0% and 99.9% are highlighted in dark grey and those invariant (100%) are highlighted in black.

Family	1,2	1	2	2
Mutation	m.14258G>A	m.14582 A>G	m.10680 G>A	m.12033 A>G
Gene	*MT-ND6*	*MT-ND6*	*MT-ND4L*	*MT-ND4*
AA_change	p.P139L	p.V31A	p.A71T	p.N425S
PolyPhen2	benign	benign	benign	benign
SIFT	neutral	neutral	neutral	neutral
FatHmm	neutral	neutral	neutral	neutral
PROVEAN	neutral	neutral	deleterious	neutral
MutationAssessor	neutral_impact	neutral_impact	high_impact	low_impact
CADD	deleterious	neutral	neutral	neutral
PANTHER	neutral	neutral	disease	neutral
PhD-SNP	neutral	neutral	disease	neutral
MtoolBox	neutral	neutral	neutral	deleterious
APOGEE_boost	N	N	N	N
GB	16/32,059	179/32,059	14/32,059	5/32,059
Frequency	19/31,735	188/31,735	14/31,735	6/31,735
Conservation				
Eukaryota	F 22%	G 49%	A 86%	N 42%
Vertebrata	F 32%	G 69%	A 97%	N 54%
Mammalia	A 37%	G 46%	A 97%	N 70%
Local	63%	85%	87%	77%
Global	71%	71%	80%	83%
Invariants	-57/+2	-2/+1	-11/+3	-8/+6

Table 2. Prediction tools and conservation analysis

Genbank-HGDP-1000 GP ID	HmtDB Genome Identifier	Haplogroup	Synonymous Private Variants	Non-coding Private Variants	Missense Private Variants	Haplogroup Diagnostic Missense Variants	Phenotype
HG00589	AS_CN_0419	F1a1	8697G>A/*MT-ATP6*	203G>C/*MT-HV2* *1709G>A/MT-RNR2* *16399A>G/MT-HV1*	14258G>A/*MT-ND6* (P139L)	9053G>A/*MT-ATP6* (S176N) 10609 T>C/MT-ND4L (M47T) 12406 G>A/MT-ND5 (V24I) 13759 G>A/MT-ND5 (A475T) 13928 G>C/MT-ND5 (S531T)	Normal
EF657644	EU_XX_0538	H1q3	5237A>G/*MT-ND2*	1009T>C/*MT-RNR1*	9948G>A/*MT-CO3* (V248I)	14258G>A/*MT-ND6* (P139L)	Normal
JX153975	EU_DK_0876	H1q3			3511A>G/*MT-ND1* (T69A)	14258G>A/*MT-ND6* (P139L)	Normal
KF161678	EU_DK_1085	H1q3			3511A>G/*MT-ND1* (T69A)	14258G>A/*MT-ND6* (P139L)	Normal
KF162479	PA_EU_DK_0471	H1q3			3511A>G/*MT-ND1* (T69A)	14258G>A/*MT-ND6* (P139L)	Diabetes
KM252740	XX_XX_5717	H1q3	11266C>T/*MT-ND4*		4084G>A/*MT-ND1* (V260D)	14258G>A/*MT-ND6* (P139L)	Normal
	PA_EU_XX_0019	H1q3				14258G>A/*MT-ND6* (P139L)	Glioblastoma
NA20811	EU_IT_0707	H1q3				14258G>A/*MT-ND6* (P139L)	Normal
	PA_EU_XX_0017	H5b	8251G>A/*MT-CO2*	16309A>G/*MT-HV1*	9966G>A/*MT-CO3* (V254I) 12033A>G/MT-ND4 (N425S) 14258G>A/MT-ND6 (P139L)		Glioblastoma
KP340158	n.a.	HV2a2	6563C>T/*MT-CO1*		14258G>A/*MT-ND6* (P139L)		n.a.
KP340159	n.a.	HV2a2	6563C>T/ *MT-CO1*		14258G>A/*MT-ND6* (P139L)		n.a.
KC878720	EU_IT_0585	K1a	6137T>C/ *MT-CO1* *6329C>T/ MT-CO1* *8994G>A/MT-ATP6* *11038A>G/MT-ND4* *15253A>G/MT-CYB*		14258G>A/*MT-ND6* (P139L) 14582A>G/MT-ND6 (V31A)	9055G>A/*MT-ATP6* (A177T) 14798T>C/MT-CYB (F18L)	Normal

Genbank-HGDP-1000 GP ID	HmtDB Genome Identifier	Haplogroup	Synonymous Private Variants	Non-coding Private Variants	Missense Private Variants	Haplogroup Diagnostic Missense Variants	Phenotype
KC533510	PA_AF_SF_0059	L0d2a1	10771A>G/*MT-ND4*		5460G>A/*MT-ND2* (A331T) 13508C>T/MT-ND5 (S391F) 14258G>A/MT-ND6 (P139L)	4025C>T/*MT-ND1* (T240M) 4225A>G/MT-ND1 (M307V) 4232T>C/MT-ND1 (I309T) 5442T>C/MT-ND2 (F325L)	Pediatric patients
NA18868	AF_NG_0078	L2a1c1a1		2242T>C/*MT-RNR2*	8584G>A/*MT-ATP6* (A20T) 14258G>A/MT-ND6 (P139L)	3308T>C/*MT-ND1* (M1T) 3338T>C/MT-ND1 (V11A) 6663A>G/MT-CO1 (I254V) 8584G>A/MT-ATP6 (A20T)	Normal
KF451170/ HGDP00647	XX_XX_6141	U1b1	9374A>G/*MT-CO3*	444A>G/*MT-DLOOP* 2352T>C/*MT-RNR2*	14258G>A/*MT-ND6* (P139L)	15110G>A/*MT-CYB* (A122T)	Normal
JN203207	EU_PL_0054	U3a1a1			3808A>G/*MT-ND1* (T168A)	10506A>G/*MT-ND4L* (T13A) 13934C>T/MT-ND5 (T533M) 14258G>A/MT-ND6 (P139L)	Normal
JQ704950	EU_IE_0218	U3a1a1	9656T>C/*MT-CO3* *14049C>T/MT-ND5*			10506A>G/*MT-ND4L* (T13A) 13934C>T/MT-ND5 (T533M) 14258G>A/MT-ND6 (P139L)	Normal
JX153017	EU_IT_0472	U3a1a1	13785C>T/*MT-ND5*			10506A>G/*MT-ND4L* (T13A) 13934C>T/MT-ND5 (T533M) 14258G>A/MT-ND6 (P139L)	Normal
HM156692	PA_XX_XX_0032	W3a1b	8251G>A/*MT-CO2*	146T>C/*MT-HV2*	3350T>C/*MT-ND1* (I15T) 14258G>A/MT-ND6 (P139L)	3505A>G/*MT-ND1* (T67A) 5046G>A/MT-ND2 (V193I) 15884G>C/MT-CYB (A380P)	Chronic Periodontitis
HM156696	PA_XX_XX_0028	W3a1b	8251G>A/*MT-CO2* *8952T>C/MT-CO2* *8994G>A/MT-CO2*	1243T>C/*MT-RNR1*	3350T>C/*MT-ND1* (I15T) 5460G>A/MT-ND2 (A331T) 14258G>A/MT-ND6 (P139L)	3505A>G/*MT-ND1* (T67A) 5046G>A/MT-ND2 (V193I) 15884G>C/MT-CYB (A380P)	Chronic Periodontitis

Table 3. Mitogenome sequences carrying the m.14258G>A/*MT-ND6*, p.P139L, in common databases

Genbank-HGDP-1000 GP ID	HmtDB Genome Identifier	Haplogroup	Synonymous Private Variants	Non-coding Private Variants	Missense Private Variants	Haplogroup Diagnostic Missense Variants	Phenotype
JN866824	PA_XX_XX_0343	B4a1e	3540T>C/*MT-ND1*	2352T>C/*MT-RNR1*	10680G>A/*MT-ND4L* (A71T)	3548T>C/*MT-ND1* (I81T)	LHON [32]
FJ986465	PA_XX_XX_0331	B4d1	13449C>T/*MT-ND5* *14239C>T/MT-ND6*	185G>A/*MT-HV2* *189A>G/MT-HV2* *489T>C/MT-HV2*	10680G>A/*MT-ND4L* (A71T) 14484T>C/MT-ND6 (M64V)	13942A>G/*MT-ND5* (T536A) 15038A>G/MT-CYB (I98V)	LHON [26]
KF540683	AS_TW_0178	D4a8			10680G>A/*MT-ND4L* (A71T)	5178C>A/*MT-ND2* (L237M) 8414C>T/MT-ATP8 (L17F) 10400C>T/MT-ND3 (T114A) 14979T>C/MT-CYB (I78T)	Normal
JN866825	PA_XX_XX_0344	D6a1	8251G>A/*MT-CO2* *11809T>C/MT-ND4* *15688C>T/MT-CYB*	16192C>T/*MT-HV1*	3745G>A/*MT-ND1* (A147T) 10680G>A/MT-ND4L (A71T) 13327A>G/MT-ND5 (T331A)	5178C>A/*MT-ND2* (L237M) 10400C>T/MT-ND3 (T114A)	LHON [32]
JX153117	EU_GR_0092	H13a2a	9824T>C/*MT-CO3*		10680G>A/*MT-ND4L* (A71T)		Normal
JQ703337	EU_NL_0018	H1b	13389C>T/*MT-ND5*		10680G>A/*MT-ND4L* (A71T)		Normal
JQ702415	XX_XX_1893	H1	4742T>C/*MT-ND2* 8865G>R/*MT-ATP6*	16075T>C/*MT-HV1* 16189T>C/*MT-HV1* 16224T>C/*MT-HV1* 16319G>A/*MT-HV1* 16324T>C/*MT-HV1*	10680G>A/*MT-ND4L* (A71T)		Normal
JQ704194	XX_XX_2693	H1t	3447A>G/*MT-ND1* *6167T>C/MT-CO1* *6293T>C/MT-CO1*	2141T>C/*MT-RNR2*	9911C>A/*MT-CO3* (F235L) 10680G>A/MT-ND4L (A71T)		Normal
KF450878/ HGDP00119	XX_XX_6433	HV	3351C>T/*MT-ND1* *3744A>G/MT-ND1* *4829A>G/MT-ND2* *11566A>G/MT-ND4* *12630G>A/MT-ND5*	16158A>T/*MT-HV1*	10680G>A/*MT-ND4L* (A71T)		Normal

Genbank-HGDP-1000 GP ID	HmtDB Genome Identifier	Haplogroup	Synonymous Private Variants	Non-coding Private Variants	Missense Private Variants	Haplogroup Diagnostic Missense Variants	Phenotype
KJ445748/ HGDP00621	XX_XX_4630	L0a1b1a		593T>C/*MT-TF*	3311C>T/*MT-ND1* (P2L) 10680G>A/MT-ND4L (A71T)	5442T>C/*MT-ND2* (F325L) 5460G>A/MT-ND2 (A331T) 5911C>T/MT-CO1 (A3V) 8566A>G/MT-ATP6 (I14V) 15431G>A/MT-CYB (A229T)	Normal
KJ669103	AF_NA_0197	L0k1a2a	3876A>G/*MT-ND1*		10680G>A/*MT-ND4L* (A71T)	5442T>C/*MT-ND2* (F325L) 7257A>G/MT-CO1 (I452V) 9136A>G/MT-ATP6 (I204V) 10920C>T/MT-ND4 (P54L) 13819T>C/MT-ND5 (F495L) 13928G>C/MT-ND5 (S531T)	Normal
GU377087	PA_XX_XX_0306	M13a1b	9053G>A/*MT-ATP6* *10646G>A/MT-ND4L*	980T>C/*MT-RNR1* *16239C>T/MT-HV1* *16391G>A/MT-HV1*	10680G>A/*MT-ND4L* (A71T)	3644T>C/*MT-ND1* (A113A) 6253T>C/MT-CO1 (M117T) 9053G>A/MT-ATP6 (S176N) 10400C>T/MT-ND3 (T114A) 13135G>A/MT-ND5 (A267T)	LHON [31]
JF742198	AS_NP_0020	M33b2	8802T>C/*MT-ATP6* *15326G>A/MT-CYB* *15514T>C/MT-CYB* *15868C>T/MT-CYB*	1438G>A/*MT-RNR1* *3202T>C/MT-RNR2*	3469C>T/*MT-ND1* (L55F) 6261G>A/MT-CO1 (A120T) 10680G>A/MT-ND4L (A71T)	10400C>T/*MT-ND3* (T114A)	Normal
KF162184	EU_DK_1441	R9b1a3			10680G>A/*MT-ND4L* (A71T)	3316G>A/*MT-ND1* (A4T) 13928G>C/MT-ND5 (S531T)	Normal

Table 4. Mitogenome sequences carrying the m.10680G>A/*MT-ND4L*, p.A71T, in common databases

Cybrid studies

To assess the pathogenic potential of the two peculiar combinations of missense variants found in Family 1 (m.14258G>A/MT-ND6 and m.14582A>G/MT-ND6) and Family 2 (m.10680G>A/MT-ND4L, m.12033A>G/MT-ND4 and m.14258G>A/MT-ND6) we generated cybrids using enucleated fibroblasts derived from the probands of Families 1a, 1b and 2, as cytoplast donors. Different cell clones were obtained harboring each the two combinations of homoplasmic variants and used for subsequent investigations. In Figure 8, the data obtained from each LHON cell line were pooled together and compared to control cybrids, matched for haplogroup, having first verified that they had very similar functional profiles. To challenge the mitochondrial oxidative phosphorylation system, we grew cybrids in a glucose-free medium containing galactose; under these conditions, the rate of glycolysis is markedly reduced and cells are forced to rely on oxidative phosphorylation for ATP production (Robinson et al., 1992). No significant differences were found in LHON cell viability compared to controls (Figure 8A). Assessment of Complex I redox activity displayed a non-significant reduction in LHON cells (Figure 8B), indicating that the combinations of variants did not affect the overall Complex I function. However, the basal and the FCCP-stimulated oxygen consumption rate (OCR) of LHON cells were significantly reduced (Figure 8C). LHON cells also displayed a metabolic shift toward glycolysis, since they showed a higher ECAR and a lower OCR when compared to controls (Figure 8D). Consistently, the CS normalized ATP synthesis, driven by Complex I substrates (malate and glutamate), was significantly reduced in LHON cells, whereas ATP synthesis was normal when driven by Complex II substrates (succinate) (Figure 8E).

Although LHON mutations have been reported to exert their pathogenic role by increasing oxidative stress (Carelli et al., 2004; Yu-Wai-Man et al., 2011), we failed to reveal any difference between mutant and control cells in terms of superoxide anion and hydrogen peroxide production (Figure 9). Overall, these data indicate that combinations of polymorphic Complex I variants induce a mild bioenergetic defect.

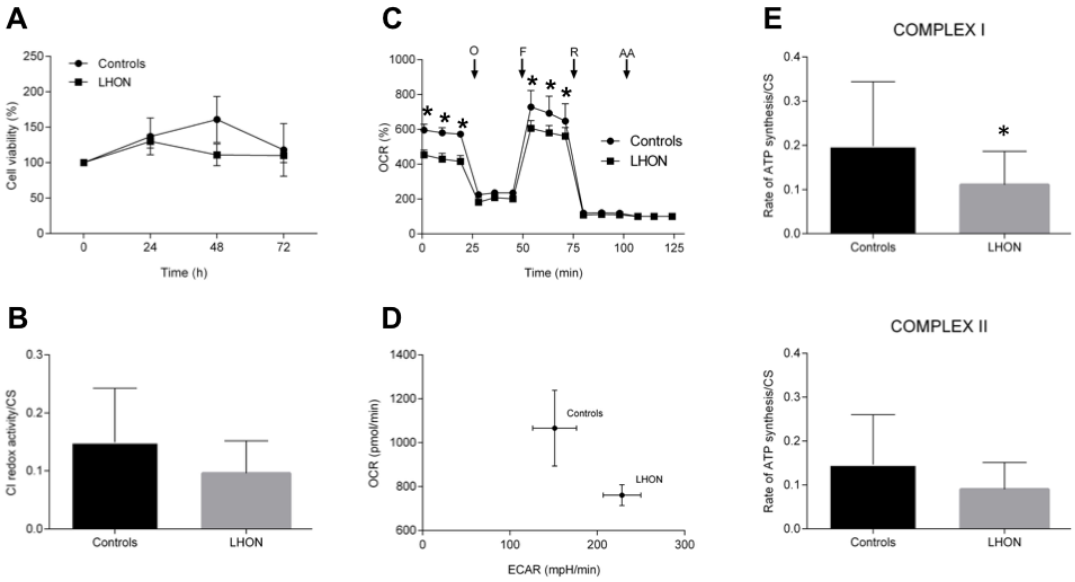

Figure 8. Biochemical characterization of cybrids clones. A. Cell viability after different time of incubation in galactose medium. Data are expressed as percentage of T0 (*n*=12; mean ± SEM). **B.** Rotenone sensitive redox activity of respiratory complex I normalized for CS activity (*n*=9; mean ± SD). **C.** OCR traces as pmol O_2/min, after the injection of 1µM oligomycin (O), 0.2µM FCCP (F), 1µM rotenone (R) and 1µM antimycin A (AA) (mean ± SD). Asterisks indicate statistical significance (*n*=3; * p<0.05). **D.** XFe Metabolic Phenogram. Basal OCR (pmol/min) and ECAR (mpH/min) rates were plotted in controls vs LHON cybrids, showing a metabolic shift in LHON cybrids towards glycolysis. **E.** ATP synthesis rates normalized for CS activity driven by complex I substrates (malate/glutamate) and complex II substrate succinate (mean ± SD). Asterisks indicate statistical significance (*n*=16; * p<0.05).

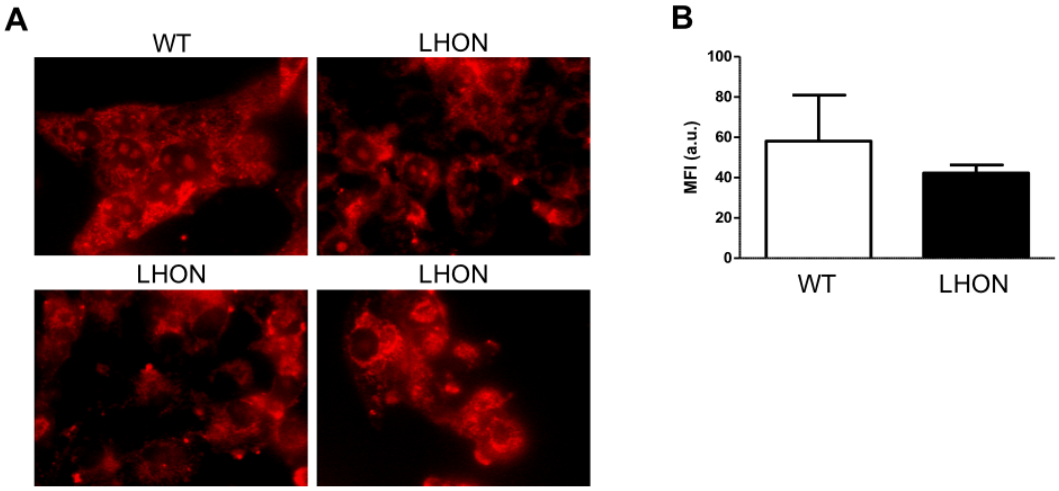

Figure 9. Production of superoxide anion and hydrogen peroxide in cybrid cell lines. A. Mitochondrial superoxide anion production determined by epifluorescence microscopy using MitoSOX™ fluorescent dye. Cells were visualized with a digital imaging system, using an inverted epifluorescence microscope (magnification x63/1.4 oil objective) at 580nm. Images are representative of 3 different experiments. **B**. Hydrogen peroxide levels were measured using H_2DCFDA by flow cytometry, as described in materials and methods. Data are mean±SD (*n*=3).

Modeling of the identified variants on the ovine Complex I structure

In order to define how such peculiar combinations of variants lead to a mild Complex I defect, we took advantage of the recently released structure of mammalian enzyme at 3.9 Å resolution, solved by cryo-electron microscopy (Fiedorczuk et al., 2016). We analyzed the position of amino acids affected by the polymorphic variants, namely m.14258G>A/MT-ND6, m.14582A>G/MT-ND6, m.10680G>A/MT-ND4L and m.12033A>G/MT-ND4 (Figure 10), but also the variants in three LHON Chinese families, with m.10680G>A/MT-ND4L found in combination with m.14484T>C/MT-ND6, m.3745G>A/MT-ND1, m.3548T>C/MT-ND1 m.3644T>C/MT-ND1, respectively (Yang et al., 2009; Zhang et al., 2012; Zou et al., 2010), and the adaptive variants (m.3745G>A/MT-ND1, m.4216T>C/MT-ND1, m.3394T>C/MT-ND1) for high altitude in Tibet (Ji et al., 2012; Kang et al., 2013) (Figure 11).

The variant m.14258A>G/*MT-ND6* shared by Families 1 and 2 induces the P139L amino acid change in humans, which corresponds to A140 in ovine Complex I. Such amino acid is located in the transversal α-helix 5 of ND6. The variant m.14582A>G/*MT-ND6* found in Family 1 generates the amino acid substitution p.V31A in humans and corresponds to G32 in the ovine complex, affecting the transmembrane α-helix 2 (TM2) of ND6. The m.10680G>A/*MT-ND4L* variant harbored by Family 2 affects the amino acid A71 of ND4L both in human and ovine Complex I. This amino acid lies in TM3 of the ND4L subunit. Lastly, the m.12033A>G/*MT-ND4* induces the amino acid substitution p.N425S in the loop between TM13 and TM14 of ND4, which faces the mitochondrial matrix. Interestingly, with the only exception of the latter amino acid change, all the other variants affect positions around the putative E-channel of Complex I (Castellana et al., 2015), suggesting that the mild functional defect found in these patients may arise from an altered proton pumping caused by the two peculiar mtDNA combinations of variants (Figure 10).

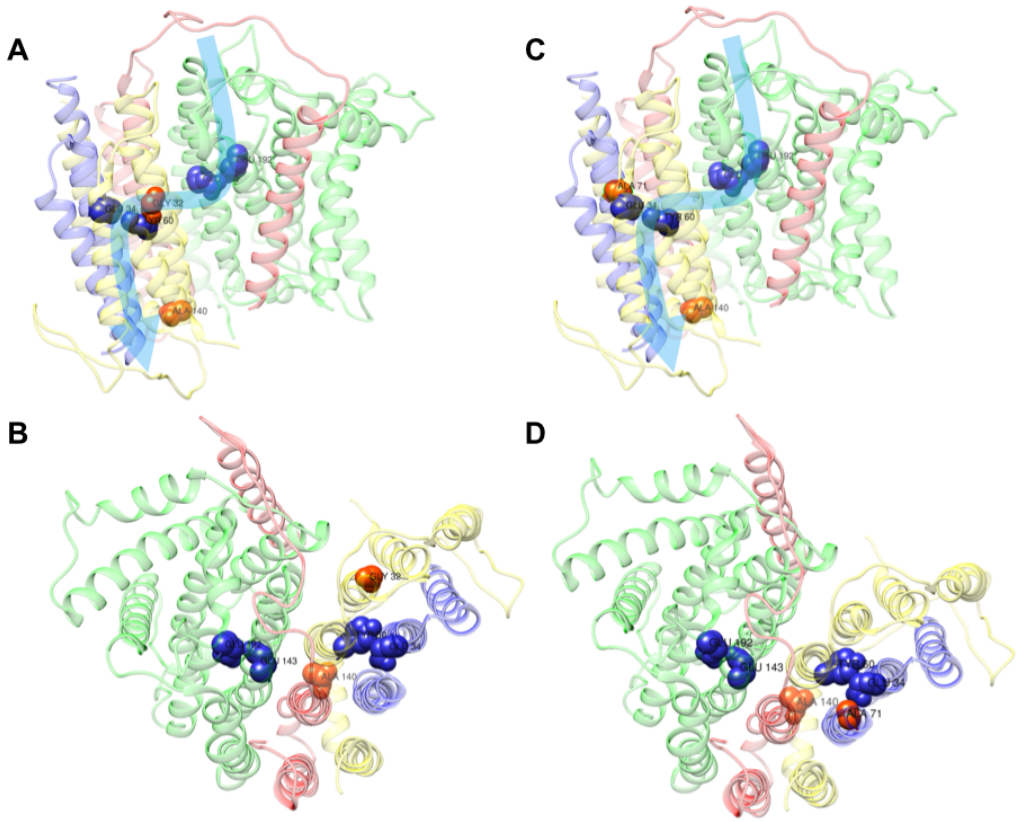

Figure 10. Complex I model. Localization of polymorphic variants on the structure of the ovine complex I, (Fiedorczuk et al., 2016) using the UCSF Chimera software. The ovine amino acids Ala140 (corresponding to human p.P139L, m.14258G>A/MT-ND6), Gly32 (corresponding to human p.V31A, m.14582A>G/MT-ND6) and Ala71 (corresponding to human p.A71T, m.10680G>A/MT-ND4L) are shown as red-labelled spheres; whereas residues Glu143/ND1, Glu192/ND1, Glu34/ND4L, Tyr60/ND6, the key residues for the E-channel (near Q site), are shown as blue-labelled spheres. The structures of ND1, ND4L, ND6 and ND3 subunits are shown as ribbons, in green, blue, yellow and red, respectively. The combination of variants in Family 1 (**A-B**) and Family 2 (**C-D**) are displayed as front (**A-C**) and upper (**B-D**) views. Light blue arrows indicate the proposed proton translocation pathway (Fiedorczuk et al., 2016).

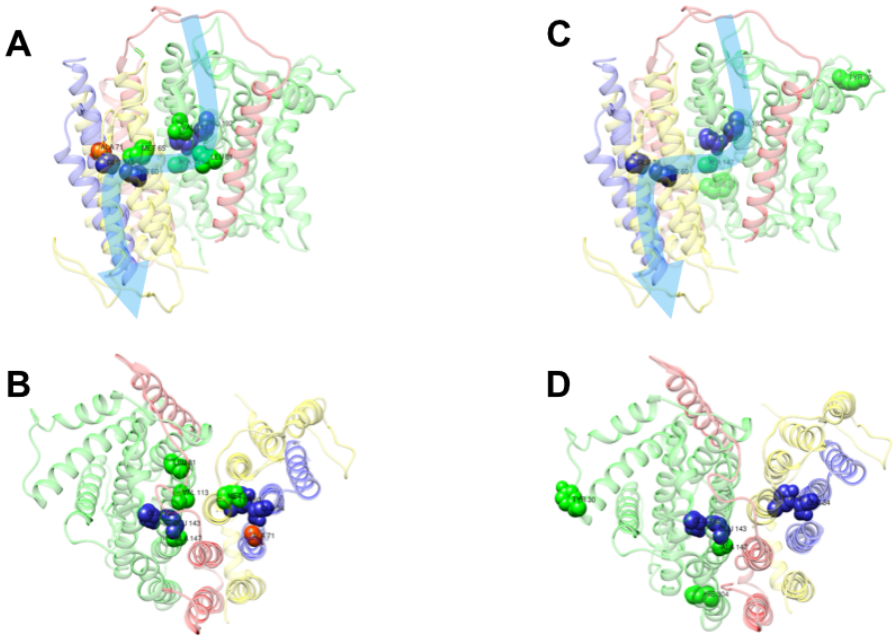

Figure 11. Combinations of mtDNA variants from three LHON Chinese families and single mtDNA variants, adaptive for high altitude in Tibet, on the ovine Complex I structure. Positioning of the combinations of variants in three LHON Chinese families (**A-B**) (Yang et al., 2009; Zhang et al., 2012; Zou et al., 2010) and the adaptive variants for high altitude in Tibet (**C-D**) (Ji et al., 2012; Kang et al., 2013) on crystallographic structure of ovine Complex I (Fiedorczuk et al., 2016), using the UCSF Chimera software. In panels A and B, the ovine amino acids Ala71 (corresponding to human p.A71T, m.10680G>A/MT-ND4L) are shown as red labelled spheres, and this variant is associated in each families with Met65 (corresponding to human p.M64V, m.14484T>C /MT-ND6), Ala147 (corresponding to human p.A147T, m.3745G>A/MT-ND1), Leu81 (corresponding to human p.I81T, m.3548T>C/MT-ND1) or Val113 (corresponding to human p.V113A, m.3644T>C/MT-ND1), shown as green labelled spheres. In panels **C** and **D**, the ovine amino acids Ala147 (corresponding to p.A147T, m.3745G>A/MT-ND1), His304 (corresponding to human p.Y139H, m.4216T>C/MT-ND1) and Tyr30 (corresponding to human p.Y30H, m.3394T>C/MT-ND1) are shown as green labelled spheres. In all panels, residues Glu143/ND1, Glu192/ND1, Glu34/ND4L, Tyr60/ND6, the key residues for the E-channel (near Q-site), are shown as blue labelled spheres (Ji et al., 2012). The backbones of ND1, ND4L, ND6 and ND3 are shown as ribbons, in green, blue, yellow and red, respectively. The variants combination in LHON Chinese families (**A**-**B**) and adaptive variants for high altitude in Tibet (**C**-**D**) are displayed as front (**A**-**C**) and upper (**B**-**D**) views. Light blue arrows indicate the proposed proton translocation pathway.

PART 2 - *Mitochondrial DNA variability in Leber's hereditary optic neuropathy*

Mitochondrial genome sequencing and haplogroup affiliation

We completely sequenced mtDNA in 147 probands, affected by LHON carrying the *m.14484T>C/MT-ND6* primary mutation, in apparently unrelated families from Europe (52 from Italy, 43 from Germany, 27 from France, 19 from UK, 3 from Spain and 3 from US, but with European ancestry).

Out of the entire cohort 28 probands were related and in table 5 the results of 119 unrelated mitochondrial genomes are shown: for each proband it is indicated the haplogroup affiliation, the private mutations not diagnostic for the haplogroup and the corresponding amino acid changes.

Haplotype	Haplogroup	Private variants non-coding	Private variants synonymous	Private variants missense
H	H	73 A>G	14968 T>C	
H	H	16093 T>C 16258 A>C 16311 T>C		9055 G>A 10680 G>A
H1a1	H		6959 C>G	
H1bm	H	1790 A>G 16171 A>T	9881 T>C 10972 A>G	14582 A>G
H1e	H		15518 C>T	
H1e1a	H	362 insAAAG 452 T>C 16093 T>C		14564 A>G
H3	H		10121 A>G 15346 G>A 15833 C>T	4639 T>C
H3c2b1	H			6261 G>A 7444 G>A
H3h	H	93 A>G 146 T>C		
H4a1a	H	16362 T>C	13497 A>G	
H4a1a1a	H	195 T>C	15172 G>A	
H5	H	16368 T>C	8251 G>A 9530 T>C	3368 T>C 7080 T>C
H5	H	73 A>G 709 G>A 5628 T>C	8251 G>A 9530 T>C	
H5b4	H	16145 G>A	6620 T>C 12501 G>A	
H6a1a	H		15784 T>C	
H7c1	H	16093 T>C	11533 C>T	
H14b	H	16162 delA	4086 C>T 5978 A>G	
H26a1	H	152 T>C 5895 insCCC	8840 A>G	
H27	H			3368 T>C
H56	H		10235 T>C	
H94	H	16093 T>C	9374 A>G 13227 C>T	
HV	H	152 T>C 16311 T>C		
V1a1	H	151 C>T 16104 C>A	4065 A>G	

V10b1	H			
J1b1a1	J	146 T>C		
J1b1a1	J	146 T>C		13135 G>A
J1b1a1	J	789 T>C 10427 G>A		
J1b1a1	J	789 T>C 10427 G>A	13743 T>C	
J1b1a1	J	146 T>C 657 G>A 789 T>C 10427 G>A	13743 T>C	
J1b1a1	J	146 T>C 16311 T>C		
J1b1a1	J	7543 A>G 16093 T>C		14861 G>A
J1b1a1b	J	15930 G>A 16256 C>T 16260 C>T	15262 T>C	3535 T>A
J1b1a1d	J	1462 G>A		4659 G>A
J1b1a1d	J			8557 G>C
J1b1a1d	J			
J1c	J	1284 T>C 5788 T>C 16114 C>T 16215 A>G 16265 A>T	4017 C>T 9425 A>G 15394 T>C	7859 G>A 13135 G>A
J1c1d	J	10031 T>C	8383 T>C	9053 G>A
J1c1d	J	183 A>G 10031 T>C	8383 T>C	9053 G>A
J1c1d	J			
J1c2	J		3375 C>T	
J1c2b	J			
J1c2c1	J			
J1c2e	J	194 C>T		
J1c2j	J			14279 G>A
J1c2j	J			4184 T>A 14279 G>A
J1c3	J	182 C>T	3372 T>C	
J1c3a	J			
J1c3b	J		10915 T>C	10609T>C
J1c3b1a	J			8989 G>A
J1c3e2	J	16325 T>C	5147 G>A	6712 A>T 9957 T>C
J1c3e2	J	16291 C>T		
J1c3f	J	709 G>A 16093 T>C		10845 C>T
J1c3f	J	709 G>A 2181 A>G	8458 A>G	10845 C>T
J1c3g	J	188 A>G 195 T>C 16243 T>C	14364 G>A	
J1c3j	J			
J1c4	J		11260 T>C	
J1c4	J		7271 A>G 13641 T>C	
J1c4	J	16189 T>C		
J1c5	J	489 T>C 16174 C>T	4209 T>C 12810 A>G	
J1c6	J	182 C>T		
J1c9	J	189 A>G 254 T>C 16343 A>G	6602 C>T 10786 T>C	12361 A>G
J1c10	J	195 T>C 198 C>T	3358 A>G 12501 G>A 12648 A>G	4561 T>C 13621 C>T

J1d1a1	J	16093 T>C 16203 A>G	15430 C>T	8812 A>G
J2a1a1	J	198 C>T 3027 T>C		3316 G>A 13712 C>T
J2a1a1a	J	16400 C>T 16497 A>G	3447 A>G 5258 A>G	9137 T>C
J2a1a1a3	J	16189 T>C		7270 T>C 8843 T>C
J2a2b1	J	185 G>A 8292 G>A 16311 T>C		
J2a2b1	J	185 G>A 8292 G>A	15409 C>T	
J2a2c	J		14569 G>A	7269 G>A
J2a2c	J			7269 G>A
J2b1	J	16265 A>T	6959 C>G	4824 A>G 8953 A>G 15315 C>T
J2b1a2	J	246 T>C	3348 A>G	
J2b1a3	J	709 G>A	13029 C>T	
J2b1a3	J	709 G>A		8743 G>A
J2b1a6	J		8557 A>C	9025 G>A
J2b1a6	J		13194 G>A	
J2b1a6	J			
J2b1b1	J	146 T>C	10124 T>C	8711 A>G
T1a1b	T			
T1a2	T	152 T>C 204 T>C 633 A>G 16185 C>T	8994 G>A 9377 A>G 10876 A>G 11239 A>G	8516 T>C 10398 A>G
T1a2	T	204 T>C 633 A>G	8640 C>T 8994 G>A 9377 A>G 10876 A>G 11239 A>G	10398 A>G
T1a2	T	204 T>C 633 A>G	8994 G>A 9377 A>G 10876 A>G 11239 A>G	10398 A>G
T1a2	T	633 A>G	8994 G>A 9377 A>G 10876 A>G 11239 A>G	10398 A>G
T2	T	490 A>G	5378 A>G 12681 T>C 12819 A>G 13194 G>A	3460 G>A 7440 T>G
T2	T	490 A>G	5378 A>G 12681 T>C 12819 A>G 13194 G>A	7440 T>G 10680 G>A
T2	T	490 A>G	5378 A>G 12681 T>C 12819 A>G 13194 G>A	7440 T>G
T2b	T	185 G>A 16178 T>C	3828 A>G	
T2b	T		3828 A>G	
T2b3b	T			
T2b25	T	16311 T>C		9067 A>G 10237 T>C

T2c1d1	T	152 T>C 182 C>T 374 A>G 5565 A>T	6644 C>T	13708 G>A
T2c1d1	T	152 T>C 374 A>G 5565 A>T 16092 T>C	6644 C>T	13708 G>A
T2c1d1	T	152 T>C 374 A>G 5565 A>T	3645 T>C 6644 C>T	13708 G>A
T2f1a	T	8270 ins9		
U1a1a1	U	513insCA 16168 C>T 16183 A>C 16215 A>G 16325 T>C	5090 T>C 6050 T>C	7257 A>G 10680 G>A 11969 G>A
U3b	U	152 T>C 2833 A>G 15940 delT	7660 T>C 13474 T>C	3523 A>G 15221 G>A
U3b	U	152 T>C 15940 delT 16172 T>C 16173 C>T 16290 C>T 16390 G>A 16497 A>G	3429 C>T 15784 T>C	3434 A>G 13105 A>G
U5a1a1	U	152 T>C 16231 T>C		11778 G>A
U5a1a2b	U	16082 C>T	4023 T>C 10535 T>C	4160 T>C
U5a1c1	U	15928 G>A		
U5b1b1	U	16093 T>C		
K1a1b1	K	5583 C>T		
K1a1b1	K	16051 A>G	8053 A>G	
K1a8	K	152 T>C 3084 A>G	9422 A>G	
B2	other		9254 A>G 9548 G>A	7119 G>A
I2a	other		9758 T>C	4216 T>C 5460 G>A 10320 G>A
I2d	other	152 T>C 16362 T>C		
L0F2b	other	4456 C>T		
L1b1a	other	200 A>G 16213 G>A	8937 T>C 11452 T>C	4123 A>G 4695 T>C
L1b1a1	other		3693 G>A	13105 A>G
L2a1a1	other	1901 C>T 5774 T>A	4161 C>T	14258 G>A
L2a1l2	other	198 C>T	7492 C>T	4136 A>G
L3e1a	other			
L3e5a	other			5460 G>A
L3e5a	other	16311 T>C 16362 T>C		9327 A>G
L3e5a	other	3290 T>C		5460 G>A 8888 T>C
M1a5	other			
N1a1a1a3	other	143 G>A 228 G>A 2955 T>C 12235 T>C	4772 T>C	8448 T>C 9103 T>C 15458 T>C

X2d1	other	16161 TA>T		8400 T>C 10680 G>A

Table 5. Mitochondrial genome of LHON probands carrying m.14484T>C/MT-ND6 mutation with haplogroup affiliation (according to www.phylotree.org - build 17) and private changes. Missense variant in coloured according scoring criteria described in the "materials and methods" as in table 6.

In the LHON cohort of probands carrying the m.14484T>C/MT-ND6 mutation we found a statistically different frequency of mitochondrial haplogroups as compared to the European population (χ^2test, p < 0,0001) (Figure 12). To understand which haplogroup generated this difference, all categories were compared to each other (*n*=15), indicating a major role for the haplogroup J and, less stringently, for haplogroup T (χ^2test with Bonferroni correction), both over-represented and stemming from the same root. On the contrary, haplogroup H was consistently under-represented and to a lesser extent haplogroups K and U, these latter two sitting on the same root.

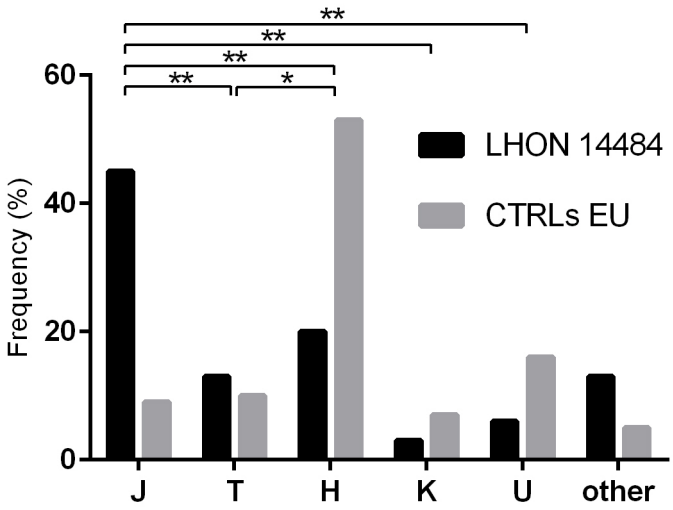

Figure 12. Frequency of European haplogroups in LHON cohort with m.14484T>C/MT-ND6 mutation and control population (*n* =10379). **p<0.001, *p<0.05.

Taking advance of having the entire mtDNA genome sequence available, and in consideration of the strong association of haplogroup J with the m.14484T>C/MT-ND6 mutation, we dissected further haplogroup J into the sub-clades. Of relevance, previous studies reported the association with specific clades of haplogroup J, i.e. J1c (Carelli et al., 2006; Hudson et al., 2007). Our current results failed to highlight any significant difference amongst any of the haplogroup J sub-clades, in particular between J1 vs J2, or their sub-clades, as compared with

the European population (χ^2test, J sub-ckades p=0.4046, J1 sub-ckades p=0.1285, J2 sub-ckades p=1.000) (Figure 13).

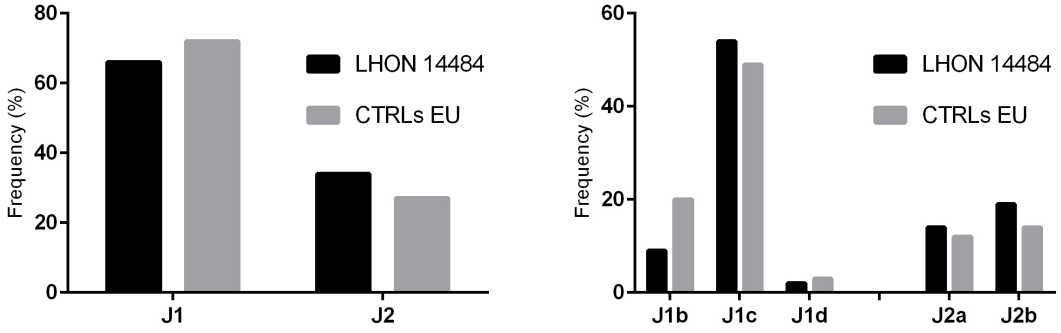

Figure 13. Frequency of J1 and J2 clades, and their subclades in 55 LHON with m.14484T>C/MT-ND6 mutation on haplogroup J background and control population (*n* =156).

Evaluation of private missense variants

We analysed all missense changes, which were not diagnostic for the haplogroups, to detect other private variants, with some possible pathogenic significance. For each variant, the amino acid residue conservation and the *in-silico* prediction values of pathogenicity were considered (Table 6).

To this end, the *on-line* tools PolyPhen2, SIFT, PANTHER and PhD-SNP have been used and conservation analysis was carried out, as detailed in the methods. According to the scoring criteria described in the "materials and methods", changes with a score of 0,66-1 points were considered pathogenic (red), with 0,5-0,65 points were considered synergistic (orange) and with 0-0,49 points neutral (black).

Nucleotide change	Gene	Amino-Acid change	Predictor tools				Conservation (%)			Invariants	
			PolyPhen2	SIFT	PANTHER	PhD-SNP	Mammals	Local	Global	-	+
m.3316G>A	MT-ND1	p.A4T	benign	neutral	NA	neutral	67	57	78	3	12
m.3368T>C	MT-ND1	p.M21T	benign	neutral	NA	neutral	92	81	78	1	1
m.3434A>G	MT-ND1	p.Y43C	benign	neutral	neutral	disease	82	86	78	2	1
m.3460G>A	MT-ND1	p.A52T	probably_damaging	neutral	neutral	disease	97	86	78	1	2
m.3523A>G	MT-ND1	p.T73A	benign	neutral	neutral	neutral	51	68	78	10	2
m.3535T>A	MT-ND1	p.L77M	probably_damaging	neutral	neutral	neutral	95	57	78	2	9
m.4123A>G	MT-ND1	p.I273V	benign	neutral	neutral	neutral	70	81	78	1	1
m.4136A>G	MT-ND1	p.Y277C	probably_damaging	neutral	disease	disease	99	86	78	3	1
m.4160T>C	MT-ND1	p.L285P	probably_damaging	neutral	disease	disease	100	100	78	1	1
m.4184T>A	MT-ND1	p.F293Y	probably_damaging	neutral	disease	neutral	100	100	78	2	1
m.4216T>C	MT-ND1	p.Y304H	benign	neutral	neutral	neutral	62	67	78	6	11
m.4561T>C	MT-ND2	p.V31A	benign	neutral	neutral	neutral	56	67	62	1	1
m.4639T>C	MT-ND2	p.I57T	benign	neutral	neutral	neutral	86	76	62	6	2
m.4659G>A	MT-ND2	p.A64T	benign	neutral	disease	disease	93	76	62	1	2
m.4695T>C	MT-ND2	p.F76L	benign	neutral	neutral	neutral	73	57	62	9	8
m.4824A>G	MT-ND2	p.T119A	benign	neutral	disease	neutral	94	81	62	1	1
m.5460G>A	MT-ND2	p.A331T	benign	neutral	neutral	neutral	46	48	62	22	7
m.6261G>A	MT-CO1	p.A120T	probably_damaging	neutral	neutral	neutral	100	100	95	1	1

m.6712A>T	MT-CO1	p.Y270F	probably_damaging	neutral	disease	disease	100	100	95	1	1
m.7080T>C	MT-CO1	p.F393L	probably_damaging	neutral	neutral	disease	100	100	95	1	2
m.7119G>A	MT-CO1	p.D406N	benign	neutral	neutral	neutral	83	90	95	4	1
m.7257A>G	MT-CO1	p.I452V	benign	neutral	neutral	neutral	77	90	95	1	2
m.7269G>A	MT-CO1	p.V456M	benign	neutral	neutral	neutral	77	86	95	1	1
m.7270T>C	MT-CO1	p.V456A	benign	deleterious	neutral	neutral	77	86	95	1	1
m.7440T>G	MT-CO1	p.S513A	benign	neutral	neutral	neutral	33	55	95	5	-
m.7859G>A	MT-CO2	p.D92N	benign	neutral	neutral	neutral	75	95	89	3	1
m.8400T>C	MT-ATP8	p.M12T	benign	neutral	neutral	neutral	55	62	46	3	39
m.8448T>C	MT-ATP8	p.M28T	benign	neutral	neutral	neutral	47	33	46	19	23
m.8516T>C	MT-ATP8	p.W51R	probably_damaging	neutral	disease	disease	100	48	46	42	4
m.8557G>C	MT-ATP6	p.A11P	possibly_damaging	neutral	neutral	disease	68	67	77	2	1
m.8557G>C	MT-ATP8	p.L64F	probably_damaging	neutral	disease	neutral	80	67	46	7	-
m.8711A>G	MT-ATP6	p.N62S	benign	neutral	neutral	neutral	83	67	77	1	3
m.8743G>A	MT-ATP6	p.V73M	benign	neutral	neutral	neutral	44	71	77	2	2
m.8812A>G	MT-ATP6	p.T96A	probably_damaging	neutral	neutral	neutral	98	95	77	1	1
m.8843T>C	MT-ATP6	p.I106T	benign	deleterious	disease	neutral	98	81	77	1	3
m.8888T>C	MT-ATP6	p.I121T	benign	neutral	neutral	neutral	71	76	77	1	1
m.8953A>G	MT-ATP6	p.I143V	probably_damaging	neutral	neutral	neutral	85	86	77	3	1
m.8989G>A	MT-ATP6	p.A155T	probably_damaging	neutral	neutral	disease	93	95	77	2	2
m.9025G>A	MT-ATP6	p.G167S	probably_damaging	deleterious	disease	disease	100	90	77	1	1
m.9053G>A	MT-ATP6	p.S176N	benign	neutral	neutral	neutral	58	76	77	1	23
m.9055G>A	MT-ATP6	p.A177T	possibly_damaging	neutral	disease	disease	90	71	77	2	22
m.9067A>G	MT-ATP6	p.M181V	benign	deleterious	neutral	neutral	90	57	77	6	18
m.9103T>C	MT-ATP6	p.F193L	benign	neutral	disease	neutral	93	62	77	18	6
m.9137T>C	MT-ATP6	p.I204T	benign	neutral	NA	neutral	66	86	77	1	7
m.9327A>G	MT-CO3	p.T41A	benign	neutral	neutral	neutral	42	71	92	5	1
m.9957T>C	MT-CO3	p.F251L	benign	neutral	neutral	disease	100	100	92	1	1
m.10237T>C	MT-ND3	p.I60T	probably_damaging	neutral	disease	disease	100	100	69	3	1
m.10320G>A	MT-ND3	p.V88I	benign	neutral	neutral	neutral	46	29	69	10	10
m.10398A>G	MT-ND3	p.T114A	benign	neutral	neutral	neutral	81	92	69	1	-
m.10609T>C	MT-ND4L	p.M47T	benign	neutral	neutral	neutral	51	48	69	13	13
m.10680G>A	MT-ND4L	p.A71T	benign	neutral	disease	disease	97	81	69	11	3
m.10845C>T	MT-ND4	p.T29I	benign	neutral	NA	neutral	36	62	77	3	6
m.11778G>A	MT-ND4	p.R340H	probably_damaging	deleterious	disease	disease	100	90	77	2	2
m.11969G>A	MT-ND4	p.A404T	benign	neutral	disease	disease	84	67	77	5	2
m.12361A>G	MT-ND5	p.T9A	unknown	neutral	NA	neutral	59	26	68	-	6
m.13105A>G	MT-ND5	p.I257V	benign	neutral	neutral	neutral	59	86	68	1	1
m.13135G>A	MT-ND5	p.A267T	benign	neutral	disease	neutral	56	67	68	4	12
m.13621C>T	MT-ND5	p.L429F	benign	neutral	disease	neutral	67	62	68	4	6
m.13708G>A	MT-ND5	p.A458T	benign	neutral	disease	disease	44	67	68	1	7
m.13712C>T	MT-ND5	p.A459V	benign	neutral	neutral	disease	46	62	68	2	6
m.14258G>A	MT-ND6	p.P139L	benign	neutral	neutral	neutral	37	38	52	57	2
m.14279G>A	MT-ND6	p.S132L	benign	neutral	neutral	neutral	60	24	52	50	9
m.14484T>C	MT-ND6	p.M64V	probably_damaging	neutral	neutral	disease	58	95	52	1	1
m.14564A>G	MT-ND6	p.V37A	benign	neutral	neutral	disease	70	67	52	1	2
m.14582A>G	MT-ND6	p.V31A	benign	neutral	neutral	neutral	47	86	52	2	1
m.14861G>A	MT-CYB	p.A39T	benign	neutral	neutral	neutral	39	81	82	2	1
m.15221G>A	MT-CYB	p.D159N	benign	neutral	neutral	disease	38	95	82	2	4
m.15315C>T	MT-CYB	p.A190V	benign	neutral	neutral	disease	41	86	82	3	6
m.15458T>C	MT-CYB	p.S238P	benign	neutral	neutral	disease	27	52	82	7	9

Table 6. Prediction tools and conservation analysis of missense private variants in LHON probands carrying m.14484T>C/MT-ND6 mutation.

This analysis confirmed the pathogenic role of the m.14484T>C, found in all probands.

We detect the co-presence of 10 other possibly pathogenic mutations in 10 different pedigrees (Table 6). In 2 families, besides the primary LHON m.14484T>C mutation, a second LHON primary mutation was found (m.3460G>A and m.11778G>A). We also found 3 possibly

pathogenic mutations in MT-ND1 (m.4136A>G, m.4160T>C, m.4184T>A), 1 in MT-ND3 (m.10237T>C), 1 in MT-ND2 (m.4659G>A), 1 in MT-CO1 (m.6712A>T), 1 in MT-CO3 (m.9957T>C), 1 in MT-ATP8 (m.8516T>C) and 2 in MT-ATP6 (m.8989G>A, m.9025G>A). Furthermore, 7 variants were predicted to be synergistic with the LHON m.14484T>C mutation: m.4824A>G in MT-ND2, m.6261G>A and m.7080T>C in MT-CO1, m.8557G>C in MT-ATP8, m.8812A>G (found in 2 families), m.8953A>G and m.9055G>A in MT-ATP6.

Phylogenetic analysis

To investigate any possible founder event, we reconstructed the phylogenetic tree starting from control population analysis in www.phylotree.org database (van Oven and Kayser, 2009). We show the branches of haplogruops J and T, because these two were the only with recurrent haplotypes (Figures 14).

A possibly ancient founder event is recognized on J1b1a1, which spread in central Europe with 3 families in Italy, 2 in France and 6 in Germany. Other founder events still occurring on haplogroup J are noticed on J1c1d, J1c2j, J1c3e2, J1c3f, J1c4 and J2b1 clades, but also on haplogroup T, in particular on T1a2, T2 and T2c1d1 clades (Figure 14).

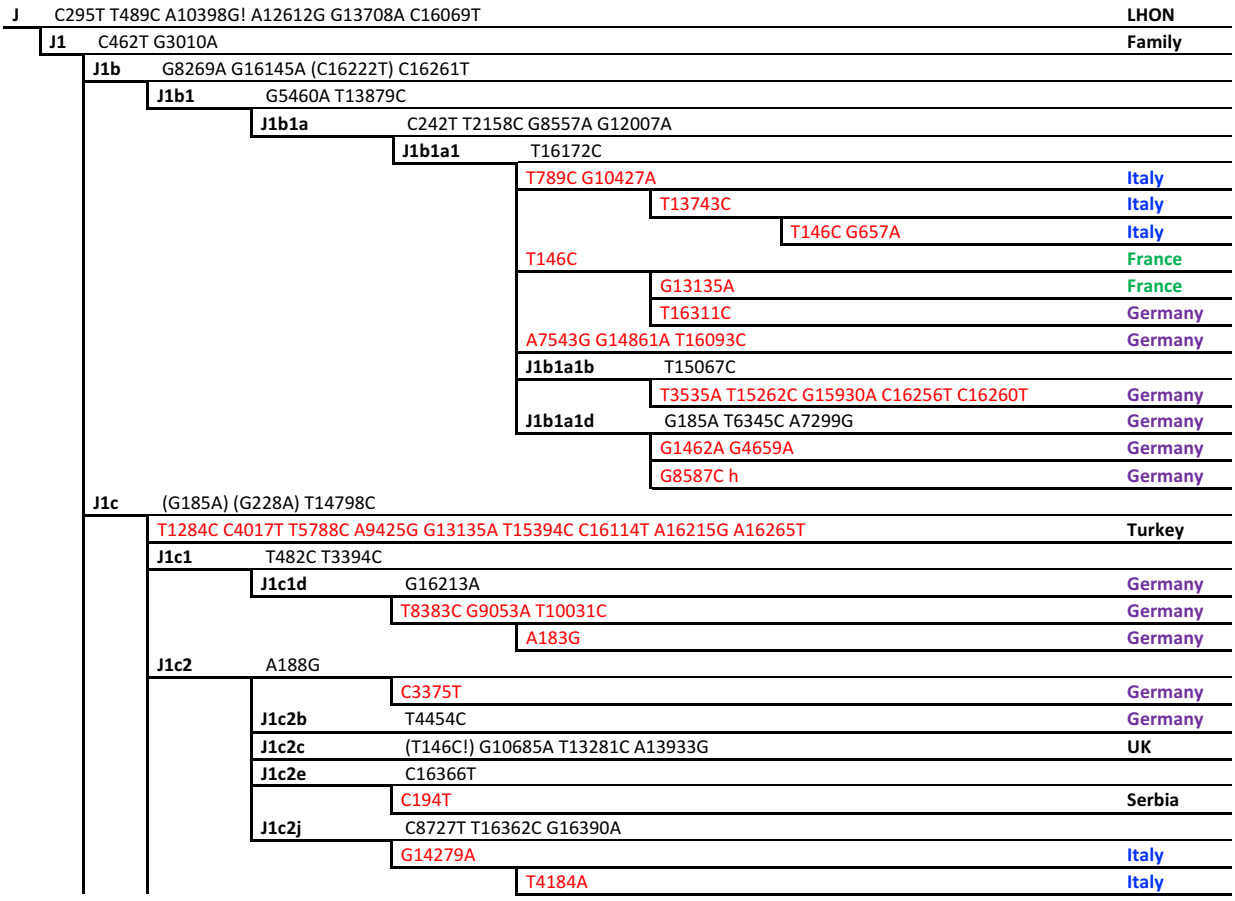

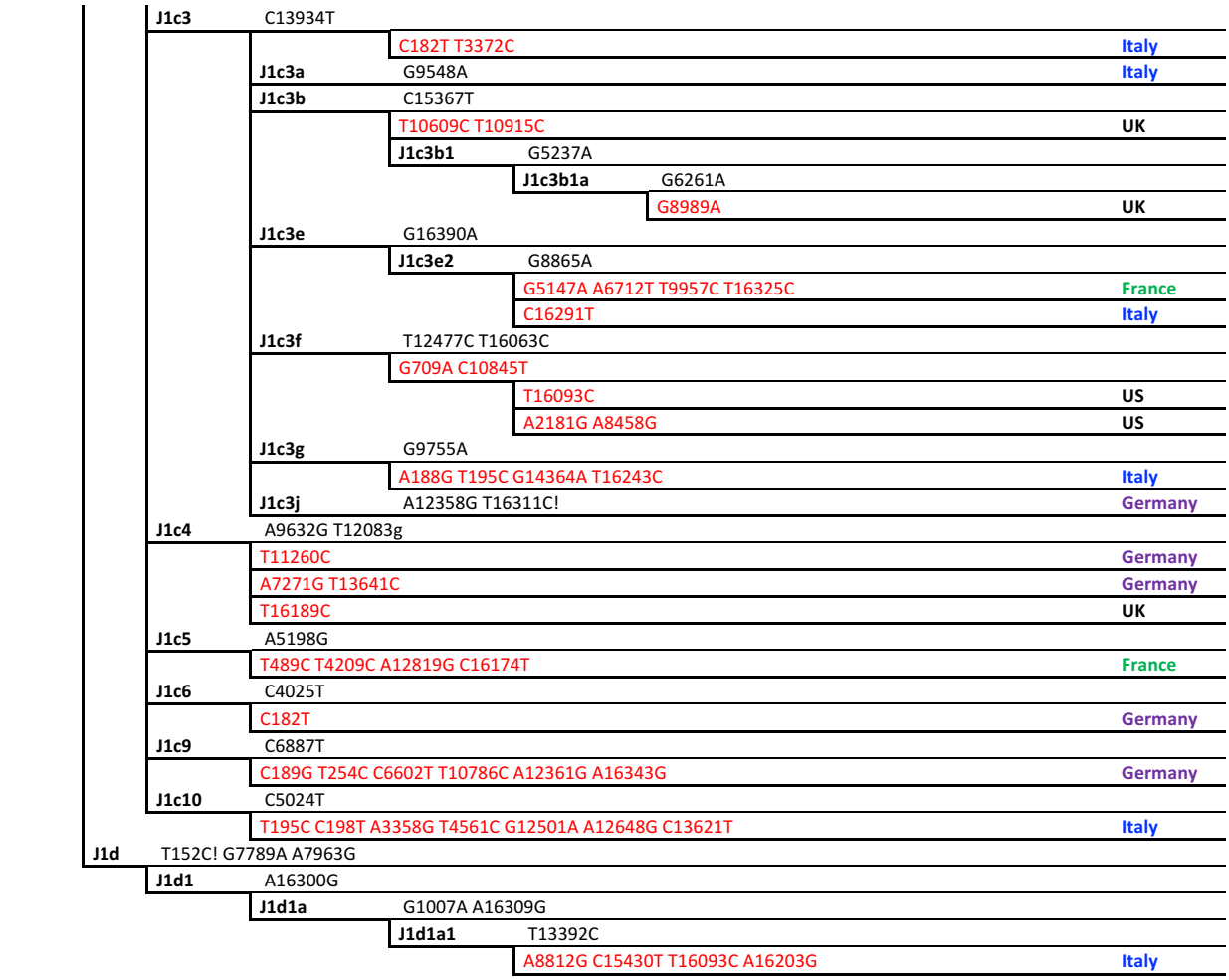
J1c3 C13934T
C182T T3372C Italy
J1c3a G9548A Italy
J1c3b C15367T
T10609C T10915C UK
J1c3b1 G5237A
J1c3b1a G6261A
G8989A UK
J1c3e G16390A
J1c3e2 G8865A
G5147A A6712T T9957C T16325C France
C16291T Italy
J1c3f T12477C T16063C
G709A C10845T
T16093C US
A2181G A8458G US
J1c3g G9755A
A188G T195C G14364A T16243C Italy
J1c3j A12358G T16311C! Germany
J1c4 A9632G T12083g
T11260C Germany
A7271G T13641C Germany
T16189C UK
J1c5 A5198G
T489C T4209C A12819G C16174T France
J1c6 C4025T
C182T Germany
J1c9 C6887T
C189G T254C C6602T T10786C A12361G A16343G Germany
J1c10 C5024T
T195C C198T A3358G T4561C G12501A A12648G C13621T Italy
J1d T152C! G7789A A7963G
J1d1 A16300G
J1d1a G1007A A16309G
J1d1a1 T13392C
A8812G C15430T T16093C A16203G Italy

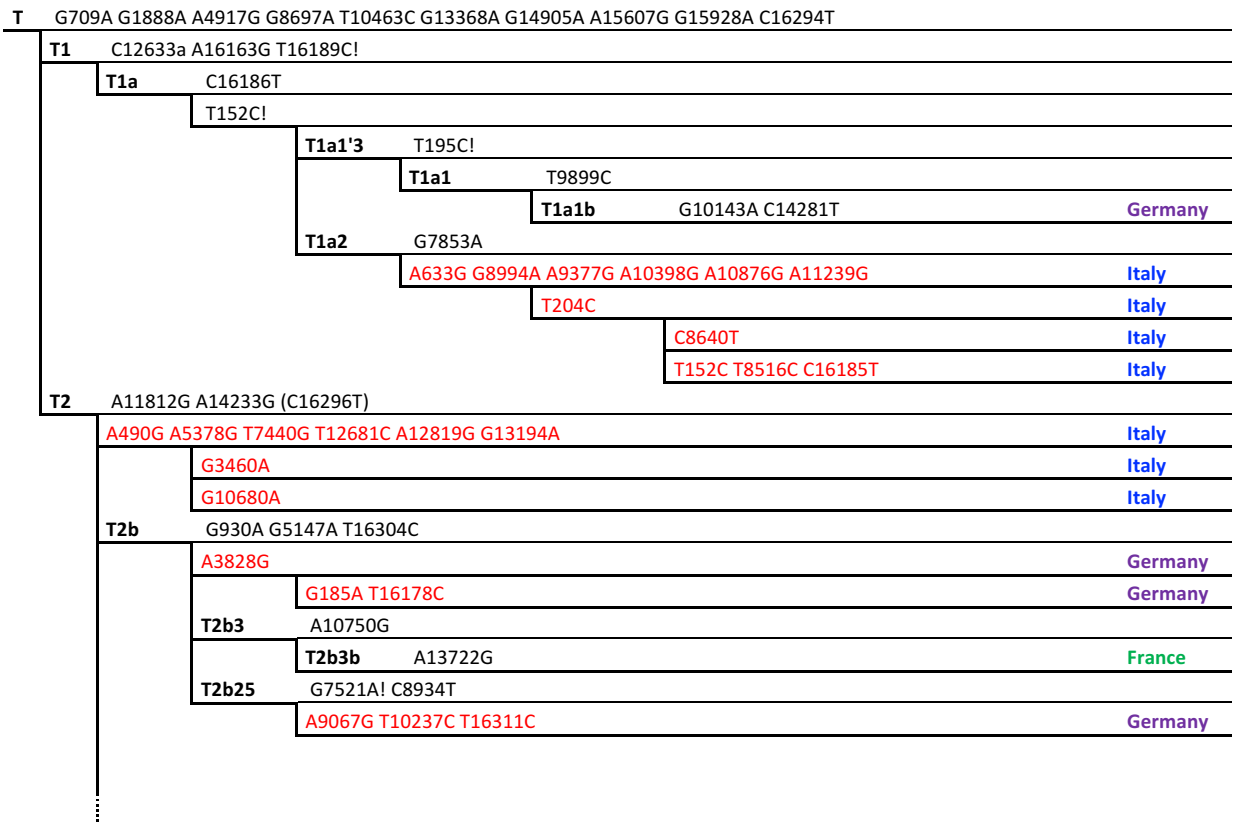
T G709A G1888A A4917G G8697A T10463C G13368A G14905A A15607G G15928A C16294T
T1 C12633a A16163G T16189C!
T1a C16186T
T152C!
T1a1'3 T195C!
T1a1 T9899C
T1a1b G10143A C14281T Germany
T1a2 G7853A
A633G G8994A A9377G A10398G A10876G A11239G Italy
T204C Italy
C8640T Italy
T152C T8516C C16185T Italy
T2 A11812G A14233G (C16296T)
A490G A5378G T7440G T12681C A12819G G13194A Italy
G3460A Italy
G10680A Italy
T2b G930A G5147A T16304C
A3828G Germany
G185A T16178C Germany
T2b3 A10750G
T2b3b A13722G France
T2b25 G7521A! C8934T
A9067G T10237C T16311C Germany

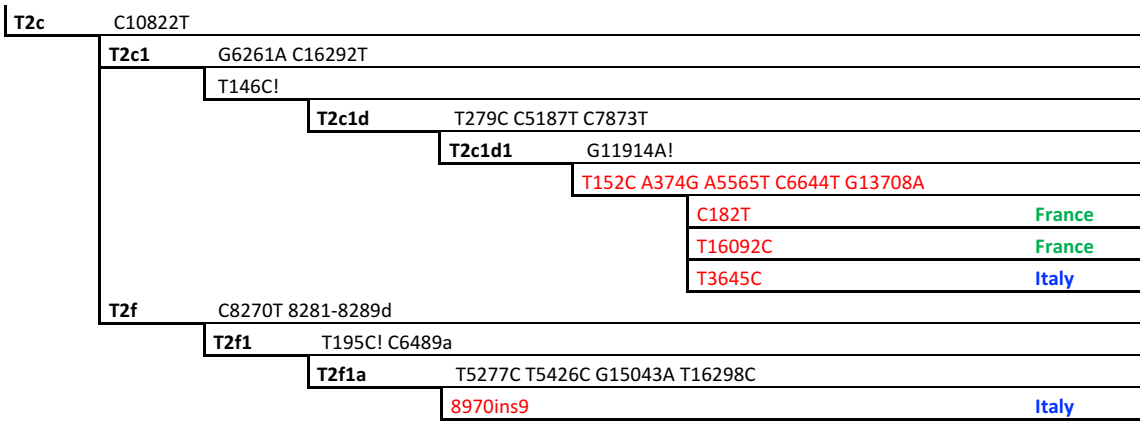

Figure 14. Phylogenetic reconstruction tree of LHON probands carrying m.14484T>C/MT-ND6 on haplogroups J and T, based on www.phylotree.org

Penetrance evaluation on available pedigree

To assess the role of haplogruop J on incomplete penetrance and male prevalence, we evaluated the number of affected versus unaffected carriers on the available reconstruction of the pedigrees (14 maternal lines on haplogruop J, 22 non-J). The results are summarized in tables 7 and 8.

	Males	
	Affected	**Unaffected**
J	27 (29.0)	66 (71.0)
non-J	42 (24.4)	130 (75.6)
All	69 (26.0)	196 (74.0)
	Females	
	Affected	**Unaffected**
J	10 (7.5)	123 (92.5)
non-J	10 (5.7)	166 (94.3)
All	20 (6.4)	289 (93.6)
	Total	
	Affected	**Unaffected**
J	37 (16.4)	189 (83.6)
non-J	52 (14.9)	296 (85.1)
All	89 (15.5)	485 (84.5)

Table 7. Frequency of affected and unaffected individuals within haplogroup J and non-J maternal lines, considering gender as variable. The data are expressed as n (%).

RATIO	Affected Male:Female	Affected:Unaffected	Male A:U	Female A:U
J	2,7	0,2	0,4	0,1
non-J	4,2	0,2	0,3	0,1
All	3,5	0,2	0,4	0,1

Table 8. Ratio of affected and unaffected individuals within haplogroup J and non-J maternal lines, considering gender as variable.

This analysis failed to highlight any significant difference. However, despite the lack af a strong evident effect, it remains a tendency towards higher penetrance of the m.14484T>C mutation on the haplogroup J background, which applies to both genders (Tables 7, 8).

PART III - *Mitochondrial DNA variability in Dominant Optic Atrophy (DOA) with mutation in OPA1 gene*

Mitochondrial genome sequencing and haplogroup affiliation

We completely sequenced the mtDNA in 112 maternally unrelated patients from 85 families carrying a dominant OPA1 mutation. The haplogroup affiliations and private variants are summarized in Table 9.

Family	Relationship	Haplogroup	Private synonimous	Private non coding	Provate tRNA/rRNA	Private missense
1	Proband	H1				6253 T>C/MT-CO1
2	Proband	U2e1	14470 T>C	228 G>A		
3	Proband	J1d3a	11061 C>G			14551 A>G/MT-ND6
4	Proband	H26	5096 T>C			
4	Maternal granfather	R1a1	7055 A>G 12906 C>T			
5	Proband	U2e2a1		16183 A>C 16182 A>C		6249 G>A/MT-CO1 14790 A>G/MT-CYB
5	Father	H5qa		152 T>C		
6	Proband	H	7630 T>C 11113 T>C		12172 A>G/MT-TH	
7	Proband	H1j				
8	Proband	H70		16192 C>T 16209 T>C		
8	Father	T2c1d1	13056 C>T 14544 G>A		12215 T>C/MT-TS2	
9	Proband	U1a3	6023 G>A 13470 A>G 9449 C>T			
10	Proband	J1c3	12477 T>C 12696 T>C			
10	Father	H10d		15884 G>A	729 T>C/MT-RNR1	10398 A>G/MT-ND3
11	Proband	V	7804 A>G		3290 T>C/MT-TL1	
12	Proband	N1b1a	14097 C>T 14323 G>A			
13	Proband	H4a1	8730 A>G			4129 A>G/MT-ND1 7853 G>A/MT-CO2
14	Proband	H3b				
15	Proband	L3b	10283 A>G			12674 A>G/MT-ND5
16	Proband	T1a1l	14311 T>C			
16	Father	K1b1c	3918 G>A 13470 A>G		1736 A>G/MT-RNR2	
18	Proband	J1c3				
18	Father	H10	7702 G>A			8896 G>C/MT-ATP6 14798 T>C/MT-CYB
19	Proband	J1c8	3657 C>A 14653 C>T			13768 T>C/MT-ND5
20	Proband	T2h				
21	Proband	U2e2a1b	7235 C>A 7418 C>T 7427 C>T 14788 T>C			14180 T>C/MT-ND6
22	Proband	H1c2				
23	Proband	H	13641 T>C		2648 T>C/MT-RNR2	
23	Father	H1u			1809 T>C/MT-RNR2	
24	Proband	H20	9410 A>G 13656 T>C	16189 T>C 16192 C>T		
25	Proband	J1c	5147 G>A 14296 A>G	16390 G>A		13145 G>A/MT-ND5

26	Proband	H65				4491 G>A/MT-ND2
27	Proband	J2b1a2	11686 C>T		5774 T>C/MT-TC	
28	Proband	X2m	6023 G>A 11944 T>C		15910 C>T/MT-TT	8866 A>G/MT-ATP6
28	Father	H1q	5201 T>C			
29	Proband	H	6305 G>A 7945 C>T 11203 C>T			
30	Proband	H5a	3744 A>G	456 C>T		4659 G>A/MT-ND2
31	Proband	H2b	4092 G>A		4386 T>C/MT-TQ	12557 C>T/MT-ND5
32	Proband	T2b4	8146 A>G			
33	Proband	HV0e	9944 T>C 14260 A>G 14389 C>T			
33	Father	J1b1a	5201 T>C			
34	Proband	K1b1a	4763 C>T 6290 C>T 15877 C>T			8084 A>G/MT-CO2
34	Father	H1e	8251 G>A	16148 C>T	15936 A>G/MT-TT	3316 G>A/MT-ND1 8833 G>A/MT-ATP6
35	Proband	J1b1a3	3714 A>G 9156 A>G 5471 G>A	188 A>G 16326 A>G		10188 A>G/MT-ND3
35	Father	U3b	5417 G>A 9770 T>C 12744 C>T	185 G>A 16162 A>T	2707 A>G/MT-RNR2	
37	Proband	HV0b		16564 A>G		8480 C>T/MT-ATP8 15119 G>A/MT-CYB
37	Nephew	H1	9932 G>A 11149 G>A			
37	Nephew	H	10232 A>G 16319 T>A	16319 G>A		
38	Proband	H10a1				
38	Daughter	K1b1c	10094 C>T 11152 T>C 11719 G>A			14258 G>A/MT-ND6
39	Proband	T2b	11929 T>C			
40	Proband	T2a1	12957 T>C 15265 C>T			
40	Cousin's son	H	4204 T>C			
40	Cousin's son	H	3666 G>A 6293 T>C 15103 C>T			7407 T>C/MT-CO1
41	Proband	U1b2	6725 C>A	16042 G>A		
42	Proband	H6a1a			5558 A>G/MT-TW	
43	Proband	N1a3a2	6743 T>C	16564 A>G 16565 C>T		
44	Proband	H10a1		16564 A>G 16565 C>T	2066 C>T/MT-RNR2	14198 G>A/MT-ND6
45	Proband	H6a1a	8227 T>C			
46	Proband	W1h1	12927 C>T	143 G>A	14727 T>C/MT-TE	
47	Proband	U5b2a1a1	14582 A>G			
48	Proband	H7	7340 G>A			
49	Proband	H63	5951 A>G 7094 T>C			8701 A>G/MT-ATP6
51	Proband	K1b1c				
51	Son	H73				
52	Proband	H1	6620 T>C 11929 T>C 14470 T>C			
53	Proband	H13a1a2b	7397 C>T	200 A>G		4491 G>A/MT-ND2 8701 A>G/MT-ATP6
54	Proband	U5a2				
55	Proband	U4c1			827 A>G/MT-RNR1 2282 C>T/MT-RNR2	13327 A>G/MT-ND5

56	Proband	T1a1	9275 A>C			8896 G>A/MT-ATP6 13879 T>C/MT-ND5
57	Proband	H1a	4736 T>C 9374 A>G			
58	Proband	H	15682 A>G			3511 A>G/MT-ND1 13889 G>A/MT-ND5
59	Proband	K1a	15466 G>A		15924 A>G/MT-TT	4917 A>G/MT-ND2 5194 C>T/MT-ND2
59	Father	H	5426 T>C 8026 A>G 14215 T>C		961 T>C/MT-RNR1	7309 T>C/MT-CO1 7754 G>A/MT-CO2
60	Proband	H7				
60	Father	U5b3	4065 A>G			3943 A>G/MT-ND1
61	Proband	L3f1b	5262 G>A 10373 G>A 11383 T>C 15670 T>C		A4343 A>G/MT-TQ 15940 delT/MT-TT	9957 T>C/MT-CO3
62	Proband	H5b	7861 T>C 14007 A>G		801 A>G/MT-RNR1	
62	Paternal grandfather	H6a1b2				11150 G>A/MT-ND4
62	Father	H5a	10172 G>A			
63	Proband	T2b	11929 T>C		2903 T>C/MT-RNR2 12172 A>G/MT-TT	10398 A>G/MT-ND3
64	Proband	U4b1a	4703 T>C 12609 T>C			13708 G>A/MT-ND5
64	Father	T1a1	14758 A>G			
65	Proband	J1b1a2b	9968 C>T			7407 T>C/MT-CO1
66	Proband	V4	3849 G>A		1657 C>T/MT-TV	
66	Father	J2b1	6959 C>T 10370 T>C		1824 T>C/MT-RNR2 15894 G>A/MT-TT	4824 A>G/MT-ND2 8953 A>G/MT-ATP6
67	Proband	J2a2b2		195 T>C 16224 T>C 16276 T>C 16564 A>G 16565 C>T		
68	Proband	H1ap	13194 G>A		2876 G>A/MT-RNR2	
69	Proband	H13a1a2b	6959 C>T	5580 T>C		
69	Father	H		5581 A>T		
70	Proband	I3a1	13395 A>G			
71	Proband	H10aq	7894 A>G 11314 A>G	16564 A>G 16565 A>T		
72	Proband	HV4	8763 T>C 14515 T>C	93 A>G 152 T>C		7805 G>A/MT-CO2
72	Father	U3b	5264 C>T 9305 G>A 14581 T>C		2272 C>T/MT-RNR2 15940 delT/MT-TT 15977 C>T/MT-TP	
73	Proband	T2	6488 T>C 11944 T>C	152 T>C		9804 G>A/MT-CO3 10750 A>G/MT-ND4L
74	Proband	U5a2d	6260 G>A 10984 C>T	16311 T>C		8887 A>G/MT-ATP6 12663 C>A/MT-ND5
74	Father	H43	11149 G>A			15773 G>A/MT-CYB
74	Cousin	H17a	7961 T>C 11455 C>T	16564 A>G 16565 C>T		
75	Proband	H5a1a	4086 C>T 11887 G>A 13194 G>A	195 T>C 513 delCA		14279 G>A/MT-ND6
76	Proband	J2b1a5	3591 G>A			7051 T>C/MT-CO1
77	Proband	H18b	4736 T>C	16561 A>T		8519 G>A/MT-ATP8
78	Proband	U5a1a1	4598 T>C			8516 T>C/MT-ATP8 8705 T>C/MT-ATP6
79	Proband	K1b1a	3714 A>G 5471 G>A 14560 G>A 15877 C>T			
80	Proband	T2b				

81	Proband	HV4a2	8763 T>C 14515 T>C			
82	Proband	J2a2c			15924 A>G/MT-TT	3508 A>G/MT-ND1
83	Proband	H	5264 C>T			
83	Father	HV1b				
84	Proband	H	4823 T>C 8865 G>A 11539 C>T		2789 C>T/MT-RNR2	
85	Proband	H	13431 C>T			
85	Father	R0a1a				
85	Cousin	T2b	4823 T>C 6935 C>T 13581 T>C			14562 C>T/MT-ND6

Table 9. Mitochondrial genome of DOA patients carrying OPA1 mutation with haplogroup affiliation (according to www.phylotree.org - build 17) and private changes. Missense variant in coloured according scoring criteria described in the "materials and methods" as in table 10.

In the OPA1 mutation cohort, as expected for a dominant disease, the frequency of mitochondrial haplogroups was not statistically different as compared to the Italian population (χ^2test, p =5741) (Figure 15).

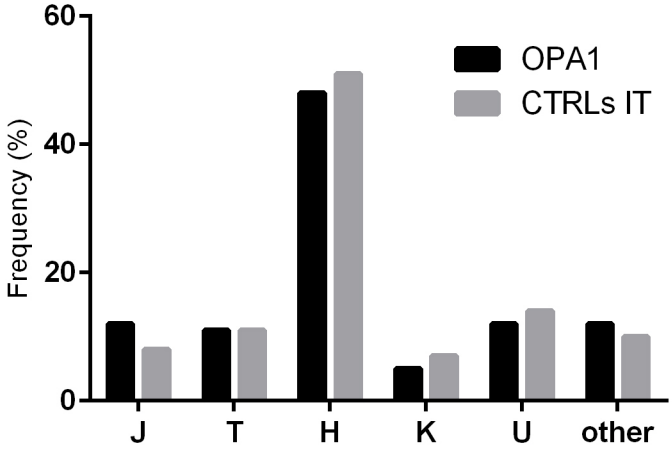

Figure 15. Frequency of European haplogroups in DOA cohort with OPA1 mutations and control population (*n* =2495). **p<0.001, *p<0.05.

Private missense variants as phenotype modifiers

We analysed all missense changes, which were not diagnostic for the haplogroups, to detect other private variants, with some possible modifying or pathogenic significance. For each variant, the amino acid residue conservation and the *in-silico* prediction values of pathogenicity were considered (Table 10). To this end, the *on-line* tools PolyPhen2, SIFT, PANTHER and PhD-SNP have been used and conservation analysis was carried out, as detailed in the methods. According to the scoring criteria described in the "materials and methods", changes with a score of 0,66-1 points were considered pathogenic (red), with 0,5-0,65 points were considered synergistic (orange) and with 0-0,49 points neutral (black).

nt change	Gene	aa change	Prediction tools				Conservation			Invariants	
			PolyPhen2	SIFT	PANTHER	PhD-SNP	Mammals	Local	Global	-	+
m.3316 G>A	MT-ND1	p.A4T	benign	neutral	NA	neutral	67	57	78	3	12
m.3508 A>G	MT-ND1	p.I68V	benign	neutral	neutral	neutral	27	67	78	5	7
m.3511 A>G	MT-ND1	p.T69A	benign	neutral	neutral	neutral	37	67	78	6	6
m.3943 A>G	MT-ND1	p.I213V	benign	neutral	neutral	neutral	86	100	78	2	2
m.4129 A>G	MT-ND1	p.T275A	benign	neutral	neutral	neutral	89	81	78	1	3
m.4491 G>A	MT-ND2	p.V8I	benign	neutral	neutral	neutral	54	39	62	5	8
m.4659 G>A	MT-ND2	p.A64T	benign	neutral	disease	disease	93	76	62	1	2
m.4824 A>G	MT-ND2	p.T119A	benign	neutral	disease	neutral	94	81	62	1	1
m.4917 A>G	MT-ND2	p.N150D	benign	neutral	disease	disease	93	43	62	15	11
m.5194 C>T	MT-ND2	p.P242L	benign	neutral	disease	neutral	38	48	62	7	8
m.6249 G>A	MT-CO1	p.A116T	benign	neutral	neutral	neutral	83	100	95	1	3
m.6253 T>C	MT-CO1	p.M117T	benign	neutral	neutral	neutral	85	100	95	2	2
m.7051 T>C	MT-CO1	p.M383T	probably_damaging	deleterious	neutral	disease	100	100	95	1	1
m.7309 T>C	MT-CO1	p.I469T	benign	deleterious	neutral	disease	100	100	95	1	1
m.7407 T>C	MT-CO1	p.Y502H	benign	neutral	neutral	neutral	71	76	95	2	1
m.7754 G>A	MT-CO2	p.D57N	benign	neutral	NA	disease	94	95	89	4	2
m.7805 G>A	MT-CO2	p.V74I	benign	neutral	NA	neutral	85	90	89	2	2
m.7853 G>A	MT-CO2	p.V90I	benign	neutral	neutral	neutral	91	95	89	1	3
m.8084 A>G	MT-CO2	p.T167A	benign	neutral	neutral	neutral	91	100	89	1	2
m.8480 C>T	MT-ATP8	p.P39S	probably_damaging	neutral	neutral	neutral	40	5	46	31	11
m.8516 T>C	MT-ATP8	p.W51R	probably_damaging	neutral	disease	disease	100	48	46	42	4
m.8519 G>A	MT-ATP8	p.E52K	probably_damaging	neutral	disease	disease	80	48	46	1	3
m.8701 A>G	MT-ATP6	p.T59A	benign	neutral	NA	neutral	37	57	77	3	2
m.8705 T>C	MT-ATP6	p.M60T	benign	neutral	NA	neutral	61	57	77	4	1
m.8833 G>A	MT-ATP6	p.A103T	probably_damaging	neutral	disease	neutral	68	90	77	5	1
m.8866 A>G	MT-ATP6	p.I114V	benign	neutral	disease	neutral	54	76	77	5	2
m.8887 A>G	MT-ATP6	p.I121V	benign	neutral	neutral	neutral	71	76	77	1	1
m.8896 G>A	MT-ATP6	p.A124T	benign	neutral	disease	disease	78	81	77	2	1
m.8896 G>C	MT-ATP6	p.A124P	benign	neutral	disease	disease	78	81	77	2	1
m.8953 A>G	MT-ATP6	p.I143V	probably_damaging	neutral	neutral	neutral	85	86	77	3	1
m.9804 G>A	MT-CO3	p.A200T	benign	neutral	neutral	disease	93	95	92	2	1
m.9957 T>C	MT-CO3	p.F251L	benign	neutral	neutral	disease	100	100	92	1	1
m.10188 A>G	MT-ND3	p.M44V	benign	neutral	neutral	neutral	81	86	69	2	3
m.10398 A>G	MT-ND3	p.T114A	benign	neutral	neutral	neutral	81	92	69	1	-
m.10750 A>G	MT-ND4L	p.N94S	benign	neutral	neutral	disease	98	93	69	1	1
m.11150 G>A	MT-ND4	p.A131T	benign	deleterious	NA	neutral	82	95	77	2	2
m.12557 C>T	MT-ND5	p.T74I	benign	neutral	NA	neutral	59	67	68	6	6
m.12663 C>A	MT-ND5	p.N109K	benign	neutral	neutral	neutral	72	86	68	1	2
m.12674 A>G	MT-ND5	p.N113S	possibly_damaging	neutral	disease	disease	36	81	68	1	4
m.13145 G>A	MT-ND5	p.S270N	benign	neutral	neutral	neutral	92	71	68	7	9
m.13327 A>G	MT-ND5	p.T331A	probably_damaging	neutral	disease	disease	95	90	68	1	1
m.13708 G>A	MT-ND5	p.A458T	benign	neutral	disease	disease	44	67	68	1	7
m.13768 T>C	MT-ND5	p.F478L	benign	neutral	disease	neutral	77	48	68	4	3
m.13879 T>C	MT-ND5	p.S515P	benign	neutral	neutral	neutral	23	29	68	18	7
m.13889 G>A	MT-ND5	p.C518Y	benign	neutral	disease	neutral	38	38	68	21	4
m.14180 T>C	MT-ND6	p.Y165C	probably_damaging	neutral	neutral	disease	26	45	52	5	4
m.14198 G>A	MT-ND6	p.T159M	probably_damaging	neutral	neutral	neutral	63	38	52	1	1
m.14258 G>A	MT-ND6	p.P139L	benign	neutral	neutral	neutral	37	38	52	57	2
m.14279 G>A	MT-ND6	p.S132L	benign	neutral	neutral	neutral	60	24	52	50	9
m.14562 C>T	MT-ND6	p.V38I	benign	neutral	neutral	neutral	72	67	52	2	1
m.14790 A>G	MT-CYB	p.N15S	benign	neutral	disease	disease	99	76	82	3	5
m.14798 T>C	MT-CYB	p.F18L	benign	neutral	neutral	neutral	89	81	82	6	2
m.15119 G>A	MT-CYB	p.A125T	benign	neutral	disease	disease	99	86	82	1	1
m.15773 G>A	MT-CYB	p.V343M	probably_damaging	neutral	disease	disease	99	76	82	4	3

Table 10. Prediction tools and conservation analysis of missense private variants in DOA patients carrying OPA1 mutation

In order to understand the influence of mitochondrial genome on the phenotype severity in patients with OPA1 gene mutation, we have analyzed the thickness of retinal nerve fiber layer (RNFL), measured by OCT (Optical Coherent Tomography), as marker of clinical outcome.

As a first step, we assessed the possible influence of private and putative pathogenic mutations (Table 10) disregarding the haplogroup affiliation on the RNFL thickness in OPA1 patients carrying or not carrying such variants. We failed to detect any differences in this comparison, considering the average RNFL thickness or sector by sector, i.e. temporal, superior, nasal, inferior (Figures 15, 16).

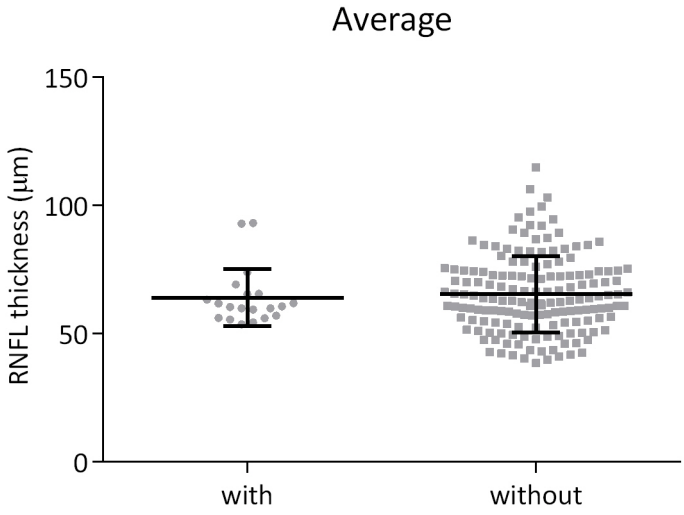

Figure 15. Scatter plot with mean±SD of average RNFL thickness in DOA patients with or without putative pathogenic mutations and synergistic variants in mtDNA.

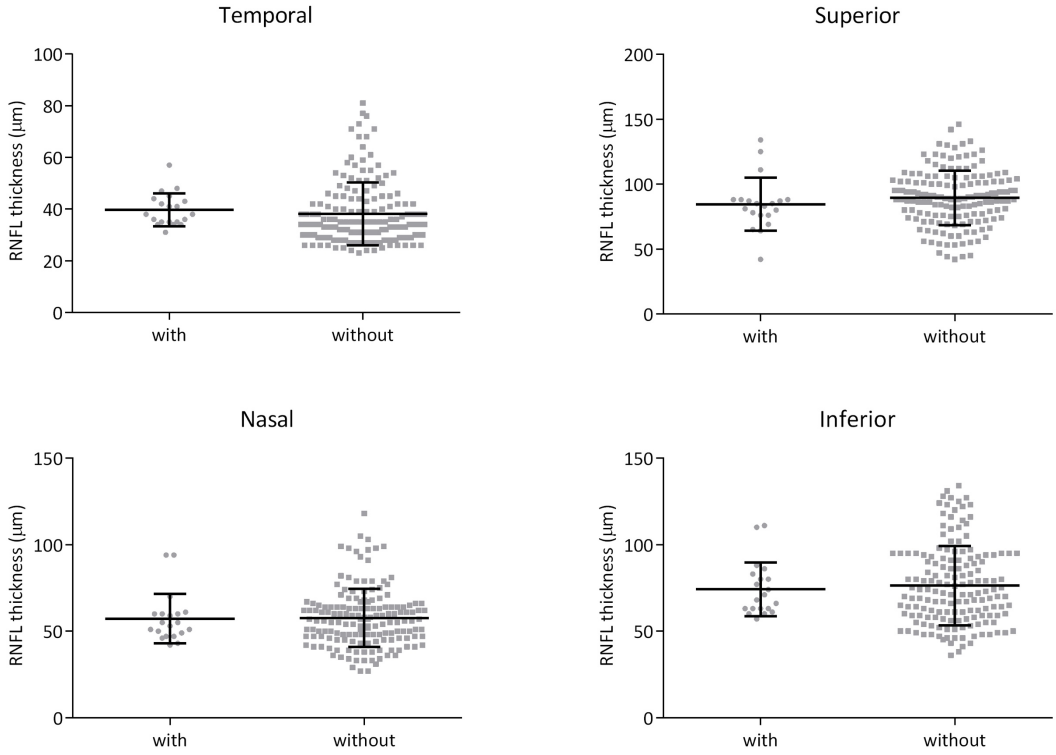

Figure 16. Scatter plot with mean±SD of RNFL thickness, split in four quadrants (Temporal, superior, nasal, inferior), in DOA patients with or without putative pathogenic mutations and synergistic variants in mtDNA

Mitochondrial haplogroups as phenotype modifier

Next, we investigated the variability of the RNFL thickness according to the different haplogroup affiliation of OPA1 patients, thus assessing the role of ancient mtDNA variation, selected and fixed during evolution as adaptive response to environmental pressure. The results are shown in Figures 17 and 18.

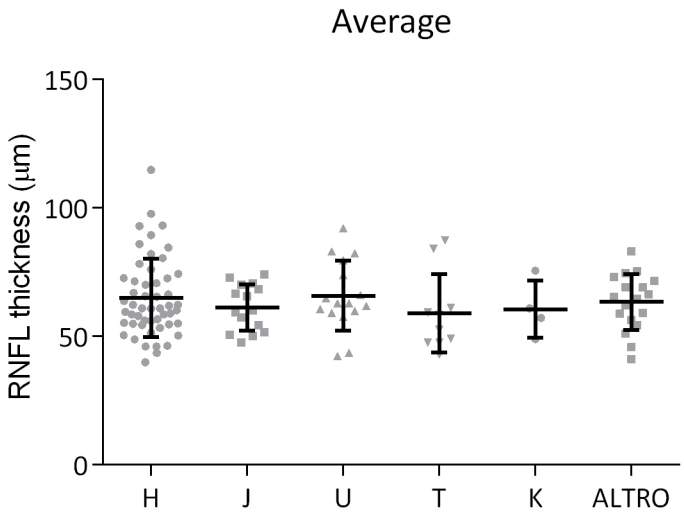

Figure 17. Scatter plot with mean±SD of average RNFL thickness in DOA patients with different mtDNA haplogroups.

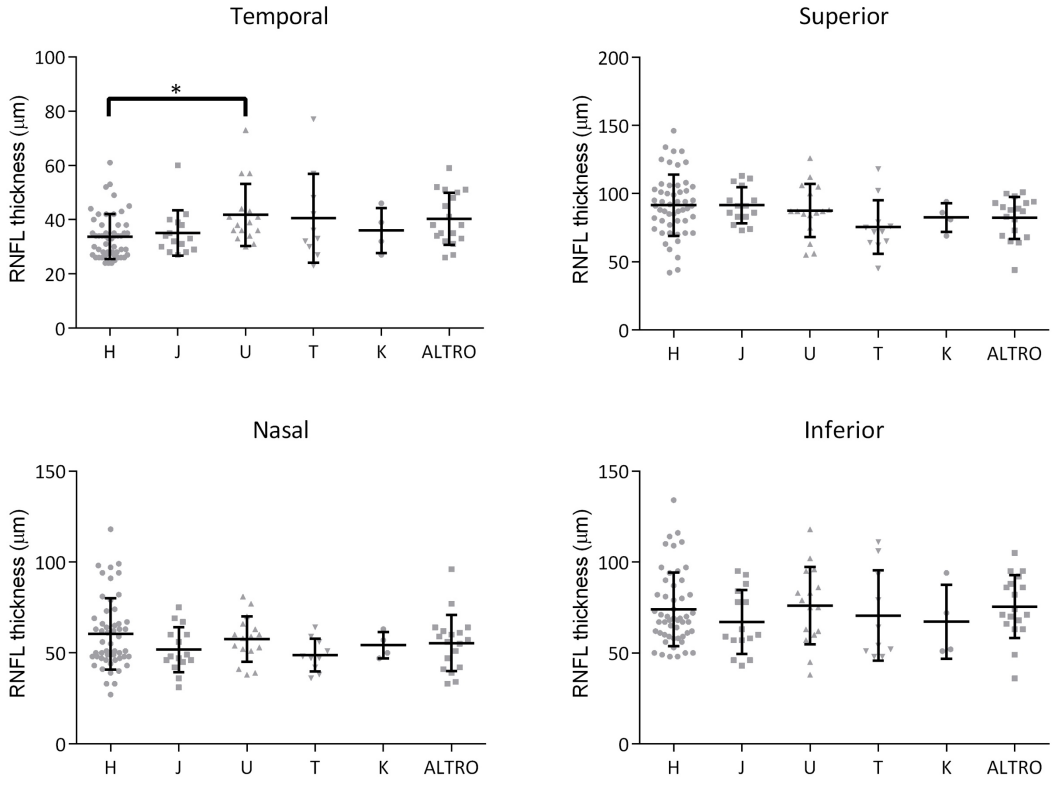

Figure 18. Scatter plot with mean±SD of RNFL thickness, split in four quadrants (Temporal, superior, nasal, inferior), in DOA patients with different mtDNA haplogroups. *p<0.01

The only statistically significant difference emerges for the temporal RNFL thickness (ANOVA, p=0.0270), thus revealing a putative protective role for haplogroup U and damaging for haplogroup H (Uncorrected Fisher's LSD, p=0.0053) (Figure 18).

Finally, we investigated the interaction between the mitochondrial and nuclear genomes, assuming that there could be a coadaptation between the two genomes and changes may influence the clinical outcome. To analyze this interaction, we evaluated the severity of the disease as a function of OPA1 mutation co-segregating or not with the mtDNA genome. In short, given the different inheritance of the two traits, an individual always inherits mtDNA from the mother, while the OPA1 mutation can be inherited from each of the two parents. Based on this last criterion, we identified 35 parent-child segregations. These were then divided into two groups:

- 19 OPA1 segregations "without" mtDNA change (mother-children segregation);
- 15 OPA1 segregations "with" mtDNA change (father-children segregation).

We have thus analyzed the difference in RNFL thickness between the two generations of each segregation group to evaluate the severity of the clinical outcome. Interestingly, in the mother-children segregation group there was a significantly increased severity of fiber loss (lower RNFL thickness) in children for the average and inferior quadrant RNFL comparison, with a similar tendency for all other quadrants (paired t-test, p=0.0186, 0.0071, respectively) (Figure 19). Noticeably, the infero-temporal fibers belong to the papillomacular bundle, which is the main target of the neurodegenerative process. Concerning the father-children segregation group, the only significant difference was found for the temporal quadrant (paired t-test, p=0.0172) (Figure 19).

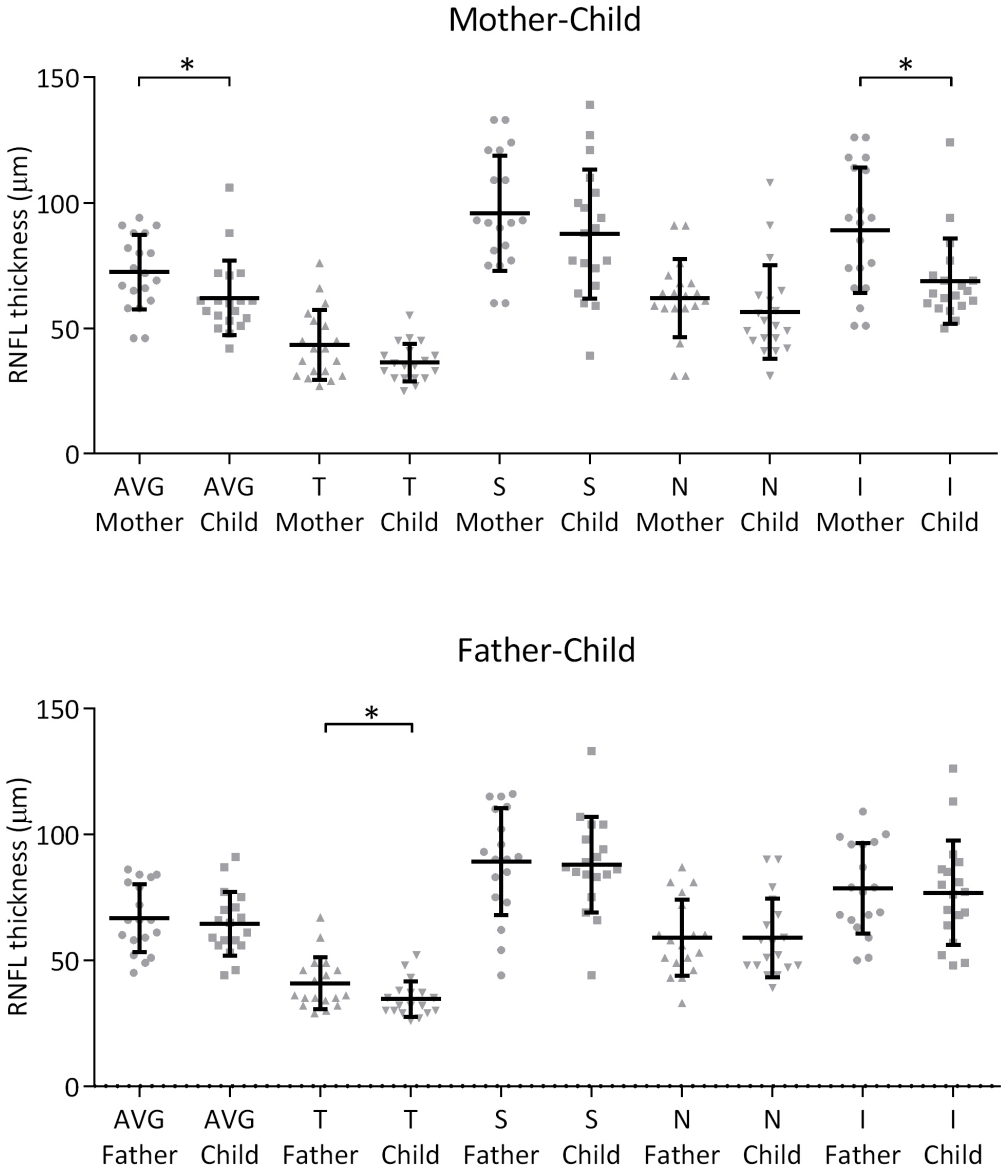

Figure 19. Scatter plot with mean±SD of differences in RNFL thickness from mother-children segregations and father-children segregations. *p<0.05

DISCUSSION

Peculiar combinations of individually non-pathogenic missense mitochondrial DNA variants cause low penetrance Leber's hereditary optic neuropathy

LHON is now well established that is a disease determined by a very mild complex I-dependent respiratory chain dysfunction, somehow borderline between functional and pathological variability, which is certainly dependent on the presence of a major predisposing pathogenic mtDNA mutation ("primary" mutation), but also largely modulated by the mitogenome sequence variation (mtDNA haplogroup with "secondary" and private mutations) (Gómez-Durán et al., 2010, 2012). Furthermore, the respiratory defect and pathogenic mechanism seem also highly modulated by environmental (Ghelli et al., 2009) and nuclear DNA factors (Carelli et al., 2003). Thus, to date, by definition in a LHON family it has always been recognized a clearly pathogenic "primary" mutation, possibly modulated by other private or mildly deleterious variants, which were usually defined as "secondary" mutations (Caporali et al., 2017).

In this study, for the first time we provide a clear evidence that in the cluster of Families 1a, 1b and 1c, all belonging to the same maternal lineage and carrying the previously unreported combination of m.14258G>A/*MT-ND6* and m.14582A>G/*MT-ND6* variants on a K1a haplogroup background (Table 3), there was no clearly "primary" pathogenic mutation. Thus, the only variants we could assign a possible pathogenic role were the missense changes affecting the ND6 subunit of complex I, here found in a previously unreported combination, otherwise individually present in the known public datasets, but on different mitogenomes (www.mitomap.org). On the clinical ground, it is worth noting that all affected members (*n*=14) of this very large family are males, indicating that most likely the combination of missense variants on the K1 mitogenome characterizing Families 1a, 1b and 1c was not sufficient to cross the threshold for triggering LHON in females. Furthermore, general penetrance of these 14 affected members was 13% over the total number of individuals on the maternal line, and 25% over the total number of males. This latter percentage is well below the usual quote of average 50% penetrance in males reported in literature (Carelli et al., 2004; Yu-Wai-Man et al., 2011).

It is also interesting to note that the mitogenomes of both Families 1 and 2 had in common the m.14258G>A/*MT-ND6* change, a mutation previously not recognized as associated with LHON. The other variant m.10680G>A/*MT-ND4L* found in Family 2 has been either found alone in pedigrees segregating cases of LHON on the maternal line (Zhang et al., 2012; Zou et al., 2010), or in association with known LHON primary mutations (Yang et al., 2009). Moreover, the mtDNA sequence variants of these previously reported cases of Chinese ancestry are found in combination with other missense changes in Complex I subunits genes, in particular in the ND1 subunit (m.3644T>C/*MT-ND1*; m.3745G>A/*MT-ND1*; m.3548T>C/*MT-ND1*) or in the ND6 subunit (m.14484T>C/*MT-ND6*), which are closely assembled with ND4L according to the currently proposed Complex I crystal structure (Figure 11, Table 4) (Fiedorczuk et al., 2016). Thus, at least the m.14258G>A/*MT-ND6* (in the present study) and m.10680G>A/*MT-ND4L* variants have been recurrently associated with LHON, either in combination with other polymorphic variants or associated with other primary mutations. However, both variants alone are also reported in the normal population, remarking their non-pathogenicity when isolated (Tables 3, 4).

To validate on the functional ground the pathogenic role of the two combinations of variants found in Families 1 and 2, the only recognized method is to demonstrate a functional defect of mitochondrial respiratory chain in the cybrid cell model, where only the patient-derived mtDNA is transferred. We observed that ATP synthesis driven by Complex I substrates and respiration as measured by OCR were significantly defective in cybrids harboring the mitogenomes from Families 1 and 2 compared to haplogroup-matched controls. Remarkably, similar to the other LHON primary mutations with the exception of m.3460G>A/*MT-ND1*, the Complex I specific activity was not reduced in cybrids carrying the two combinations of variants (Carelli et al., 1997, 1999). Thus, even if other reports proposed that combinations of different variants might exert the equivalent pathogenic role of the single primary LHON mutation (Zhang et al., 2012; Zou et al., 2010), we here provide for the first time experimental evidence of the respiratory chain impairment from a functional point of view. Interestingly, the now available crystal structure of Complex I revealed that the large majority of these variants, either those found in the Italian Families 1 and 2, as well as those reported in Chinese families (Zhang et al., 2012; Zou et al., 2010) are located in close proximity to the predicted E-channel for proton translocation (Figures 10, 11), contributed by all three ND6, ND4L and ND1

subunits. Genetic variation along this pathway may alter the efficiency of proton translocation, ultimately affecting the energy conserving function of Complex I.

These results substantially change the general criteria used to date for the diagnosis of LHON, and, more in general, for the assessment of pathogenicity of mtDNA variants. In the case of the three branches of Family 1, we performed complete mtDNA sequencing because there was a clear evidence of maternal recurrence of a phenotype undistinguishable from classic LHON despite the absence of the three common LHON mutations. However, also the sequencing of the entire mitogenome in our entire cohort of Italian LHON families revealed the presence of multiple variants potentially relevant for LHON pathogenesis, beside the known primary LHON mutations. Therefore, we propose complete mitogenome sequencing as the gold standard for LHON diagnosis, to disclose possible unique combinations of variants, or double/triple mutants. In brief, the definition of a pathogenic mtDNA mutation becomes blurrier than ever, and only the accurate consideration of population-dependent mtDNA structure, combined with functional analyses using the cybrid cell model, may lead to its final validation. A good example for such a scenario is the m.3394T>C/*MT-ND1*, which might act as an adaptive variant selected for high altitudes in Tibet, while exerting a pathogenic effect on other mtDNA backgrounds and predisposing to LHON in China (Ji et al., 2012). Closely similar, other two adaptive variants for high altitude in Tibet, i.e. m.3745G>A/*MT-ND1* and m.4216T>C/*MT-ND1*, were also implicated in LHON (Kang et al., 2013). The m.3745G>A/*MT-ND1* was in fact found in combination with m.10680G>A/*MT-ND4L* in a Chinese LHON Family (Yang et al., 2009), whereas the m. 4216T>C/*MT-ND1* variant is at the shared root of the Western Eurasian haplogroups J and T, both possibly affecting the E-channel for proton pumping (Figure 11).

Mitochondrial DNA variability in Leber's hereditary optic neuropathy

The background mitogenome variability may be associated as a modifying factor to the "primary" mutations in LHON, this being particularly evident for the m.14484T>C/MT-ND6 mutation. In fact, according to the current literature the mitochondrial haplogroup J is well established to be a modifier of penetrance for this mutation, with the strongest association compared with the other LHON primary mutations, whereas non-J mtDNA backgrounds

display a very reduced penetrance for the m.14484T>C/MT-ND6 mutation (Carelli et al., 2006; Howell et al., 2003a; Hudson et al., 2007; Palanichamy et al., 2004).

However, all previous studies on LHON cohorts did not analyze the entire sequence of mitogenomes, but only a few SNPs, which are diagnostic markers of haplogrups, or at best included in some studies the sequence of the control region, with only a few pedigrees analyzed, i.e. 6 and 33 respectively (Carelli et al., 2006; Hudson et al., 2007). Thus, we decided to collect all available LHON families carrying the m.14484T>C/MT-ND6 mutation in Europe and perform the complete sequence analysis of the mitogenomes, to dissect the genetic variability and its relevance for this specific LHON primary mutation. We collected, thanks to a relevant international effort and collaborations, and analyzed 147 probands from apparently unrelated families. Our results confirmed the strong association with haplogroup J. The 45% of this LHON cohort, carrying the m.14484T>C/MT-ND6 mutation, had a haplogroup J background as compared to the 9% in controls, further reproducing the results reported by previous studies (Carelli et al., 2006; Hudson et al., 2007; Torroni et al., 1997). However, in our hands the association was weaker than in previous reports: in the first report (Torroni et al., 1997) the patients analyzed were only two, both with J haplogroup, whereas a following study found a 66.7% (4 out 6) of mutational events on J haplogroup (Carelli et al., 2006). Finally, the largest study ever by Hudson and colleagues reported a haplogroup J frequency of 99% in 851 LHON carrying m.14484T>C/MT-ND6 mutation, but this figure was reached by considering all individuals on the 33 available maternal lineages (Hudson et al., 2007).

Furthermore, the other difference we have observed between haplogroups T and H in our cohort may be due to the reduced frequency of haplogroup H, as counterpart of the J predominance, or to a milder modifier role of haplogruop T, which shares the common phylogenetic root as haplogroup J. This latter interpretation is corroborated by the normal distribution we have found by dissecting the haplogroup J sub-clades, compared to controls, failing to confirm the previously proposed preferential association of the J1 clade with the m.14484T>C/MT-ND6 mutation (Carelli et al., 2006; Hudson et al., 2007).

A side result of our sequencing analysis of such a large number of mitogenomes is the correction of previous haplogroup affiliation in some families, which was wrong. The previous analysis was carried out by RFLP, considering only a limited number of diagnostic variants for each haplogroup. In particular, the presence of the change m.10398A>G/MT-ND3 was

discriminating between haplogroup J and haplogroup T, while the change m.4216T>C/MT-ND1 was at the root of haplogroups J and T. From our new analysis, however, these changes were private variants, outside the canonical mtDNA background, confirming the complexity of the mitogenome variation.

The assessment of a possible functional impact of the missense private variants, besides the m.14484T>C/MT-ND6 mutation, was based on amino acid conservation and *on-line* prediction tools, and revealed in some instances double mutants and synergistic changes.

In 2 independent families, besides the primary LHON m.14484T>C/MT-ND6 mutation, a second LHON "primary" mutation was found (m.3460G>A/MT-ND1 and m.11778G>A/MT-ND4). This kind of event, though rare, was already reported in one family with both m.3460G>A and m.11778G>A and 6 families with both m.14484T>C and m.11778G>A (Brown et al., 2001; Catarino et al., 2017; Cruz-Bermúdez et al., 2016; Howell et al., 2002; Riordan-Eva et al., 1995; Tonska et al., 2008). Most cases carried the second "primary" mutation in a heteroplasmic state, besides one primary homoplasmic changes, and the coexistence of two primary mutations did not apparently modify the phenotype, most cases displaying a classic LHON (Catarino et al., 2017). Only in two families the double mutation seemed to increase the proportion of affected females, impacting on the male:female ratio (Catarino et al., 2017; Howell et al., 2002).

Other variants in CI subunits genes were predicted to be pathogenic: the m.4136A>G/MT-ND1, m.4160T>C/MT-ND1, m.4184T>A/MT-ND1, m.10237T>C/MT-ND3. The m.4160T>C/MT-ND1 (p.L285P) was already associated with LHON in an Australian family (Queensland family) carrying also the m.14484T>C/MT-ND6 and affected by a complex multisystemic neurological disorder compatible with the definition of LHON "plus" (Howell et al., 1991, 1995). The sequence analysis of this family was limited to the CI subunits genes only, and based on the reported data (Howell et al., 1991) the haplogroup affiliation of this Australian family is compatible with haplogroup U, carrying some diagnostic variants for this haplogroup (m.14647A>G/MT-ND6 and m.12372G>A/MT-ND6, both in MT-ND6). The family carrying the same combination of variants (m.4160T>C/MT-ND1 + m.14484T>C/MT-ND6) identified in our cohort is originally from France and showed the same haplogroup, U5a1a12b, suggesting a possible founder event or a migration of a female in Australia, even though the Queensland family was thought to be originally from Scotland. Furthermore, in a branch of the large

Australian pedigree there was a third m.4136A>G/MT-ND1 variant, which was proposed as an intragenic suppressor, ameliorating the complex neurological phenotype associated with complex I deficiency (Howell et al., 1991).

The m.4160T>C/MT-ND1 was also reported in patients with thymidine phosphorylase deficiency, as somatic mtDNA point mutation (Nishigaki et al., 2003) and in a healthy control (Lippold et al., 2014). Thus, the specific pathogenic role of this change affecting a conserved position remains uncertain.

The m.4136A>G/MT-ND1 (p.Y277C) variant was found in 49 controls, on 26 independent mtDNA backgrounds, but never on L2a1l2 (www.mitomap.org), as in our French proband, and it was also previously found associated to m.11778G>A/MT-ND4 LHON mutation in Italy, with a possible synergic role (La Morgia et al., 2008).

The m.4184T>A/MT-ND1 (p.F293Y) variant has never been found in the control population (www.mitomap.org); moreover, the same position, but with a different nucleotide change T>G causing a different amino acid substitution (p.F293C), was found mutated in a Russian LHON family carrying also the m.3460G>A/MT-ND1, on haplogroup T1 (Povalko et al., 2005).

The m.10237T>C/MT-ND3 (p.I60T) was found in 54 controls, on 20 independent mtDNA backgrounds, but never on the haplogroup T2b25 sub-clade (www.mitomap.org), as in our German proband. The same mutation was found in a Hungarian LHON patient not carrying the common primary mutations (Horvath et al., 2002).

The m.4659G>A/MT-ND2 (p.A64T) was found in 57 controls, on 27 independent mtDNA backgrounds, but never on the haplogroup J1b1a1d sub-clade (www.mitomap.org), as in our German proband. This variant was postulated to increase the risk of developing Parkinson disease (Khusnutdinova et al., 2008), and it also is a marker of haplogroup H2a1n.

Other putative “secondary” pathogenic mutations were found in CIV and CV subunits: m.6712A>T/MT-CO1, m.8516T>C/MT-ATP8, m.8989G>A/MT-ATP6, m.9025G>A/MT-ATP6 and m.9957T>C/MT-CO3. All these variants are rare, found a few times in the normal population (1, 4, 10, 24, 27, respectively), and never associated with pathologic phenotypes (www.mitomap.org). The only exception is the m.9957T>C/MT-CO3 variant, previously associated with several forms of mitochondrial encephalomyopathy: mitochondrial encephalomyopathy, lactic acidosis and stroke-like episodes (MELAS) (Manfredi et al., 1995), chronic progressive external ophthalmoplegia (CPEO) (Liu et al., 2011), and non-arteritic

ischemic optic neuropathy (Abu-Amero et al., 2005). A cell study on cybrids carrying this mutation showed a normal respiration, but increased ROS production (Lenaz et al., 2004).

The putative synergistic variants (m.4824A>G/MT-ND2, m.6261G>A/MT-CO1, m.7080T>C/MT-CO1, m.8557G>C/MT-ATP8, m.8812A>G/MT-ATP6, m.8953A>G/MT-ATP6, m.9055G>A/MT-ATP6) were found in 57, 1052, 253, 40, 18, 46, 4, 1769, 27 controls, respectively. All variants were not associated with any neurological conditions, except for the m.6261G>A/MT-CO1 and m.9055G>A/MT-ATP6 variants. The m.6261G>A/MT-CO1 variant, besides being found in cancer as a somatic mutation, was also associated with a LHON-like optic neuropathy in a patient negative for primary LHON mutations, on haplogroup T2 (Abu-Amero and Bosley, 2006). Moreover, this variant is a marker of several haplogroups (www.phylotree.org), which lowers its possible pathogenic role as a primary mutation. The m.9055G>A/MT-ATP6, in the frame of an association study of mitochondrial haplogroups and Parkinson disease, was assigned a putative protective effect for women (van der Walt et al., 2003). The same variant was studied in metabolic disease, failing to find any association (Saxena et al., 2006). After all considered, the m.9055G>A/MT-ATP6 is a marker of haplogroup K (www.phylotree.org), and was found on the haplogroup H in our case.

The phylogenetic analysis showed that some families cluster into a common origin, suggesting founder events. In particular, 11 probands, apparently independent from the geographical point of view, share the common J1b1a1 root, and diverged in at least 5 separate branches, which were country-related. There were similar events on J1c1d in Germany, on J1c2j, T1a2, T2 in Italy, on T2c1d1 in both Italy and France. All these cases may be the result of a founder effect, assuming that the m.14484T>C/MT-ND6 mutational event occurred early during the evolution and became fixed. Alternatively, the LHON mutational events might have arisen independently, suggesting that some mitogenomes could predispose to mutagenesis at position m.14484T. According to Carelli and colleagues (Carelli et al., 2006), the six Italian LHON families originally studied in their previous report carried the m.14484T>C/MT-ND6 mutation on independent mitochondrial backgrounds, thus the preferential association of the m.14484T>C/MT-ND6 LHON mutation with haplogroup J1 was interpreted as not due to founder events but to a true mtDNA background effect. It was also proposed that the specific combination of amino acid changes in the cytochrome b is the possible cause of the mtDNA background effect, and that this may occur affecting the supercomplex formation, by co-

assembling respiratory-chain complexes I and III (Carelli et al., 2006). However, differently from the Italian population, a clear major founder event that might have occurred 900–1,800 years ago has been recognized in Northern Europe (Dutch and French population) and in Canada (French-Canadian population) on haplogroup J1c1d (Howell et al., 2003b). The association of m.14484T>C/MT-ND6 mutation with haplogroup J does not apply to non-European population: for example, a study of an Indian LHON cohort showed an association with different mtDNA backgrounds (F1c1, M31a, U2a, M*, I1, M6, M3a1, and R30a), as independent mutational events (Khan et al., 2013).

Finally, on the clinical ground, penetrance in LHON families carrying the m.14484T>C/MT-ND6 mutation on haplogroup J was higher than those on non-J haplogroups. This was a non-significant tendency that applied to both genders. Unfortunately, besides the association studies there are no published data on this issue, with the actual calculation of penetrance in in large cohorts of families, except for a few maternal lineages (Caporali et al., 2017). Moreover, as reported in literature, the ratio between affected males and females was 7.7:1 (Macmillan et al., 1998; Yu-Wai-Man and Chinnery, 2016). In our cohort, this ratio is about half (3.5:1), and in the haplogroup J background families it decreases to 2.7:1, while in the non-J was 4.2:1. Thus, the contribution of haplogroup J seems to be limited to a slight increase of penetrance, especially true in females carrying the m.14484T>C/MT-ND6 mutation.

Mitochondrial DNA variability in Dominant Optic Atrophy (DOA) with OPA1 mutations

Hypothetically, the mtDNA background may be also a modifier in DOA families carrying a mutation in the OPA1 gene, considering the consolidated role of mitogenome variability in LHON and the clinical and pathophysiological similarities between DOA and LHON. The mitochondrial haplogroups have been already investigated in DOA, and these studies failed to reveal any association (Han et al., 2006; Pierron et al., 2009). Our results confirmed this finding, as expected for a dominantly inherited disorder (Figure 15). We used the same mtDNA sequencing approach for DOA as for the m.14484T>C/MT-ND6 LHON cohort, and we have analyzed all private missense changes to detect the presence of putative pathogenic mutations or synergistic variants, besides the normal population-specific variability (Table 10). This analysis revealed 10 changes with a possible pathogenic role. Most of them are reported as rare population polymorphisms (www.mitomap.org). Both the m.4659G>A/MT-ND2

(p.A64T) and m.9957T>C/MT-CO3 variants were already found in our m.14484T>C/MT-ND6 LHON cohort, as well as associated to other neurological disorders. The m.4659G>A/MT-ND2 was postulated to increase the risk of developing Parkinson disease (Khusnutdinova et al., 2008), and is also a marker of haplogroup H2a1n. As commented in the previous paragraph, the m.9957T>C/MT-CO3 was found in 27 individuals, healthy controls and patients, and was previously associated with several form of mitochondrial encephalomyopathy (Abu-Amero et al., 2005; Liu et al., 2011; Manfredi et al., 1995) and its pathogenicity evaluated on cybrids (Lenaz et al., 2004). However, the pathogenic role of this mutation is now questioned based on our current results. Next, the m.15773 G>A/MT-CYB (p.V343M) was found in 39 controls, in 28 independent backgrounds, but never on H43 haplogroup, and, in particularly, was found associated with the m.11778G>A/MT-ND4 LHON mutation, with a possible synergic role (La Morgia et al., 2008) supporting a putative role in modulating neurodegeneration.

Furthermore, the putative synergic variants m.4824 A>G/MT-ND2, m.7754 G>A/MT-CO2, m.7805 G>A/MT-CO2, m.8896 G>A/MT-ATP6, m.8953 A>G/MT-ATP6, m.12674 A>G/MT-ND5, m.14180 T>C/MT-ND6, found in the DOA cohort, were also found in 1052, 19, 334, 28, 4, 11, 138 controls respectively, and never associated with a pathological condition.

We thus investigated the mitogenome variability as a possible modifier in the DOA clinical outcome, evaluating the haplogroup association with the RNFL thickness, as evaluated by OCT and reliable readout of disease severity. First, we analyzed the effect of the putative pathogenic mutations and synergistic variant found in mtDNA. These mutations did not impinge on the clinical outcome of DOA patients (Figures 15, 16).

Second, we evaluated the mitogenomes variability, fixed by evolution (Figures 16, 17), finding that DOA patients on the haplogroup U background maintain a significantly higher RNFL thickness on the temporal quadrant as compared with those carrying haplogroup H. Remarkably, the specificity for the temporal fibers, which are the main disease target, possibly indicates a real protective role. Noticeably, haplogroup H is the most frequent in Europe and often found to be more prevalent in healthy control subjects than in patient study groups (Mueller et al., 2012), but sometime was also associated as risk factor, i.e. for late onset Alzheimer's disease (Santoro et al., 2010). Haplogroup U is the second most frequent, and haplogroup K stems from it as sub-clade. Haplogroup U has also been associated with several clinical conditions, i.e. psychosis in bipolar disorder (Frye et al., 2017), reduction of physical

performance (Arjmand et al., 2017), or severe progression of knee osteoarthritis (Rego-Pérez et al., 2008). However, this haplohgroup as a whole, or in association with its sub-clade K, has also been assigned a protective role for Parkinson disease, a neurodegenerative disorder with a clear involvement of mitochondrial dysfunction, particularly of complex I, in its pathogenesis (Giannoccaro et al., 2017). This latter observation further supports that OPA1-related DOA, which has a documented complex I defect (Zanna et al., 2008), may benefit of a protective effect from the association with haplogroup U, in analogy with Parkinson disease.

Last, we evaluated the effect of the interaction between the mitochondrial and nuclear genomes. This approach is based on the widely discussed issue of preferntial coadaptation between the nuclear and mitochondrial genomes, thus involving in the clinical outcome of DOA the co-inheritance of mtDNA changes with the OPA1 mutation (Figure 18). To this end, we compared the clinical severity, assessed as RNFL thickness in the two possible segregations mother-child (same mitogenome) vs father-child (change of the mitogenome haplogroup). This analysis revealed that the mother-children segregations displayed a statistically significant worsening of the clinical outcome, particularly on the average and inferior quadrant RNFL thickness, with the other quadrants (temporal, superior and nasal) presenting the same trend. On the contrary, the only significant difference in the father-children segregations was on the temporal quadrant, with a similar outcome on the other quadrants and on the average assessment. These results strongly indicate that the nuclear genome variation seems to play the major role on severity of DOA carrying dominant OPA1 mutations, as exemplified in the mother-child segregations where the mitogenome remains the same.

Common features between LHON and DOA

Interestingly, the otherwise normal variants found in the peculiar pathogenic combination in the two independent LHON families, were also found in both LHON and DOA cohorts. The m.14258G>A/MT-ND6 was found in one proband of the m.14484T>C/MT-ND6 LHON cohort, on a L2a1a1 mtDNA background, and in one patient with OPA1 mutation, on a K1a background. The m.10680G>A/MT-ND4L variant was found in 4 families on H, T2, U1a1a1 and X2d1 haplogroups, only in the LHON cohort. The m.14582A>G/MT-ND6 variant was found in 1 case on H1bm haplogroup, while the m.12033A>G/MT-ND4 was not found in any proband of the two LHON and DOA cohorts. These findings confirm the association of these variants

with LHON, especially the m.10680G>A/MT-ND4L, and their relative frequency in the population, although rare.

CONCLUSIONS

The current study provides genetic and functional evidence that specific and previously unreported combinations of missense mtDNA variants, which individually obey the definition of population polymorphisms, may exert a sufficient pathogenic potential for being causative of low-penetrance LHON.

This finding seems to be the extreme end of a wide and complex molecular landscape clearly implicating the interaction of the haplogroup-specific variants, as well as the private variants, with the clearly pathogenic mutations, as in the case of the LHON cohort carrying the m.14258G>A/MT-ND6 mutation. This interaction seems to be very strong also in the LHON cohort carrying the primary m.14484T>C/MT-ND6 mutation. The association with the haplogroup J root highlights this complex interplay, revealing also the importance of geographic mitogenome stratification with the occurrence of multiple founder events in Europe, as well as the possibility that certain mitogenomes may predispose to mutagenesis, which becomes eventually fixed during evolution.

More complex and still completely open is the scenario in DOA, where we documented a minor effect that could be ascribed to the mitogenome variation, as compared with what it seems a stronger role of nDNA modifying effect.

Overall, this study highlights the complexities of mtDNA sequence variability, introducing a perspective that will necessarily change the approach for assigning the pathogenic role to single or peculiar combinations of mtDNA variants, and modifying the criteria for diagnostics in mitochondrial human diseases (Montoya et al., 2009).

MATERIALS AND METHODS

Patients

Total DNA was extracted by standard methods from blood cells, urinary sediment epithelium and skeletal muscle after informed consent and approval of the internal review board at University of Bologna for Italian patients.

For the Europen LHON cohort carrying m.14484T>C/MT-ND6 mutation the informal consent was approved by local review board and total DNA was extract from blood.

The LHON cohort are composed by 147 probands: 52 from Italy (Prof. Carelli, University of Bologna, Institute of Neurological Sciences; Prof. Federico, University of Siena; Dr. Garavaglia and Dr. Zeviani, Besta Institute, Milan), 43 from Germany (Prof. Wissinger, University of Tubingen; Prof. Klopstok, University of Munich), 27 from France (Dr. Amati Bonneau, University of Angers), 19 from UK (Prof. Cinnery, University of Chambridge), 3 from Spain (Prof. Montoya, University of Saragozza) and 3 from US (Prof. Sadun, Doheny Eye Centers-UCLA), but with European ancestry.

The dominant optic atrophy (DOA), carrying OPA1 mutations, are composed by 85 families with 112 maternally unrelated patients. The variants are described according to OPA1 transcript variant 1 (RefSeq: NM_015560.2) (Table 11). All patients were referred to Prof. Valerio Carelli, at Neurophthamology Clinic (IRCCS Institute of Neurological Science, University of Bologna).

Family	Mutation	Effect	Family	Mutation	Effect
1	c.1334G>A	p.R445H	44	c.1899_90del	p.E630FfsX2
2	c.889C>T	p.Q297X	45	c.2771_2773del	p.K924del
3	c.1212+1G>A	Splice defect	46	c.2733_2734del	p.E912GfsX7
4	c.1807G>C	p.D603H	47	c.931G>C	p.A311P
5	c.1516+1G>A	Splice defect	48	c.2825_2828del	p.V942EfsX25
6	c.815T>C	p.L272P	49	c.1212+5G>C	Splice defect
7	c.2708_2711del	p.V903GfsX3	50	c.1334G>A	p.R445H
8	c.1146A>G	p.I382M	51	c.2713C>T	p.R905X
9	c.1516+1G>A	Splice defect	52	c.1669C>T	p.R557X
10	c.1516+1G>C	Splice Defect	53	c.2713C>T	p.R905X
11	c.2708_2711del	p.V903GfsX3	54	c.2215C>T	p.Q739X
12	c.2569C>T	p.R857X	55	c.2825_2828del	p.V942EfsX25
13	c.1724_1725del	p.E575fsX576	56	c.1410_1443+5del	p.D470fsX
14	c.1770G>A	Exon Skipping	57	c.1346_47insC	p.T449fsX
15	c.2470C>T	p.R824X	58	c.1462A>G	p.G488R
16	c.751delG	p.D251MfsX13	59	c.2708_2711del	p.V903GfsX3

17	c.631_634del	p.D211KfsX16	60	c.2708_2711del	p.V903GfsX3
18	c.2729T>A	p.V910D	61	c.984+3A>T	Splice Defect
19	c.703C>T	p.R235X	62	c.984+3A>T	Splice Defect
20	c.2825_2828del	p.V942EfsX25	63	c.2825_2828del	p.V942EfsX25
21	c.2708-2A>T	Splice Defect	64	c.1334G>A	p.R445H
22	c.2482delG	p.V828X	65	c.2771_2773del	p.K924del
23	c.2819-2A>C	Exon Skipping	66	c.2726del	p.N909MfsX58
24	c.2341C>T	p.R781W	67	c.869G>A	p.R290Q
25	c.1444-1G>C	Splice defect	68	c.869G>A	p.R290Q
26	c.2341C>T	p.R781W	69	c.870+5G>A	Splice Defect
27	c.1196T>A	p.L399X	70	c.2331C>A	p.Y777X
28	c.2708_2711del	p.V903GfsX3	71	c.1484C>T	p.A495V
29	c.893G>A	p.S298N	72	c.113_130del	p.R38_S43del
30	c.2496+1G>A	Splice defect	73	c.869G>A	p.R290Q
31	c.1609del	p.H537fs540X	74	c.1778T>C	p.L593P
32	c.869G>A	p.R290Q	75	c.2671_2694dup	p.891_898dup8
33	c.751delG c.2341C>T	p.D251MfsX13 p.R781W	76	del exons21-23	-
34	c.2131C>T	p.R711X	77	c.2825_2828del	p.V942EfsX25
35	c.1212+3A>T	Splice defect	78	c.889C>T	p.Q297X
36	c.869G>A	p.R290Q	79	c.2331C>A	p.Y777X
37	c.1462A>G	p.G488R	80	del exons2-11	-
38	c.2708_2711del	p.V903GfsX3	81	c.703C>T	p.R235X
39	c.751delG	p.D251MfsX13	82	c.784-21_784-22InsAluYb8	Exon Skipping
40	c.1587del	p.L529fs534X	83	c.1316G>T	p.G439V
41	c.869G>A	p.R290Q	84	c.1187T>G	p.L396P
42	c.869G>A	p.R290Q	85	c.2815del	p.L939Sfs28
43	del exon19	-			

Table 11. OPA1 mutation

The RNFL (retinal nerve fibers layer) thickness was evaluated in 91 patients, from 49 families, by the Stratus OCT (Optical Coherent Tomography), at Prof. Valerio Carelli's Neurophthamology Clinic (IRCCS Institute of Neurological Science, University of Bologna) and Dr. Piero Barboni's clinic (Studio Oculistico d'Azeglio, Bologna). Data are shown in Table 12.

Family	**Relationship**	**OD**					**OS**				
		AVG	**T**	**S**	**N**	**I**	**AVG**	**T**	**S**	**N**	**I**
3	Proband	52	38	77	48	46	48	29	73	45	43
4	Brother	64	33	66	71	85	43	36	53	41	43
4	Maternal granfather	75	35	93	77	95	83	35	98	96	105
4	Mother	87	38	123	63	123	95	35	142	73	128
4	Proband	46	33	71	33	48	55	26	80	48	67
5	Father	55	35	71	46	67	49	24	74	40	50
5	Proband	66	30	100	58	75	65	34	87	60	79
7	Proband	59	26	92	55	61	64	28	95	61	71
8	Father	84	77	102	51	106	87	57	118	64	111
8	Proband	89	44	101	98	116	85	42	106	82	109
10	Proband	73	27	106	75	84	70	34	109	60	78
12	Proband	62	32	88	57	71	59	31	90	51	63
13	Sister	100	64	130	79	125	73	26	89	53	122
14	Proband	61	24	94	65	60	57	28	88	46	64

18	Father	56	34	65	51	74	62	35	85	47	80
18	Proband	68	39	83	56	95	71	35	113	47	88
18	Paternal aunt	59	38	88	51	61	60	36	88	55	63
19	Proband	59	32	86	60	60	60	60	91	31	59
22	Brother	98	49	131	97	114	115	61	146	118	134
22	Mother	85	45	122	79	92	91	45	120	103	95
22	Maternal Granmother	89	76	90	61	131	75	55	95	55	96
22	Proband	71	26	123	67	67	73	27	131	63	70
23	Father	66	40	94	64	68	65	31	85	56	90
23	Proband	82	34	105	99	90	73	26	102	81	82
23	Sister	65	36	94	68	64	64	34	88	60	73
26	Mother	92	81	115	64	110	95	71	133	62	116
26	Proband	59	26	100	50	59	62	34	107	47	62
27	Proband	67	30	91	67	78	74	40	95	69	93
27	Sister	78	49	106	64	94	77	42	103	71	91
28	Father	76	45	101	62	97	86	52	103	91	97
28	Proband	73	51	101	59	82	69	52	73	56	95
29	Proband	46	34	59	33	59	40	42	42	27	50
30	Proband	93	43	125	94	110	93	34	134	94	111
32	Mother	57	38	76	54	61	74	68	77	98	55
32	Proband	61	29	88	65	61	62	41	87	60	59
32	Proband	61	48	76	56	64	58	42	79	59	54
32	Maternal aunt	65	25	99	61	76	67	31	102	57	80
35	Father	63	36	86	54	75	58	33	84	51	62
35	Proband	57	28	95	49	57	54	31	83	46	57
36	Proband	52	45	60	45	59	42	29	47	35	55
37	Nephew	58	27	83	49	73	59	33	91	41	69
37	Nephew	103	68	128	93	124	106	71	122	105	127
37	Proband	69	48	81	60	88	65	45	83	47	86
38	Daughter	49	27	69	50	51	57	32	81	63	52
38	Proband	62	30	87	63	69	60	28	99	49	62
39	Sister	60	31	84	53	71	54	30	82	39	64
40	Son	72	47	89	61	95	72	54	90	57	89
40	Proband	48	23	72	47	48	49	27	75	42	51
45	Proband	69	54	86	58	79	73	53	92	48	98
48	Mother	68	29	90	74	80	70	31	93	67	89
48	Proband	54	27	71	63	56	60	38	82	59	61
52	Proband	66	35	101	50	80	72	32	112	68	79
54	Brother	75	28	118	79	74	82	34	92	99	102
54	Cousin	63	46	102	55	49	50	27	76	45	53
54	Proband	80	41	105	77	95	92	73	112	66	118
55	Proband	74	57	85	70	83	61	38	88	60	57
57	Mother	78	33	104	64	112	82	29	114	64	123
57	Proband	53	26	94	43	50	61	34	106	48	56
57	Sister	74	40	112	69	77	70	34	108	45	91
60	Father	83	43	106	81	102	82	44	126	63	96
60	Proband	66	29	80	74	82	67	29	88	73	79
61	Brother	54	47	42	49	77	56	44	76	43	60
61	Mother	60	31	80	60	68	56	35	69	55	63
61	Proband	54	41	64	42	71	na	na	na	na	na
62	Father	61	38	89	51	67	55	25	77	50	68
62	Paterna granfather	46	28	53	50	53	51	35	71	51	49
62	Proband	56	27	80	48	70	55	24	91	48	58
62	Sister of paternal granfather	40	25	55	36	46	48	39	60	38	54

64	Father	43	36	45	38	52	48	32	62	48	48
64	Proband	59	57	56	41	83	63	39	75	52	86
66	Father	na	na	na	na	na	66	42	111	46	63
66	Proband	41	26	68	34	36	46	27	69	39	49
68	Mother	50	47	63	34	55	42	37	56	27	47
68	Proband	50	35	70	39	58	50	30	63	43	65
68	Sister	59	33	89	44	69	63	44	91	53	65
69	Proband	70	34	108	66	72	71	35	95	69	87
70	Mother	62	26	84	62	77	60	28	78	59	74
70	Proband	66	38	100	61	66	56	34	87	41	63
72	Paternal aunt	84	55	108	54	120	86	58	109	50	127
73	Proband	59	33	64	47	93	53	30	65	36	79
74	Proband	44	36	63	38	38	42	31	55	39	45
74	Sister	39	30	54	29	41	43	31	54	39	47
75	Proband	78	29	123	79	81	80	42	121	66	94
78	Brother	62	41	87	59	60	60	36	87	53	63
78	Proband	57	35	76	50	66	63	34	78	61	80
79	Proband	76	46	94	57	94	61	39	86	47	72
81	Proband	65	33	89	62	74	59	38	65	64	70
82	Proband	51	28	74	42	58	50	33	86	36	46
83	Father	51	59	44	33	68	na	na	na	na	na
83	Proband	44	38	44	44	48	na	na	na	na	na
85	Father	75	50	93	64	92	72	51	94	55	86

Table 12. RNFL thickness by OCT of DOA patient carrying OPA1 muations
OD: Right eye, OS: Left eye; AVG: average; T: temporal; S: superior; N: nasal; I: inferior.

Sanger mtDNA sequencing

Direct sequence analysis of the entire mtDNA molecule was performed on total DNA, by Sanger (Torroni et al., 2001). The protocol consists in 11 amplicons (Table 13). The PCR mixture contained 50 ng of DNA, 0.5U GoTaq® G2 Flexi DNA Polymerase 5U/µl (Promega), 1x Colorless GoTaq® Flexi Buffer 5X (Promega), 200 µM PCR nucleotides mix (Life Technologies), 200 µMeach primers (Sigma-Aldrich), in a final volume of 25 µl. The cycle conditions were 94°C for 5 min, 30 cycles of 30 sec at 94°C, 30 sec at 55°C, 72°C for 30 sec, and a final extensionof 7 min at 72°C.

Primer	**Position (mtDNA)**		**Sequence (5' →3')**	**Length product (bp)**
1F	14900	149191	GCCATGCACTACTCACCAGA	1760
1R	90	71	AATGCTATCGCGTGCATACC	
2F	16458	16477	CCCATAACACTTGGGGGTAG	1682
2R	1570	1549	TGTAAGTTGGGTGCTTTGTGTT	
3F	1404	1425	ACTTAAGGGTCGAAGGTGGATT	1832
3R	3235	3214	CTTAACAAACCCTGTTCTTGGG	
4F	2932	2951	GGGATAACAGCGCAATCCTA	1607
4R	4538	4519	GCTTAGCGCTGTGATGAGTG	
5F	4366	4387	AAAATTCTCCGTGCCACCTATC	1659
5R	6024	6003	TTATGTTGTTTATGCGGGGAAA	

6F	5871	5892	GCTTCACTCAGCCATTTTACCT	1747
6R	7617	7596	TCTTGTAGACCTACTTGCGCTG	
7F	7356	7379	GTAGAAGAACCCTCCATAAACCTG	1822
7R	9177	9154	TAGAAGTGTGAAAACGTAGGCTTG	
8F	8896	8914	GCCCTAGCCCACTTCTTACC	1740
8R	10728	10708	GGCCATATGTGTTGGAGATTG	
9F	10466	10485	CCAAATGCCCCTCATTTACA	1774
9R	12240	12221	GGGGCATGAGTTAGCAGTTC	
10F	12014	12035	CTCACCCACCACATTAACAACA	1816
10R	13829	13808	AGTCCTAGGAAAGTGACAGCGA	
11F	13504	13525	TACTCCAAAGACCACATCATCG	1804
11R	15307	9184	GAAGGGCAAGATGAAGTGAAAG	

Table 13. 11 amplicons primer list for mitochondrial genome amplification

PCR product was displayed through electrophoretic run on agarose gel (1%), with the addition of GelStar (Lonza) at UV light, using as size marker GeneRuler 100 bp Plus DNA Ladder (Thermo Scientific). PCR products were purified with magnetic beads (AMPure XP, Beckman Coulter) following the manufacturer instructions.

The sequencing reaction mixture contained 100-200 ng of DNA template, 0.5% DMSO (dimethyl sulfoxide), 1.5µl of Sequencing Buffer 5X, 200µM of Primer, 1µl of BigDye Terminator 3.1 Cycle Sequencing Kit (Life Techonologies), in a final volume of 10µl

The cycle conditions were 25 cycles of 10 sec at 96°C, 5 sec at 50°C, 4 min at 60°C. For each amplicon three primers were used to sequence and their details are shown in Table 14.

Amplicon	**Position (mtDNA)**		**Sequence(5'-3')**
1	14948	14967	CACATCACTCGAGACGTAAA
1	15564	15583	ATTTCCTATTCGCCTACACA
1	58	39	AATACCAAATGCATGGAGAG
2	16522	16541	TAAAGCCTAAATAGCCCACA
2	584	603	TAGCTTACCTCCTCAAAGCA
2	1060	1079	AAGACCCAAACTGGGATTAG
3	1445	1464	GAGTGCTTAGTTGAACAGGG
3	2047	2066	TTTAAATTTGCCCACAGAAC
3	2509	2528	ATCACCTCTAGCATCACCAG
4	3067	3088	TGAGTTCAGACCGGAGTAAT
4	3540	3561	TCTCACCATCGCTCTTCTAC
4	4010	4029	ACACCCTCACCACTACAATC
5	4410	4429	CAGCTAAATAAGCTATCGGG
5	5014	5033	CCTCAATTACCCACATAGGA
5	5544	5563	TCAAAGCCCTCAGTAAGTTG
6	6041	6060	CCTTCTAGGTAACGACCACA
6	6473	6492	CACAGCAGTCCTACTTCTCC
6	7027	7046	CCCACTTCCACTATGTCCTA

7	7416	7435	TTCGAAGAACCCGTATACAT
7	7987	8006	ACTCCTTGACGTTGACAATC
7	8505	8524	ATAACAAACCCTGAGAACCA
8	8975	8992	TCATTCAACCAATAGCCC
8	9589	9608	AAGTCCCACTCCTAAACACA
8	10147	10166	ACATAGAAAAATCCACCCCT
9	10498	10519	TAGCATTTACCATCTCACTTCT
9	11081	11100	ATAACATTCACAGCCACAGA
9	11644	11663	CCTCGTAGTAACAGCCATTC
10	12114	12132	ACATCATTACCGGGTTTTC
10	12611	12630	ATTCATCCCTGTAGCATTGT
10	13134	13153	AGCAGAAAATAGCCCACTAA
11	13596	13615	CGCCTATAGCACTCGAATAA
11	14115	14134	CCCACTCATCCTAACCCTAC
11	14646	14665	CACTCAACAGAAACAAAGCA

Table 14. Primer list for mitochondrial genome sequencing

Sequence analysis was performed using the Sequencer 4.10 software (Gene Codes), comparing with the reference mitochondrial DNA sequence, rRCS (NC_012920) (Andrews et al., 1999).

NGS mtDNA sequencing

The Next Generation Sequencing (NGS) protocol consists in two long PCR amplicons (9.1 kb and 11.2 kb) (Stawski, 2013) and we amplified using Q5 High-Fidelity DNA Polymerase (with fidelity 280 times higher than Taq) (New England Biolabs). The PCR mixture contained 50 ng of DNA, 1U Q5 High-Fidelity DNA Polymerase (New England Biolabs), 1x Q5 Reaction Buffer (New England Biolabs), 200 µM PCR nucleotides mix (Life Technologies), 500 µM each primer (Sigma-Aldrich), in a final volume of 25 µl. The cycle conditions were 94°C for 5 min, 30 cycles of 30 sec at 94°C, 30 sec at 55°C, 72°C for 30 sec, and a final extensionof 7 min at 72°C (Table 15).

Primer	**Position (mtDNA)**		**Sequence (5'-3')**	**Length product (bp)**
MTL-F1	9397	9416	AAAGCACATACCAAGGCCAC	9064
MTL-R1	1892	1873	TTGGCTCTCCTTGCAAAGTT	
MTL-F2	15195	15214	TATCCGCCATCCCATACATT	11170
MTL-R2	9796	9773	AATGTTGAGCCGTAGATGCC	

Table 15. NGS primer list for mitochondrial genome amplification

PCR product was displayed through electrophoretic run on agarose gel (1%), with the addition of GelStar (Lonza) at UV light, using as size marker EZ Load™ 1 kb Molecular Ruler (Bio-Rad).

PCR products were purified with magnetic beads (AMPure XP, Beckman Coulter) following the manufacturer instructions.

The library was constructed by Nextera XT DNA Library Preparation Kit (Illumina, San Diego, CA). After fluorimetric quantification, using Quantus Fluorometer with Quantifluor dsDNA System (Pomega), the target DNA were diluted to the final concentration of 0,4 ng µL. The first step is tagmentation reaction, using "NexteraXT Transposome", which fragment DNA adding simultaneously DNA adapters ends. The reaction, in a final volume of 20 µl, contains 2 ng of DNA, 10 µl TD (Tagment DNA Buffer), 5 µl of ATM (Amplicon Tagment Mix), incubated at 55°C for 5 min, and immediately added 5 µl of NT (Neutralize Tagment Buffer) and incubated at 25°C for 5 min.

Then, a PCR amplification (Limited-Cycle PCR) added the Index 1 (i7), Index 2 (i5), and full adapter sequences to the tagmented DNA from the previous step. Every sample had a unique index combination, to be distinguished in the sequences reaction. 15 µL of NPM (Nextera PCR Master Mix), 5 µL of index 1 primers (N7XX) and 5 µL of index primers 2 (S5XX) are added. Themalcycler program is 72°C for 3 min, 95°C for 30 sec, 12 cycles at 95°C for 10 sec, 55°C for 30 sec, 72°C for 30 sec, final extention at 72°C for 5 min and hold at 10°C.

The PCR product were purified using magnetic beads, AMPure XP (Beckman-Coulter), following the manufacturer instructions, and quantified with fluorimetric method Quantus Fluorometer with Quantifluor dsDNA System (Promega). The normalized DNA were pooled. The pool where quantified and concentration is converted from ng/ µL to nM, according with this formula:

$$(concetration\ in\ ng/\mu l)\ /\ (660\ g/mol\ x\ average\ library\ size)\ x\ 10^6 = concentration\ in\ nM$$

where 660g/mol represents the mean value of the molar mass of a pair of dsDNA bases, assuming that average size of the bases is 650 bp. Pool were diluted to a final concentration of 4 nM.

5 µL of the 4nM library are added to 5 µL of fresh NaOH 0,2 N, mixed and incubated at room temperature for 5 min for DNA denaturation. A volume of 990 µL of cold Hybridization Buffer are added to obtain a library final concentration of 20 pM. Simultaneously, the PhiX control library, mixing mtDNA library with 1% of PhiX in 600 µL final volume, was carried out on the

MiSeq (Illumina) sequencer.

The sequencing parameters consisted in 150 cycles in Paired End (2x150) on MiSeq Reagent Kit v3, 600 cycles (Illumina).

Sequence output given from sequencer is a file in FASTAQ format, where each base call is associated to a "quality score". Through instrument software (MiSeq Reporter), sequences are aligned to the mitochondrial genome reference sequence, rCRS (revised Cambridge Reference Sequence), creating the alignment file (BAM) and identifying also sequences variants (variant calling), listing in a VCF file (Variant Call File).

Population frequencies of missense mutations and the mtDNA backgrounds on which they were observed were recovered from two public databases, Mitomap (http://www.mitomap.org) and HmtDB (http://www.hmtdb.uniba.it) (Lott et al., 2013; Rubino et al., 2012). Haplogroup affiliations of mitogenomes were assigned according to PhyloTree (www.phylotree.org) (van Oven and Kayser, 2009).

Protein conservation analysis and homology modelling

Protein conservation analysis and pathogenicity prediction were carried out considering *in silico* protocol (Polyphen2, SIFT, FatHmm, PROVEAN, MutationAssessor, CADD, PANTHER, PhD-SNP, MtoolBox, APOGEE_boost) (Achilli et al., 2012), available on MitImpact 2.7 databases (mitimpact.css-mendel.it) (Castellana et al., 2015), and conservation analysis on mammals, evaluating the amino acid residue conservation (> 70%), local conservation value > global storage value, invariant residue included in "-4/+4" range. An average score (0-1) for each missense variant has been calculated and changes with a score of 0,66-1 points were considered pathogenic, with a score of 0,5-0,65 points were considered synergistic and with 0-0,49 points neutral.

Positioning of amino acid changes on the 3D structure of respiratory Complex I was performed using UCSF Chimera 1.11.2 (www.cgl.ucsf.edu/chimera/) using as a template the molecular model of ovine respiratory Complex I (PDB file 5LNK) (Fiedorczuk et al., 2016).

mtDNA copy number quantification

Absolute quantification of mtDNA relative to nuclear DNA (nDNA) was performed by a real-time PCR based method using the LightCycler480 (Roche). This method is a multiplex assay

based on hydrolysis probe chemistry. A mtDNA fragment (ND2 gene) and a nDNA fragment (FasL gene) were co-amplified by multiplex polymerase chain reaction according to the primers, probes and conditions previously published (Cossarizza et al., 2003). These two fragments were cloned tale to tale in a vector and serial dilutions were used to construct a standard curve, obtaining a ratio of 1:1 of the reference molecules. Primers and probes sequences and PCR conditions are available on request.

Skeletal muscle investigation

Tibialis anterior muscle biopsy was carried out and routine histological and histoenzymatic analysis, including cytochrome c oxidase (COX) and succinic dehydrogenase (SDH) activity staining, were performed (Dubowitz et al., 2013). Respiratory chain complexes and citrate synthase (CS) redox enzymatic activities were determined on skeletal muscle homogenates as previously reported with minor modifications (Caporali et al., 2013; Trounce et al., 1996). Measurements were performed at 37°C by using a dual-wavelength spectrophotometer (V550 Jasco Europe, Italy), under constant stirring of the samples diluted in the assay buffer (50 mM KH_2PO_4 (pH 7.6), 1 mM EDTA, 2.5 mg/ml BSA). For Complex I NADH:DB:DCIP oxidoreductase activity was assessed in the presence of 60 µM DCIP (λ_{max}: 600 nm; ε_{DCIP}: $mM^{-1}\,cm^{-1}$), 70 µM DB, 0.3 mM KCN and 200 µM NADH (Janssen et al., 2007), after the subtraction of 1 µM rotenone-insensitive activity. The antimycin A-sensitive ubiquinol:cytochrome *c* reductase activity of Complex III was determined in the presence of 50 µM decylbenzoquinol (DBH_2), 0.3 mM KCN and 20 µM bovine heart cytochrome *c* (λ_{max}: 550–540 nm; $\varepsilon_{cyt\,c}$ = 19.1 $mM^{-1}\,cm^{-1}$). The Complex II+ III activity was measured as the succinate:cytochrome *c* reductase activity in the presence of 5 mM succinate, 0.3 mM KCN and 20 µM bovine heart cytochrome *c*, after the subtraction of 5 mM malonate- and 1 µM antimycin A-insensitive activity. The Complex IV activity was determined adding 60 µM of reduced bovine heart cytochrome *c*, after subtraction of 0.3 mM KCN-insensitive activity. Data were corrected for citrate synthase activity (Trounce et al., 1996) and protein content measured with Bradford assay. Skeletal muscle biopsies also underwent transmission electron microscopy (TEM) analyses using standard procedures.

Generation and maintenance of cybrids

Cybrid cell lines were generated in Dr. Monica Montopoli's Laboratory (Department of Pharmaceutical and Pharmacological Sciences, University of Padova) from patient's skin fibroblasts and 143B.Tk$^-$ cells, as previously described (King and Attardi, 1996). Cybrids were grown in Dulbecco's modified Eagle medium (DMEM) supplemented with 10% fetal calf serum (South America source from Gibco, Life Technologies), 2 mM L-glutamine, 100 U/ml penicillin, 100 μg/ml streptomycin, in an incubator with a humidified atmosphere of 5% CO_2 at 37 °C.

Cell viability assessment

For viability experiments, cells ($4x10^4$ cells/cm^2) were seeded in 24 well plates and incubated for different times in glucose-free DMEM supplemented with 5 mmol/L galactose, 5 mmol/L Na-pyruvate and 5% FBS (DMEM-galactose). Viability was determined using the colorimetric sulforhodamine B (SRB) assay (Scarlatti et al., 2003). Briefly, at the end of incubation time, cells were fixed with 50% trichloroacetic acid (TCA) for 1 hour at 4°C, washed 5 times with H_2O and dried for 1 hour at room temperature. Cells were then stained with SRB 0.4% diluted in 1% acetic acid for 1 hour at room temperature, washed 4 times with 1% acetic acid. SRB was solubilized with 10 mM Tris-HCl pH 9.8. The absorbance of SRB was detected by measuring the SRB absorbance at 570 nm with a VICTOR^3 Multilabel Plate Counter (PerkinElmer Life).

Oxygen consumption rate

Oxygen consumption rate (OCR) and extracellular acidification rate (ECAR) were measured in adherent cells with an XFe^{24} Extracellular Flux Analyzer (Seahorse Bioscience, Billerica, MA, USA), as previously described (Iommarini et al., 2014). OCR and ECAR were measured under basal conditions and after the sequential addition of 1μM oligomycin, 0.2 μM FCCP (carbonylcyanide-p-trifluoromethoxyphenyl hydrazone, Sigma-Aldrich, Milan, Italy), 1 μM rotenone and 1 μM antimycin A. Data were normalized on SRB-based cell quantification and expressed either as rate (pmol O_2/min or mpH/min) or as percentage of OCR compared to non-mitochondrial residual OCR.

ATP synthesis

The rate of mitochondrial ATP synthesis was measured in digitonin-permeabilized cybrids using the previously described luciferin/luciferase assay, with minor modifications (Giorgio et al., 2012). Briefly, after trypsinization, cells were resuspended ($10x10^6$/mL) in buffer A (10 mM KCl, 25 mM Tris-HCl, 2 mM EDTA, 0.1% bovine serum albumin, 10 mM potassium phosphate, 0.1 mM $MgCl_2$ (pH 7.4)), kept for 15 minutes at room temperature, and then incubated with 50 µg/mL digitonin for 1 minute. After centrifugation, the cells pellet was resuspended in buffer A and aliquots were taken to measure ATP synthesis, protein content, and CS activity. Aliquots of cells were incubated with 5 mM malate plus 5 mM pyruvate (complex I–driven substrates) in the presence or absence of 10 µg/mL oligomycin, or with 10 mM succinate plus 2 µg/mL rotenone (Complex II–driven substrate), and 0.2 mM ADP for 1 and 3 minutes. The amount of ATP was measured as described (Zanna et al., 2005). Adenosine 5'-triphosphate (ATP) Bioluminescent Assay Kit was from Sigma Aldrich. Data were normalized on protein content measured by Bradford assay and the rate of ATP synthesis was expressed as a ratio on CS activity (Trounce et al., 1996).

Reactive oxygen species (ROS) assessment

Mitochondrial superoxide production was determined by fluorescent microscopy incubating cells with 2.5 µm MitoSOX™ (Life Technologies) for 30 min at 37°C. MitoSOX-Red fluorescence was determined at 580 nm with a digital imaging system using an inverted epifluorescence microscope with 63X/1.4 oil objective (Nikon Eclipse Ti-U, Nikon, Japan). Images were captured with a back-illuminated Photometrics Cascade CCD camera system (Roper Scientific) with 500 ms exposure time and elaborated with Metamorph acquisition/analysis software (Universal Imaging Corp.).

Hydrogen peroxide was determined after incubation with 5 µM of 2,7-dichlorodihydrofluorescein diacetate (H_2DCFDA, Life Technologies). H_2DCFDA fluorescence was measured at 535 nm using a multilabel counter Wallac 1420 (PerkinElmer, Turku, Finland).

Statistical analyses

Statistical analysis was performed using the Prism 6 software (GraphPad), choosing ordinary one-way ANOVA with multiple comparison, applying Tukey test, as correction test, or $\chi 2$ tests

were performed, corrected with Bonferroni test. Data were considered significantly different for p-values < 0.05.

BIBLIOGRAPHY

Abrahams, J.P., Leslie, A.G., Lutter, R., and Walker, J.E. (1994). Structure at 2.8 A resolution of F1-ATPase from bovine heart mitochondria. Nature *370*, 621–628.

Abu-Amero, K.K., and Bosley, T.M. (2006). Mitochondrial abnormalities in patients with LHON-like optic neuropathies. Invest. Ophthalmol. Vis. Sci. *47*, 4211–4220.

Abu-Amero, K.K., Bosley, T.M., Bohlega, S., and Hansen, E. (2005). Mitochondrial T9957C mutation in association with NAION and seizures but not MELAS. Ophthalmic Genet. *26*, 31–36.

Achilli, A., Iommarini, L., Olivieri, A., Pala, M., Hooshiar Kashani, B., Reynier, P., La Morgia, C., Valentino, M.L., Liguori, R., Pizza, F., et al. (2012). Rare primary mitochondrial DNA mutations and probable synergistic variants in Leber's hereditary optic neuropathy. PLoS ONE *7*, e42242.

Al Rawi, S., Louvet-Vallée, S., Djeddi, A., Sachse, M., Culetto, E., Hajjar, C., Boyd, L., Legouis, R., and Galy, V. (2011). Postfertilization autophagy of sperm organelles prevents paternal mitochondrial DNA transmission. Science *334*, 1144–1147.

Albring, M., Griffith, J., and Attardi, G. (1977). Association of a protein structure of probable membrane derivation with HeLa cell mitochondrial DNA near its origin of replication. Proc Natl Acad Sci U S A *74*, 1348–1352.

Alexander, C., Votruba, M., Pesch, U.E., Thiselton, D.L., Mayer, S., Moore, A., Rodriguez, M., Kellner, U., Leo-Kottler, B., Auburger, G., et al. (2000). OPA1, encoding a dynamin-related GTPase, is mutated in autosomal dominant optic atrophy linked to chromosome 3q28. Nat. Genet. *26*, 211–215.

Amati-Bonneau, P., Valentino, M.L., Reynier, P., Gallardo, M.E., Bornstein, B., Boissière, A., Campos, Y., Rivera, H., de la Aleja, J.G., Carroccia, R., et al. (2008). OPA1 mutations induce mitochondrial DNA instability and optic atrophy "plus" phenotypes. Brain *131*, 338–351.

Anderson, S., Bankier, A.T., Barrell, B.G., de Bruijn, M.H., Coulson, A.R., Drouin, J., Eperon, I.C., Nierlich, D.P., Roe, B.A., Sanger, F., et al. (1981). Sequence and organization of the human mitochondrial genome. Nature *290*, 457–465.

Andrews, R.M., Kubacka, I., Chinnery, P.F., Lightowlers, R.N., Turnbull, D.M., and Howell, N. (1999). Reanalysis and revision of the Cambridge reference sequence for human mitochondrial DNA. Nat. Genet. *23*, 147.

Arjmand, S., Khaledi, N., Fayazmilani, R., Lotfi, A.S., and Tavana, H. (2017). Association of mitochondrial DNA haplogroups with elite athletic status in Iranian population. Meta Gene *11*, 81–84.

Attardi, G., and Schatz, G. (1988). Biogenesis of mitochondria. Annu. Rev. Cell Biol. *4*, 289–333.

Azar, A., Devlin, K., Mell, J., Giovannetti, T., Pirrone, V., Nonnemacher, M., Jacobson, J., Wigdhal, B., Dampier, W., Lee, E., et al. (2017). Mitochondrial haplogroup influences motor function in long-term HIV-1 infected individuals. Experimental Gerontology *94*, 113.

Bach, D., Pich, S., Soriano, F.X., Vega, N., Baumgartner, B., Oriola, J., Daugaard, J.R., Lloberas, J., Camps, M., Zierath, J.R., et al. (2003). Mitofusin-2 determines mitochondrial network

architecture and mitochondrial metabolism. A novel regulatory mechanism altered in obesity. J. Biol. Chem. *278*, 17190–17197.

Balaban, R.S. (1990). Regulation of oxidative phosphorylation in the mammalian cell. Am. J. Physiol. *258*, C377-389.

Barboni, P., Savini, G., Parisi, V., Carbonelli, M., La Morgia, C., Maresca, A., Sadun, F., De Negri, A.M., Carta, A., Sadun, A.A., et al. (2011). Retinal nerve fiber layer thickness in dominant optic atrophy measurements by optical coherence tomography and correlation with age. Ophthalmology *118*, 2076–2080.

Barboni, P., Savini, G., Cascavilla, M.L., Caporali, L., Milesi, J., Borrelli, E., La Morgia, C., Valentino, M.L., Triolo, G., Lembo, A., et al. (2014). Early macular retinal ganglion cell loss in dominant optic atrophy: genotype-phenotype correlation. Am. J. Ophthalmol. *158*, 628–636.e3.

Behar, D.M., Villems, R., Soodyall, H., Blue-Smith, J., Pereira, L., Metspalu, E., Scozzari, R., Makkan, H., Tzur, S., Comas, D., et al. (2008). The dawn of human matrilineal diversity. Am. J. Hum. Genet. *82*, 1130–1140.

Belenguer, P., and Pellegrini, L. (2013). The dynamin GTPase OPA1: more than mitochondria? Biochim. Biophys. Acta *1833*, 176–183.

de Brito, O.M., and Scorrano, L. (2008). Mitofusin 2 tethers endoplasmic reticulum to mitochondria. Nature *456*, 605–610.

Brown, M.D., Voljavec, A.S., Lott, M.T., Torroni, A., Yang, C.C., and Wallace, D.C. (1992). Mitochondrial DNA complex I and III mutations associated with Leber's hereditary optic neuropathy. Genetics *130*, 163–173.

Brown, M.D., Sun, F., and Wallace, D.C. (1997). Clustering of Caucasian Leber hereditary optic neuropathy patients containing the 11778 or 14484 mutations on an mtDNA lineage. Am. J. Hum. Genet. *60*, 381–387.

Brown, M.D., Allen, J.C., Van Stavern, G.P., Newman, N.J., and Wallace, D.C. (2001). Clinical, genetic, and biochemical characterization of a Leber hereditary optic neuropathy family containing both the 11778 and 14484 primary mutations. Am. J. Med. Genet. *104*, 331–338.

Brown, T.A., Tkachuk, A.N., Shtengel, G., Kopek, B.G., Bogenhagen, D.F., Hess, H.F., and Clayton, D.A. (2011). Superresolution fluorescence imaging of mitochondrial nucleoids reveals their spatial range, limits, and membrane interaction. Mol. Cell. Biol. *31*, 4994–5010.

Brown, W.M., George, M., and Wilson, A.C. (1979). Rapid evolution of animal mitochondrial DNA. Proc Natl Acad Sci U S A *76*, 1967–1971.

Cai, X., Wang, X., Li, S., Qian, J., Qian, D., Chen, F., Yang, Y., Yuan, Z., Xu, J., Bai, Y., et al. (2009). Association of Mitochondrial DNA Haplogroups with Exceptional Longevity in a Chinese Population. PLoS One *4*.

Caporali, L., Ghelli, A.M., Iommarini, L., Maresca, A., Valentino, M.L., La Morgia, C., Liguori, R., Zanna, C., Barboni, P., De Nardo, V., et al. (2013). Cybrid studies establish the causal link between the mtDNA m.3890G>A/MT-ND1 mutation and optic atrophy with bilateral brainstem lesions. Biochim. Biophys. Acta *1832*, 445–452.

Caporali, L., Maresca, A., Capristo, M., Del Dotto, V., Tagliavini, F., Valentino, M.L., La Morgia,

C., and Carelli, V. (2017). Incomplete penetrance in mitochondrial optic neuropathies. Mitochondrion *36*, 130–137.

Carelli, V. (2015). Keeping in shape the dogma of mitochondrial DNA maternal inheritance. PLoS Genet. *11*, e1005179.

Carelli, V., Ghelli, A., Ratta, M., Bacchilega, E., Sangiorgi, S., Mancini, R., Leuzzi, V., Cortelli, P., Montagna, P., Lugaresi, E., et al. (1997). Leber's hereditary optic neuropathy: biochemical effect of 11778/ND4 and 3460/ND1 mutations and correlation with the mitochondrial genotype. Neurology *48*, 1623–1632.

Carelli, V., Ghelli, A., Bucchi, L., Montagna, P., De Negri, A., Leuzzi, V., Carducci, C., Lenaz, G., Lugaresi, E., and Degli Esposti, M. (1999). Biochemical features of mtDNA 14484 (ND6/M64V) point mutation associated with Leber's hereditary optic neuropathy. Ann. Neurol. *45*, 320–328.

Carelli, V., Vergani, L., Bernazzi, B., Zampieron, C., Bucchi, L., Valentino, M., Rengo, C., Torroni, A., and Martinuzzi, A. (2002). Respiratory function in cybrid cell lines carrying European mtDNA haplogroups: implications for Leber's hereditary optic neuropathy. Biochim. Biophys. Acta *1588*, 7–14.

Carelli, V., Giordano, C., and d'Amati, G. (2003). Pathogenic expression of homoplasmic mtDNA mutations needs a complex nuclear-mitochondrial interaction. Trends Genet. *19*, 257–262.

Carelli, V., Ross-Cisneros, F.N., and Sadun, A.A. (2004). Mitochondrial dysfunction as a cause of optic neuropathies. Prog Retin Eye Res *23*, 53–89.

Carelli, V., Achilli, A., Valentino, M.L., Rengo, C., Semino, O., Pala, M., Olivieri, A., Mattiazzi, M., Pallotti, F., Carrara, F., et al. (2006). Haplogroup effects and recombination of mitochondrial DNA: novel clues from the analysis of Leber hereditary optic neuropathy pedigrees. Am. J. Hum. Genet. *78*, 564–574.

Carelli, V., La Morgia, C., Valentino, M.L., Barboni, P., Ross-Cisneros, F.N., and Sadun, A.A. (2009). Retinal ganglion cell neurodegeneration in mitochondrial inherited disorders. Biochim. Biophys. Acta *1787*, 518–528.

Carelli, V., Musumeci, O., Caporali, L., Zanna, C., La Morgia, C., Del Dotto, V., Porcelli, A.M., Rugolo, M., Valentino, M.L., Iommarini, L., et al. (2015). Syndromic parkinsonism and dementia associated with OPA1 missense mutations. Ann. Neurol. *78*, 21–38.

Carelli, V., d'Adamo, P., Valentino, M.L., La Morgia, C., Ross-Cisneros, F.N., Caporali, L., Maresca, A., Loguercio Polosa, P., Barboni, P., De Negri, A., et al. (2016). Parsing the differences in affected with LHON: genetic versus environmental triggers of disease conversion. Brain *139*, e17–e17.

Castellana, S., Rónai, J., and Mazza, T. (2015). MitImpact: an exhaustive collection of pre-computed pathogenicity predictions of human mitochondrial non-synonymous variants. Hum. Mutat. *36*, E2413-2422.

Catarino, C.B., Ahting, U., Gusic, M., Iuso, A., Repp, B., Peters, K., Biskup, S., von Livonius, B., Prokisch, H., and Klopstock, T. (2017). Characterization of a Leber's hereditary optic neuropathy (LHON) family harboring two primary LHON mutations m.11778G>A and m.14484T>C of the mitochondrial DNA. Mitochondrion *36*, 15–20.

Chalkia, D., Singh, L.N., Leipzig, J., Lvova, M., Derbeneva, O., Lakatos, A., Hadley, D., Hakonarson, H., and Wallace, D.C. (2017). Association Between Mitochondrial DNA Haplogroup Variation and Autism Spectrum Disorders. JAMA Psychiatry *74*, 1161–1168.

Chan, D.C. (2012). Fusion and fission: interlinked processes critical for mitochondrial health. Annu. Rev. Genet. *46*, 265–287.

Chen, H., Detmer, S.A., Ewald, A.J., Griffin, E.E., Fraser, S.E., and Chan, D.C. (2003). Mitofusins Mfn1 and Mfn2 coordinately regulate mitochondrial fusion and are essential for embryonic development. J. Cell Biol. *160*, 189–200.

Chen, H., McCaffery, J.M., and Chan, D.C. (2007). Mitochondrial fusion protects against neurodegeneration in the cerebellum. Cell *130*, 548–562.

Chinnery, P.F., and Hudson, G. (2013). Mitochondrial genetics. Br Med Bull *106*, 135–159.

Clayton, D.A. (1991). Replication and transcription of vertebrate mitochondrial DNA. Annu. Rev. Cell Biol. *7*, 453–478.

Cossarizza, A., Riva, A., Pinti, M., Ammannato, S., Fedeli, P., Mussini, C., Esposito, R., and Galli, M. (2003). Increased mitochondrial DNA content in peripheral blood lymphocytes from HIV-infected patients with lipodystrophy. Antivir. Ther. (Lond.) *8*, 315–321.

Costa, M.D., Pereira, J.B., Pala, M., Fernandes, V., Olivieri, A., Achilli, A., Perego, U.A., Rychkov, S., Naumova, O., Hatina, J., et al. (2013). A substantial prehistoric European ancestry amongst Ashkenazi maternal lineages. Nat Commun *4*, 2543.

Cruz-Bermúdez, A., Vicente-Blanco, R.J., Hernández-Sierra, R., Montero, M., Alvarez, J., González Manrique, M., Blázquez, A., Martín, M.A., Ayuso, C., Garesse, R., et al. (2016). Functional Characterization of Three Concomitant MtDNA LHON Mutations Shows No Synergistic Effect on Mitochondrial Activity. PLoS ONE *11*, e0146816.

Darrouzet, E., Moser, C.C., Dutton, P.L., and Daldal, F. (2001). Large scale domain movement in cytochrome bc(1): a new device for electron transfer in proteins. Trends Biochem. Sci. *26*, 445–451.

Delettre, C., Lenaers, G., Griffoin, J.M., Gigarel, N., Lorenzo, C., Belenguer, P., Pelloquin, L., Grosgeorge, J., Turc-Carel, C., Perret, E., et al. (2000). Nuclear gene OPA1, encoding a mitochondrial dynamin-related protein, is mutated in dominant optic atrophy. Nat. Genet. *26*, 207–210.

Delettre, C., Lenaers, G., Pelloquin, L., Belenguer, P., and Hamel, C.P. (2002). OPA1 (Kjer type) dominant optic atrophy: a novel mitochondrial disease. Mol. Genet. Metab. *75*, 97–107.

Dibrova, D.V., Cherepanov, D.A., Galperin, M.Y., Skulachev, V.P., and Mulkidjanian, A.Y. (2013). Evolution of cytochrome bc complexes: from membrane-anchored dehydrogenases of ancient bacteria to triggers of apoptosis in vertebrates. Biochim. Biophys. Acta *1827*, 1407–1427.

DiMauro, S., and Schon, E.A. (2008). Mitochondrial disorders in the nervous system. Annu. Rev. Neurosci. *31*, 91–123.

DiMauro, S., Schon, E.A., Carelli, V., and Hirano, M. (2013). The clinical maze of mitochondrial neurology. Nat Rev Neurol *9*, 429–444.

Dokianakis, E., and Ladoukakis, E.D. (2014). Different degree of paternal mtDNA leakage

between male and female progeny in interspecific Drosophila crosses. Ecol Evol *4*, 2633–2641.

Dotto, V.D., Mishra, P., Vidoni, S., Fogazza, M., Maresca, A., Caporali, L., McCaffery, J.M., Cappelletti, M., Baruffini, E., Lenaers, G., et al. (2017). OPA1 Isoforms in the Hierarchical Organization of Mitochondrial Functions. Cell Reports *19*, 2557–2571.

Dubowitz, V., Sewry, C.A., Oldfors, A., and Lane, R.J.M. (2013). Muscle biopsy: a practical approach (Oxford, England? Saunders Elsevier).

Fernández-Silva, P., Enriquez, J.A., and Montoya, J. (2003). Replication and transcription of mammalian mitochondrial DNA. Exp. Physiol. *88*, 41–56.

Ferré, M., Caignard, A., Milea, D., Leruez, S., Cassereau, J., Chevrollier, A., Amati-Bonneau, P., Verny, C., Bonneau, D., Procaccio, V., et al. (2015). Improved locus-specific database for OPA1 mutations allows inclusion of advanced clinical data. Hum. Mutat. *36*, 20–25.

Fiedorczuk, K., Letts, J.A., Degliesposti, G., Kaszuba, K., Skehel, M., and Sazanov, L.A. (2016). Atomic structure of the entire mammalian mitochondrial complex I. Nature *538*, 406–410.

Frank, M., Duvezin-Caubet, S., Koob, S., Occhipinti, A., Jagasia, R., Petcherski, A., Ruonala, M.O., Priault, M., Salin, B., and Reichert, A.S. (2012). Mitophagy is triggered by mild oxidative stress in a mitochondrial fission dependent manner. Biochim. Biophys. Acta *1823*, 2297–2310.

Frey, T.G., and Mannella, C.A. (2000). The internal structure of mitochondria. Trends Biochem. Sci. *25*, 319–324.

Frezza, C., Cipolat, S., Martins de Brito, O., Micaroni, M., Beznoussenko, G.V., Rudka, T., Bartoli, D., Polishuck, R.S., Danial, N.N., De Strooper, B., et al. (2006). OPA1 controls apoptotic cristae remodeling independently from mitochondrial fusion. Cell *126*, 177–189.

Friedman, J.R., and Nunnari, J. (2014). Mitochondrial form and function. Nature *505*, 335.

Frye, M.A., Ryu, E., Nassan, M., Jenkins, G.D., Andreazza, A.C., Evans, J.M., McElroy, S.L., Oglesbee, D., Highsmith, W.E., and Biernacka, J.M. (2017). Mitochondrial DNA sequence data reveals association of haplogroup U with psychosis in bipolar disorder. Journal of Psychiatric Research *84*, 221–226.

Fusté, J.M., Wanrooij, S., Jemt, E., Granycome, C.E., Cluett, T.J., Shi, Y., Atanassova, N., Holt, I.J., Gustafsson, C.M., and Falkenberg, M. (2010). Mitochondrial RNA polymerase is needed for activation of the origin of light-strand DNA replication. Mol. Cell *37*, 67–78.

Ghelli, A., Porcelli, A.M., Zanna, C., Vidoni, S., Mattioli, S., Barbieri, A., Iommarini, L., Pala, M., Achilli, A., Torroni, A., et al. (2009). The background of mitochondrial DNA haplogroup J increases the sensitivity of Leber's hereditary optic neuropathy cells to 2,5-hexanedione toxicity. PLoS ONE *4*, e7922.

Ghezzi, D., Marelli, C., Achilli, A., Goldwurm, S., Pezzoli, G., Barone, P., Pellecchia, M.T., Stanzione, P., Brusa, L., Bentivoglio, A.R., et al. (2005). Mitochondrial DNA haplogroup K is associated with a lower risk of Parkinson's disease in Italians. Eur. J. Hum. Genet. *13*, 748–752.

Giacchetti, M., Monticelli, A., De Biase, I., Pianese, L., Turano, M., Filla, A., De Michele, G., and Cocozza, S. (2004). Mitochondrial DNA haplogroups influence the Friedreich's ataxia phenotype. J. Med. Genet. *41*, 293–295.

Giannoccaro, M.P., La Morgia, C., Rizzo, G., and Carelli, V. (2017). Mitochondrial DNA and primary mitochondrial dysfunction in Parkinson's disease. Mov. Disord. *32*, 346–363.

Giordano, C., Montopoli, M., Perli, E., Orlandi, M., Fantin, M., Ross-Cisneros, F.N., Caparrotta, L., Martinuzzi, A., Ragazzi, E., Ghelli, A., et al. (2011). Oestrogens ameliorate mitochondrial dysfunction in Leber's hereditary optic neuropathy. Brain *134*, 220–234.

Giordano, C., Iommarini, L., Giordano, L., Maresca, A., Pisano, A., Valentino, M.L., Caporali, L., Liguori, R., Deceglie, S., Roberti, M., et al. (2014). Efficient mitochondrial biogenesis drives incomplete penetrance in Leber's hereditary optic neuropathy. Brain *137*, 335–353.

Giorgio, V., Petronilli, V., Ghelli, A., Carelli, V., Rugolo, M., Lenaz, G., and Bernardi, P. (2012). The effects of idebenone on mitochondrial bioenergetics. Biochim. Biophys. Acta *1817*, 363–369.

Gomes, L.C., Di Benedetto, G., and Scorrano, L. (2011). During autophagy mitochondria elongate, are spared from degradation and sustain cell viability. Nat. Cell Biol. *13*, 589–598.

Gómez-Durán, A., Pacheu-Grau, D., López-Gallardo, E., Díez-Sánchez, C., Montoya, J., López-Pérez, M.J., and Ruiz-Pesini, E. (2010). Unmasking the causes of multifactorial disorders: OXPHOS differences between mitochondrial haplogroups. Hum. Mol. Genet. *19*, 3343–3353.

Gómez-Durán, A., Pacheu-Grau, D., Martínez-Romero, I., López-Gallardo, E., López-Pérez, M.J., Montoya, J., and Ruiz-Pesini, E. (2012). Oxidative phosphorylation differences between mitochondrial DNA haplogroups modify the risk of Leber's hereditary optic neuropathy. Biochim. Biophys. Acta *1822*, 1216–1222.

Griffin, E.E., Graumann, J., and Chan, D.C. (2005). The WD40 protein Caf4p is a component of the mitochondrial fission machinery and recruits Dnm1p to mitochondria. J. Cell Biol. *170*, 237–248.

Gustafsson, C.M., Falkenberg, M., and Larsson, N.-G. (2016). Maintenance and Expression of Mammalian Mitochondrial DNA. Annual Review of Biochemistry *85*, 133–160.

Gyllensten, U., Wharton, D., Josefsson, A., and Wilson, A.C. (1991). Paternal inheritance of mitochondrial DNA in mice. Nature *352*, 255–257.

Hällberg, B.M., and Larsson, N.-G. (2014). Making proteins in the powerhouse. Cell Metab. *20*, 226–240.

Han, J., Thompson-Lowrey, A.J., Reiss, A., Mayorov, V., Jia, H., Biousse, V., Newman, N.J., and Brown, M.D. (2006). OPA1 mutations and mitochondrial DNA haplotypes in autosomal dominant optic atrophy. Genet. Med. *8*, 217–225.

Horvath, J., Horvath, R., Karcagi, V., Komoly, S., and Johns, D.R. (2002). Sequence analysis of Hungarian LHON patients not carrying the common primary mutations. J. Inherit. Metab. Dis. *25*, 323–324.

Howell, N., Kubacka, I., Xu, M., and McCullough, D.A. (1991). Leber hereditary optic neuropathy: involvement of the mitochondrial ND1 gene and evidence for an intragenic suppressor mutation. Am. J. Hum. Genet. *48*, 935–942.

Howell, N., Kubacka, I., Halvorson, S., Howell, B., McCullough, D.A., and Mackey, D. (1995). Phylogenetic analysis of the mitochondrial genomes from Leber hereditary optic neuropathy pedigrees. Genetics *140*, 285–302.

Howell, N., Miller, N.R., Mackey, D.A., Arnold, A., Herrnstadt, C., Williams, I.M., and Kubacka, I. (2002). Lightning strikes twice: Leber hereditary optic neuropathy families with two

pathogenic mtDNA mutations. J Neuroophthalmol *22*, 262–269.

Howell, N., Herrnstadt, C., Shults, C., and Mackey, D.A. (2003a). Low penetrance of the 14484 LHON mutation when it arises in a non-haplogroup J mtDNA background. Am. J. Med. Genet. A *119A*, 147–151.

Howell, N., Oostra, R.-J., Bolhuis, P.A., Spruijt, L., Clarke, L.A., Mackey, D.A., Preston, G., and Herrnstadt, C. (2003b). Sequence Analysis of the Mitochondrial Genomes from Dutch Pedigrees with Leber Hereditary Optic Neuropathy. Am J Hum Genet *72*, 1460–1469.

Hudson, G., Carelli, V., Spruijt, L., Gerards, M., Mowbray, C., Achilli, A., Pyle, A., Elson, J., Howell, N., La Morgia, C., et al. (2007). Clinical expression of Leber hereditary optic neuropathy is affected by the mitochondrial DNA-haplogroup background. Am. J. Hum. Genet. *81*, 228–233.

Hudson, G., Amati-Bonneau, P., Blakely, E.L., Stewart, J.D., He, L., Schaefer, A.M., Griffiths, P.G., Ahlqvist, K., Suomalainen, A., Reynier, P., et al. (2008). Mutation of OPA1 causes dominant optic atrophy with external ophthalmoplegia, ataxia, deafness and multiple mitochondrial DNA deletions: a novel disorder of mtDNA maintenance. Brain *131*, 329–337.

Iommarini, L., Maresca, A., Caporali, L., Valentino, M.L., Liguori, R., Giordano, C., and Carelli, V. (2012). Revisiting the issue of mitochondrial DNA content in optic mitochondriopathies. Neurology *79*, 1517–1519.

Iommarini, L., Kurelac, I., Capristo, M., Calvaruso, M.A., Giorgio, V., Bergamini, C., Ghelli, A., Nanni, P., De Giovanni, C., Carelli, V., et al. (2014). Different mtDNA mutations modify tumor progression in dependence of the degree of respiratory complex I impairment. Hum. Mol. Genet. *23*, 1453–1466.

Ishihara, N., Eura, Y., and Mihara, K. (2004). Mitofusin 1 and 2 play distinct roles in mitochondrial fusion reactions via GTPase activity. J. Cell. Sci. *117*, 6535–6546.

Ishihara, N., Nomura, M., Jofuku, A., Kato, H., Suzuki, S.O., Masuda, K., Otera, H., Nakanishi, Y., Nonaka, I., Goto, Y.-I., et al. (2009). Mitochondrial fission factor Drp1 is essential for embryonic development and synapse formation in mice. Nat. Cell Biol. *11*, 958–966.

Janssen, A.J.M., Trijbels, F.J.M., Sengers, R.C.A., Smeitink, J.A.M., van den Heuvel, L.P., Wintjes, L.T.M., Stoltenborg-Hogenkamp, B.J.M., and Rodenburg, R.J.T. (2007). Spectrophotometric assay for complex I of the respiratory chain in tissue samples and cultured fibroblasts. Clin. Chem. *53*, 729–734.

Ji, F., Sharpley, M.S., Derbeneva, O., Alves, L.S., Qian, P., Wang, Y., Chalkia, D., Lvova, M., Xu, J., Yao, W., et al. (2012). Mitochondrial DNA variant associated with Leber hereditary optic neuropathy and high-altitude Tibetans. Proc. Natl. Acad. Sci. U.S.A. *109*, 7391–7396.

Ji, Y., Zhang, A.-M., Jia, X., Zhang, Y.-P., Xiao, X., Li, S., Guo, X., Bandelt, H.-J., Zhang, Q., and Yao, Y.-G. (2008). Mitochondrial DNA haplogroups M7b1'2 and M8a affect clinical expression of leber hereditary optic neuropathy in Chinese families with the m.11778G-->a mutation. Am. J. Hum. Genet. *83*, 760–768.

Jiang, P., Liang, M., Zhang, C., Zhao, X., He, Q., Cui, L., Liu, X., Sun, Y.-H., Fu, Q., Ji, Y., et al. (2016). Biochemical evidence for a mitochondrial genetic modifier in the phenotypic manifestation of Leber's hereditary optic neuropathy-associated mitochondrial DNA mutation. Hum. Mol. Genet. *25*, 3613–3625.

Johns, D.R., and Berman, J. (1991). Alternative, simultaneous complex I mitochondrial DNA mutations in Leber's hereditary optic neuropathy. Biochem. Biophys. Res. Commun. *174*, 1324–1330.

Johns, D.R., and Neufeld, M.J. (1991). Cytochrome b mutations in Leber hereditary optic neuropathy. Biochem. Biophys. Res. Commun. *181*, 1358–1364.

Johnston, P.B., Gaster, R.N., Smith, V.C., and Tripathi, R.C. (1979). A clinicopathologic study of autosomal dominant optic atrophy. Am. J. Ophthalmol. *88*, 868–875.

Kaewsutthi, S., Phasukkijwatana, N., Joyjinda, Y., Chuenkongkaew, W., Kunhapan, B., Tun, A.W., Suktitipat, B., and Lertrit, P. (2011). Mitochondrial haplogroup background may influence Southeast Asian G11778A Leber hereditary optic neuropathy. Invest. Ophthalmol. Vis. Sci. *52*, 4742–4748.

Kalman, B., Li, S., Chatterjee, D., O'Connor, J., Voehl, M.R., Brown, M.D., and Alder, H. (1999). Large scale screening of the mitochondrial DNA reveals no pathogenic mutations but a haplotype associated with multiple sclerosis in Caucasians. Acta Neurol. Scand. *99*, 16–25.

Kang, L., Zheng, H.-X., Chen, F., Yan, S., Liu, K., Qin, Z., Liu, L., Zhao, Z., Li, L., Wang, X., et al. (2013). mtDNA lineage expansions in Sherpa population suggest adaptive evolution in Tibetan highlands. Mol. Biol. Evol. *30*, 2579–2587.

Kashatus, D.F., Lim, K.-H., Brady, D.C., Pershing, N.L.K., Cox, A.D., and Counter, C.M. (2011). RALA and RALBP1 regulate mitochondrial fission at mitosis. Nat. Cell Biol. *13*, 1108–1115.

Khan, N.A., Govindaraj, P., Soumittra, N., Srilekha, S., Ambika, S., Vanniarajan, A., Meena, A.K., Uppin, M.S., Sundaram, C., Taly, A.B., et al. (2013). Haplogroup Heterogeneity of LHON Patients Carrying the m.14484T>C Mutation in India. Invest. Ophthalmol. Vis. Sci. *54*, 3999–4005.

Khusnutdinova, E., Gilyazova, I., Ruiz-Pesini, E., Derbeneva, O., Khusainova, R., Khidiyatova, I., Magzhanov, R., and Wallace, D.C. (2008). A mitochondrial etiology of neurodegenerative diseases: evidence from Parkinson's disease. Ann. N. Y. Acad. Sci. *1147*, 1–20.

King, M.P., and Attardi, G. (1996). Isolation of human cell lines lacking mitochondrial DNA. Meth. Enzymol. *264*, 304–313.

Kivisild, T. (2015). Maternal ancestry and population history from whole mitochondrial genomes. Investigative Genetics *6*, 3.

Kjer, P., Jensen, O.A., and Klinken, L. (1983). Histopathology of eye, optic nerve and brain in a case of dominant optic atrophy. Acta Ophthalmol (Copenh) *61*, 300–312.

Koshiba, T., Detmer, S.A., Kaiser, J.T., Chen, H., McCaffery, J.M., and Chan, D.C. (2004). Structural basis of mitochondrial tethering by mitofusin complexes. Science *305*, 858–862.

Krüger, J., Hinttala, R., Majamaa, K., and Remes, A.M. (2010). Mitochondrial DNA haplogroups in early-onset Alzheimer's disease and frontotemporal lobar degeneration. Mol Neurodegener *5*, 8.

La Morgia, C., Achilli, A., Iommarini, L., Barboni, P., Pala, M., Olivieri, A., Zanna, C., Vidoni, S., Tonon, C., Lodi, R., et al. (2008). Rare mtDNA variants in Leber hereditary optic neuropathy families with recurrence of myoclonus. Neurology *70*, 762–770.

La Morgia, C., Caporali, L., Gandini, F., Olivieri, A., Toni, F., Nassetti, S., Brunetto, D., Stipa, C.,

Scaduto, C., Parmeggiani, A., et al. (2014a). Association of the mtDNA m.4171C>A/MT-ND1 mutation with both optic neuropathy and bilateral brainstem lesions. BMC Neurol *14*, 116.

La Morgia, C., Carbonelli, M., Barboni, P., Sadun, A.A., and Carelli, V. (2014b). Medical management of hereditary optic neuropathies. Front Neurol *5*, 141.

Lamminen, T., Huoponen, K., Sistonen, P., Juvonen, V., Lahermo, P., Aula, P., Nikoskelainen, E., and Savontaus, M.L. (1997). mtDNA haplotype analysis in Finnish families with leber hereditary optic neuroretinopathy. Eur. J. Hum. Genet. *5*, 271–279.

Lancaster, C.R., and Kröger, A. (2000). Succinate: quinone oxidoreductases: new insights from X-ray crystal structures. Biochim. Biophys. Acta *1459*, 422–431.

Lee, M.W., Lee, E.Y., Lai, G.H., Kennedy, N.W., Posey, A.E., Xian, W., Ferguson, A.L., Hill, R.B., and Wong, G.C.L. (2017). Molecular Motor Dnm1 Synergistically Induces Membrane Curvature To Facilitate Mitochondrial Fission. ACS Cent Sci *3*, 1156–1167.

Lenaers, G., Hamel, C., Delettre, C., Amati-Bonneau, P., Procaccio, V., Bonneau, D., Reynier, P., and Milea, D. (2012). Dominant optic atrophy. Orphanet J Rare Dis *7*, 46.

Lenaz, G., Baracca, A., Carelli, V., D'Aurelio, M., Sgarbi, G., and Solaini, G. (2004). Bioenergetics of mitochondrial diseases associated with mtDNA mutations. Biochim. Biophys. Acta *1658*, 89–94.

Lippold, S., Xu, H., Ko, A., Li, M., Renaud, G., Butthof, A., Schröder, R., and Stoneking, M. (2014). Human paternal and maternal demographic histories: insights from high-resolution Y chromosome and mtDNA sequences. Investig Genet *5*, 13.

Liu, C.-H., Liou, C.-W., Liu, C.-H., Kuo, H.-C., Chu, C.-C., and Huang, C.-C. (2011). Chronic progressive external ophthalmoplegia with T9957C mitochondrial DNA mutation in a Taiwanese patient. Acta Neurol Taiwan *20*, 53–58.

Liu, X., Weaver, D., Shirihai, O., and Hajnóczky, G. (2009). Mitochondrial "kiss-and-run": interplay between mitochondrial motility and fusion-fission dynamics. EMBO J. *28*, 3074–3089.

Lodi, R., Montagna, P., Cortelli, P., Iotti, S., Cevoli, S., Carelli, V., and Barbiroli, B. (2000). "Secondary" 4216/ND1 and 13708/ND5 Leber's hereditary optic neuropathy mitochondrial DNA mutations do not further impair in vivo mitochondrial oxidative metabolism when associated with the 11778/ND4 mitochondrial DNA mutation. Brain *123 (Pt 9)*, 1896–1902.

Losón, O.C., Song, Z., Chen, H., and Chan, D.C. (2013). Fis1, Mff, MiD49, and MiD51 mediate Drp1 recruitment in mitochondrial fission. Mol. Biol. Cell *24*, 659–667.

Lott, M.T., Leipzig, J.N., Derbeneva, O., Xie, H.M., Chalkia, D., Sarmady, M., Procaccio, V., and Wallace, D.C. (2013). mtDNA Variation and Analysis Using Mitomap and Mitomaster. Curr Protoc Bioinformatics *44*, 1.23.1-26.

Luo, S.-M., Ge, Z.-J., Wang, Z.-W., Jiang, Z.-Z., Wang, Z.-B., Ouyang, Y.-C., Hou, Y., Schatten, H., and Sun, Q.-Y. (2013). Unique insights into maternal mitochondrial inheritance in mice. Proc. Natl. Acad. Sci. U.S.A. *110*, 13038–13043.

Macaulay, V., Hill, C., Achilli, A., Rengo, C., Clarke, D., Meehan, W., Blackburn, J., Semino, O., Scozzari, R., Cruciani, F., et al. (2005). Single, rapid coastal settlement of Asia revealed by analysis of complete mitochondrial genomes. Science *308*, 1034–1036.

Mackey, D., and Howell, N. (1992). A variant of Leber hereditary optic neuropathy characterized by recovery of vision and by an unusual mitochondrial genetic etiology. Am. J. Hum. Genet. *51*, 1218–1228.

Macmillan, C., Kirkham, T., Fu, K., Allison, V., Andermann, E., Chitayat, D., Fortier, D., Gans, M., Hare, H., Quercia, N., et al. (1998). Pedigree analysis of French Canadian families with T14484C Leber's hereditary optic neuropathy. Neurology *50*, 417–422.

Man, P.Y.W., Griffiths, P.G., Brown, D.T., Howell, N., Turnbull, D.M., and Chinnery, P.F. (2003). The Epidemiology of Leber Hereditary Optic Neuropathy in the North East of England. Am J Hum Genet *72*, 333–339.

Mancuso, M., Conforti, F.L., Rocchi, A., Tessitore, A., Muglia, M., Tedeschi, G., Panza, D., Monsurrò, M., Sola, P., Mandrioli, J., et al. (2004). Could mitochondrial haplogroups play a role in sporadic amyotrophic lateral sclerosis? Neurosci. Lett. *371*, 158–162.

Manfredi, G., Schon, E.A., Moraes, C.T., Bonilla, E., Berry, G.T., Sladky, J.T., and DiMauro, S. (1995). A new mutation associated with MELAS is located in a mitochondrial DNA polypeptide-coding gene. Neuromuscul. Disord. *5*, 391–398.

Marelli, C., Amati-Bonneau, P., Reynier, P., Layet, V., Layet, A., Stevanin, G., Brissaud, E., Bonneau, D., Durr, A., and Brice, A. (2011). Heterozygous OPA1 mutations in Behr syndrome. Brain *134*, e169; author reply e170.

Milea, D., Sander, B., Wegener, M., Jensen, H., Kjer, B., Jørgensen, T.M., Lund-Andersen, H., and Larsen, M. (2010). Axonal loss occurs early in dominant optic atrophy. Acta Ophthalmol *88*, 342–346.

Milone, M., Younge, B.R., Wang, J., Zhang, S., and Wong, L.-J. (2009). Mitochondrial disorder with OPA1 mutation lacking optic atrophy. Mitochondrion *9*, 279–281.

Miralles Fusté, J., Shi, Y., Wanrooij, S., Zhu, X., Jemt, E., Persson, Ö., Sabouri, N., Gustafsson, C.M., and Falkenberg, M. (2014). In Vivo Occupancy of Mitochondrial Single-Stranded DNA Binding Protein Supports the Strand Displacement Mode of DNA Replication. PLoS Genet *10*.

Mishmar, D., Ruiz-Pesini, E., Golik, P., Macaulay, V., Clark, A.G., Hosseini, S., Brandon, M., Easley, K., Chen, E., Brown, M.D., et al. (2003). Natural selection shaped regional mtDNA variation in humans. Proc. Natl. Acad. Sci. U.S.A. *100*, 171–176.

Mishra, P., Carelli, V., Manfredi, G., and Chan, D.C. (2014). Proteolytic cleavage of Opa1 stimulates mitochondrial inner membrane fusion and couples fusion to oxidative phosphorylation. Cell Metab. *19*, 630–641.

Mitchell, P. (1961). Coupling of Phosphorylation to Electron and Hydrogen Transfer by a Chemi-Osmotic type of Mechanism. Nature *191*, 144.

Montoya, J., López-Gallardo, E., Díez-Sánchez, C., López-Pérez, M.J., and Ruiz-Pesini, E. (2009). 20 years of human mtDNA pathologic point mutations: carefully reading the pathogenicity criteria. Biochim. Biophys. Acta *1787*, 476–483.

Mueller, E.E., Brunner, S.M., Mayr, J.A., Stanger, O., Sperl, W., and Kofler, B. (2012). Functional differences between mitochondrial haplogroup T and haplogroup H in HEK293 cybrid cells. PLoS ONE *7*, e52367.

Nicholls, T.J., and Minczuk, M. (2014). In D-loop: 40 years of mitochondrial 7S DNA. Exp.

Gerontol. *56*, 175–181.

Nishigaki, Y., Martí, R., Copeland, W.C., and Hirano, M. (2003). Site-specific somatic mitochondrial DNA point mutations in patients with thymidine phosphorylase deficiency. J. Clin. Invest. *111*, 1913–1921.

Ojala, D., Montoya, J., and Attardi, G. (1981). tRNA punctuation model of RNA processing in human mitochondria. Nature *290*, 470–474.

Olichon, A., Baricault, L., Gas, N., Guillou, E., Valette, A., Belenguer, P., and Lenaers, G. (2003). Loss of OPA1 perturbates the mitochondrial inner membrane structure and integrity, leading to cytochrome c release and apoptosis. J. Biol. Chem. *278*, 7743–7746.

Otera, H., Ohsakaya, S., Nagaura, Z.-I., Ishihara, N., and Mihara, K. (2005). Export of mitochondrial AIF in response to proapoptotic stimuli depends on processing at the intermembrane space. EMBO J. *24*, 1375–1386.

van Oven, M., and Kayser, M. (2009). Updated comprehensive phylogenetic tree of global human mitochondrial DNA variation. Hum. Mutat. *30*, E386-394.

Palanichamy, M.G., Sun, C., Agrawal, S., Bandelt, H.-J., Kong, Q.-P., Khan, F., Wang, C.-Y., Chaudhuri, T.K., Palla, V., and Zhang, Y.-P. (2004). Phylogeny of mitochondrial DNA macrohaplogroup N in India, based on complete sequencing: implications for the peopling of South Asia. Am. J. Hum. Genet. *75*, 966–978.

Parisi, M.A., and Clayton, D.A. (1991). Similarity of human mitochondrial transcription factor 1 to high mobility group proteins. Science *252*, 965–969.

Payne, B.A.I., Wilson, I.J., Yu-Wai-Man, P., Coxhead, J., Deehan, D., Horvath, R., Taylor, R.W., Samuels, D.C., Santibanez-Koref, M., and Chinnery, P.F. (2013). Universal heteroplasmy of human mitochondrial DNA. Hum. Mol. Genet. *22*, 384–390.

Pello, R., Martín, M.A., Carelli, V., Nijtmans, L.G., Achilli, A., Pala, M., Torroni, A., Gómez-Durán, A., Ruiz-Pesini, E., Martinuzzi, A., et al. (2008). Mitochondrial DNA background modulates the assembly kinetics of OXPHOS complexes in a cellular model of mitochondrial disease. Hum. Mol. Genet. *17*, 4001–4011.

Pezzi, P.P., De Negri, A.M., Sadun, F., Carelli, V., and Leuzzi, V. (1998). Childhood Leber's hereditary optic neuropathy (ND1/3460) with visual recovery. Pediatr. Neurol. *19*, 308–312.

Pierron, D., Ferré, M., Rocher, C., Chevrollier, A., Murail, P., Thoraval, D., Amati-Bonneau, P., Reynier, P., and Letellier, T. (2009). OPA1-related dominant optic atrophy is not strongly influenced by mitochondrial DNA background. BMC Medical Genetics *10*, 70.

Pinhasi, R., Thomas, M.G., Hofreiter, M., Currat, M., and Burger, J. (2012). The genetic history of Europeans. Trends Genet. *28*, 496–505.

Povalko, N., Zakharova, E., Rudenskaia, G., Akita, Y., Hirata, K., Toyojiro, M., and Koga, Y. (2005). A new sequence variant in mitochondrial DNA associated with high penetrance of Russian Leber hereditary optic neuropathy. Mitochondrion *5*, 194–199.

Praefcke, G.J.K., and McMahon, H.T. (2004). The dynamin superfamily: universal membrane tubulation and fission molecules? Nat. Rev. Mol. Cell Biol. *5*, 133–147.

Puomila, A., Hämäläinen, P., Kivioja, S., Savontaus, M.-L., Koivumäki, S., Huoponen, K., and Nikoskelainen, E. (2007). Epidemiology and penetrance of Leber hereditary optic neuropathy

in Finland. Eur. J. Hum. Genet. *15*, 1079–1089.

Pyle, A., Hudson, G., Wilson, I.J., Coxhead, J., Smertenko, T., Herbert, M., Santibanez-Koref, M., and Chinnery, P.F. (2015). Extreme-Depth Re-sequencing of Mitochondrial DNA Finds No Evidence of Paternal Transmission in Humans. PLoS Genet. *11*, e1005040.

Qu, J., Zhou, X., Zhang, J., Zhao, F., Sun, Y.-H., Tong, Y., Wei, Q.-P., Cai, W., Yang, L., West, C.E., et al. (2009). Extremely Low Penetrance of Leber's Hereditary Optic Neuropathy in 8 Han Chinese Families Carrying the ND4 G11778A Mutation. Ophthalmology *116*, 558–564.e3.

Rampelt, H., Zerbes, R.M., van der Laan, M., and Pfanner, N. (2017). Role of the mitochondrial contact site and cristae organizing system in membrane architecture and dynamics. Biochimica et Biophysica Acta (BBA) - Molecular Cell Research *1864*, 737–746.

Rego-Pérez, I., Fernández-Moreno, M., Fernández-López, C., Arenas, J., and Blanco, F.J. (2008). Mitochondrial DNA haplogroups: role in the prevalence and severity of knee osteoarthritis. Arthritis Rheum. *58*, 2387–2396.

Richards, M.B., Soares, P., and Torroni, A. (2016). Palaeogenomics: Mitogenomes and Migrations in Europe's Past. Curr. Biol. *26*, R243-246.

Riordan-Eva, P., Sanders, M.D., Govan, G.G., Sweeney, M.G., Da Costa, J., and Harding, A.E. (1995). The clinical features of Leber's hereditary optic neuropathy defined by the presence of a pathogenic mitochondrial DNA mutation. Brain *118 (Pt 2)*, 319–337.

Robinson, B.H., Petrova-Benedict, R., Buncic, J.R., and Wallace, D.C. (1992). Nonviability of cells with oxidative defects in galactose medium: a screening test for affected patient fibroblasts. Biochem. Med. Metab. Biol. *48*, 122–126.

Rojansky, R., Cha, M.-Y., and Chan, D.C. (2016). Elimination of paternal mitochondria in mouse embryos occurs through autophagic degradation dependent on PARKIN and MUL1. Elife *5*.

Rouzier, C., Bannwarth, S., Chaussenot, A., Chevrollier, A., Verschueren, A., Bonello-Palot, N., Fragaki, K., Cano, A., Pouget, J., Pellissier, J.-F., et al. (2012). The MFN2 gene is responsible for mitochondrial DNA instability and optic atrophy "plus" phenotype. Brain *135*, 23–34.

Rubino, F., Piredda, R., Calabrese, F.M., Simone, D., Lang, M., Calabrese, C., Petruzzella, V., Tommaseo-Ponzetta, M., Gasparre, G., and Attimonelli, M. (2012). HmtDB, a genomic resource for mitochondrion-based human variability studies. Nucleic Acids Res. *40*, D1150-1159.

Ruiz-Pesini, E., Lapeña, A.-C., Díez-Sánchez, C., Pérez-Martos, A., Montoya, J., Alvarez, E., Díaz, M., Urriés, A., Montoro, L., López-Pérez, M.J., et al. (2000). Human mtDNA Haplogroups Associated with High or Reduced Spermatozoa Motility. Am J Hum Genet *67*, 682–696.

Ruiz-Pesini, E., Mishmar, D., Brandon, M., Procaccio, V., and Wallace, D.C. (2004). Effects of purifying and adaptive selection on regional variation in human mtDNA. Science *303*, 223–226.

Sadun, F., De Negri, A.M., Carelli, V., Salomao, S.R., Berezovsky, A., Andrade, R., Moraes, M., Passos, A., Belfort, R., da Rosa, A.B., et al. (2004). Ophthalmologic findings in a large pedigree of 11778/Haplogroup J Leber hereditary optic neuropathy. Am. J. Ophthalmol. *137*, 271–277.

Sagan, L. (1967). On the origin of mitosing cells. J. Theor. Biol. *14*, 255–274.

Santoro, A., Salvioli, S., Raule, N., Capri, M., Sevini, F., Valensin, S., Monti, D., Bellizzi, D.,

Passarino, G., Rose, G., et al. (2006). Mitochondrial DNA involvement in human longevity. Biochimica et Biophysica Acta (BBA) - Bioenergetics *1757*, 1388–1399.

Santoro, A., Balbi, V., Balducci, E., Pirazzini, C., Rosini, F., Tavano, F., Achilli, A., Siviero, P., Minicuci, N., Bellavista, E., et al. (2010). Evidence for sub-haplogroup h5 of mitochondrial DNA as a risk factor for late onset Alzheimer's disease. PLoS ONE *5*, e12037.

Sato, M., and Sato, K. (2011). Degradation of paternal mitochondria by fertilization-triggered autophagy in C. elegans embryos. Science *334*, 1141–1144.

Sato, M., and Sato, K. (2013). Maternal inheritance of mitochondrial DNA by diverse mechanisms to eliminate paternal mitochondrial DNA. Biochim. Biophys. Acta *1833*, 1979–1984.

Saxena, R., de Bakker, P.I.W., Singer, K., Mootha, V., Burtt, N., Hirschhorn, J.N., Gaudet, D., Isomaa, B., Daly, M.J., Groop, L., et al. (2006). Comprehensive association testing of common mitochondrial DNA variation in metabolic disease. Am. J. Hum. Genet. *79*, 54–61.

Scarlatti, F., Sala, G., Somenzi, G., Signorelli, P., Sacchi, N., and Ghidoni, R. (2003). Resveratrol induces growth inhibition and apoptosis in metastatic breast cancer cells via de novo ceramide signaling. FASEB J. *17*, 2339–2341.

Schon, E.A., DiMauro, S., and Hirano, M. (2012). Human mitochondrial DNA: roles of inherited and somatic mutations. Nat. Rev. Genet. *13*, 878–890.

Schwartz, M., and Vissing, J. (2002). Paternal inheritance of mitochondrial DNA. N. Engl. J. Med. *347*, 576–580.

Seelert, H., and Dencher, N.A. (2011). ATP synthase superassemblies in animals and plants: two or more are better. Biochim. Biophys. Acta *1807*, 1185–1197.

Shin, W.S., Tanaka, M., Suzuki, J., Hemmi, C., and Toyo-oka, T. (2000). A Novel Homoplasmic Mutation in mtDNA with a Single Evolutionary Origin as a Risk Factor for Cardiomyopathy. Am J Hum Genet *67*, 1617–1620.

Skuder, P., Plomin, R., McClearn, G.E., Smith, D.L., Vignetti, S., Chorney, M.J., Chorney, K., Kasarda, S., Thompson, L.A., Detterman, D.K., et al. (1995). A polymorphism in mitochondrial DNA associated with IQ? Intelligence *21*, 1–11.

Skulachev, V.P. (2001). Mitochondrial filaments and clusters as intracellular power-transmitting cables. Trends Biochem. Sci. *26*, 23–29.

Stawski, H. (2013). Preparing whole genome human mitochondrial DNA libraries for Next Generation Sequencing using Illumina® Nextera® XT. Western Carolina University.

Stone, E.M., Newman, N.J., Miller, N.R., Johns, D.R., Lott, M.T., and Wallace, D.C. (1992). Visual recovery in patients with Leber's hereditary optic neuropathy and the 11778 mutation. J Clin Neuroophthalmol *12*, 10–14.

Stotland, A., and Gottlieb, R.A. (2015). Mitochondrial quality control: Easy come, easy go. Biochim. Biophys. Acta *1853*, 2802–2811.

Sutovsky, P., Moreno, R.D., Ramalho-Santos, J., Dominko, T., Simerly, C., and Schatten, G. (1999). Ubiquitin tag for sperm mitochondria. Nature *402*, 371–372.

Szabadkai, G., Bianchi, K., Várnai, P., De Stefani, D., Wieckowski, M.R., Cavagna, D., Nagy, A.I.,

Balla, T., and Rizzuto, R. (2006). Chaperone-mediated coupling of endoplasmic reticulum and mitochondrial Ca2+ channels. J. Cell Biol. *175*, 901–911.

Taylor, R.W., and Turnbull, D.M. (2005). Mitochondrial DNA mutations in human disease. Nat. Rev. Genet. *6*, 389–402.

Temperley, R., Richter, R., Dennerlein, S., Lightowlers, R.N., and Chrzanowska-Lightowlers, Z.M. (2010). Hungry codons promote frameshifting in human mitochondrial ribosomes. Science *327*, 301.

Tonska, K., Kurzawa, M., Ambroziak, A.M., Korwin-Rujna, M., Szaflik, J.P., Grabowska, E., Szaflik, J., and Bartnik, E. (2008). A family with 3460G>A and 11778G>A mutations and haplogroup analysis of Polish Leber hereditary optic neuropathy patients. Mitochondrion *8*, 383–388.

Torroni, A., Carelli, V., Petrozzi, M., Terracina, M., Barboni, P., Malpassi, P., Wallace, D.C., and Scozzari, R. (1996). Detection of the mtDNA 14484 mutation on an African-specific haplotype: implications about its role in causing Leber hereditary optic neuropathy. Am. J. Hum. Genet. *59*, 248–252.

Torroni, A., Petrozzi, M., D'Urbano, L., Sellitto, D., Zeviani, M., Carrara, F., Carducci, C., Leuzzi, V., Carelli, V., Barboni, P., et al. (1997). Haplotype and phylogenetic analyses suggest that one European-specific mtDNA background plays a role in the expression of Leber hereditary optic neuropathy by increasing the penetrance of the primary mutations 11778 and 14484. Am. J. Hum. Genet. *60*, 1107–1121.

Torroni, A., Rengo, C., Guida, V., Cruciani, F., Sellitto, D., Coppa, A., Calderon, F.L., Simionati, B., Valle, G., Richards, M., et al. (2001). Do the four clades of the mtDNA haplogroup L2 evolve at different rates? Am. J. Hum. Genet. *69*, 1348–1356.

Trounce, I.A., Kim, Y.L., Jun, A.S., and Wallace, D.C. (1996). Assessment of mitochondrial oxidative phosphorylation in patient muscle biopsies, lymphoblasts, and transmitochondrial cell lines. Meth. Enzymol. *264*, 484–509.

Vidoni, S., Zanna, C., Rugolo, M., Sarzi, E., and Lenaers, G. (2013). Why Mitochondria Must Fuse to Maintain Their Genome Integrity. Antioxid Redox Signal *19*, 379–388.

Wakabayashi, J., Zhang, Z., Wakabayashi, N., Tamura, Y., Fukaya, M., Kensler, T.W., Iijima, M., and Sesaki, H. (2009). The dynamin-related GTPase Drp1 is required for embryonic and brain development in mice. J. Cell Biol. *186*, 805–816.

Walker, J.E. (2013). The ATP synthase: the understood, the uncertain and the unknown. Biochem. Soc. Trans. *41*, 1–16.

Wallace, D.C., Singh, G., Lott, M.T., Hodge, J.A., Schurr, T.G., Lezza, A.M., Elsas, L.J., and Nikoskelainen, E.K. (1988). Mitochondrial DNA mutation associated with Leber's hereditary optic neuropathy. Science *242*, 1427–1430.

van der Walt, J.M., Nicodemus, K.K., Martin, E.R., Scott, W.K., Nance, M.A., Watts, R.L., Hubble, J.P., Haines, J.L., Koller, W.C., Lyons, K., et al. (2003). Mitochondrial polymorphisms significantly reduce the risk of Parkinson disease. Am. J. Hum. Genet. *72*, 804–811.

van der Walt, J.M., Dementieva, Y.A., Martin, E.R., Scott, W.K., Nicodemus, K.K., Kroner, C.C., Welsh-Bohmer, K.A., Saunders, A.M., Roses, A.D., Small, G.W., et al. (2004). Analysis of

European mitochondrial haplogroups with Alzheimer disease risk. Neurosci. Lett. *365*, 28–32.

Wells, R.C., Picton, L.K., Williams, S.C.P., Tan, F.J., and Hill, R.B. (2007). Direct binding of the dynamin-like GTPase, Dnm1, to mitochondrial dynamics protein Fis1 is negatively regulated by the Fis1 N-terminal arm. J. Biol. Chem. *282*, 33769–33775.

Yang, J., Zhu, Y., Tong, Y., Zhang, Z., Chen, L., Chen, S., Cao, Z., Liu, C., Xu, J., and Ma, X. (2009). The novel G10680A mutation is associated with complete penetrance of the LHON/T14484C family. Mitochondrion *9*, 273–278.

Yang, T.-L., Guo, Y., Shen, H., Lei, S.-F., Liu, Y.-J., Li, J., Liu, Y.-Z., Yu, N., Chen, J., Xu, T., et al. (2011). Genetic Association Study of Common Mitochondrial Variants on Body Fat Mass. PLoS One *6*.

Youle, R.J., and Karbowski, M. (2005). Mitochondrial fission in apoptosis. Nat. Rev. Mol. Cell Biol. *6*, 657–663.

Yu-Wai-Man, P., and Chinnery, P.F. (2016). Leber Hereditary Optic Neuropathy. In GeneReviews®, M.P. Adam, H.H. Ardinger, R.A. Pagon, S.E. Wallace, L.J. Bean, H.C. Mefford, K. Stephens, A. Amemiya, and N. Ledbetter, eds. (Seattle (WA): University of Washington, Seattle), p.

Yu-Wai-Man, P., Griffiths, P.G., Gorman, G.S., Lourenco, C.M., Wright, A.F., Auer-Grumbach, M., Toscano, A., Musumeci, O., Valentino, M.L., Caporali, L., et al. (2010). Multi-system neurological disease is common in patients with OPA1 mutations. Brain *133*, 771–786.

Yu-Wai-Man, P., Griffiths, P.G., and Chinnery, P.F. (2011). Mitochondrial optic neuropathies - disease mechanisms and therapeutic strategies. Prog Retin Eye Res *30*, 81–114.

Yu-Wai-Man, P., Spyropoulos, A., Duncan, H.J., Guadagno, J.V., and Chinnery, P.F. (2016). A multiple sclerosis-like disorder in patients with OPA1 mutations. Ann Clin Transl Neurol *3*, 723–729.

Zanna, C., Ghelli, A., Porcelli, A.M., Martinuzzi, A., Carelli, V., and Rugolo, M. (2005). Caspase-independent death of Leber's hereditary optic neuropathy cybrids is driven by energetic failure and mediated by AIF and Endonuclease G. Apoptosis *10*, 997–1007.

Zanna, C., Ghelli, A., Porcelli, A.M., Karbowski, M., Youle, R.J., Schimpf, S., Wissinger, B., Pinti, M., Cossarizza, A., Vidoni, S., et al. (2008). OPA1 mutations associated with dominant optic atrophy impair oxidative phosphorylation and mitochondrial fusion. Brain *131*, 352–367.

Zhang, A.-M., Jia, X., Guo, X., Zhang, Q., and Yao, Y.-G. (2012). Mitochondrial DNA mutation m.10680G > A is associated with Leber hereditary optic neuropathy in Chinese patients. J Transl Med *10*, 43.

Zhao, X., Li, N., Guo, W., Hu, X., Liu, Z., Gong, G., Wang, A., Feng, J., and Wu, C. (2004). Further evidence for paternal inheritance of mitochondrial DNA in the sheep (Ovis aries). Heredity (Edinb) *93*, 399–403.

Zou, Y., Jia, X., Zhang, A.-M., Wang, W.-Z., Li, S., Guo, X., Kong, Q.-P., Zhang, Q., and Yao, Y.-G. (2010). The MT-ND1 and MT-ND5 genes are mutational hotspots for Chinese families with clinical features of LHON but lacking the three primary mutations. Biochem. Biophys. Res. Commun. *399*, 179–185.